# IDENTIFICATION OF OXLDL-INDUCED OXIDATIVE STRESS SOURCES IN CARDIOVASCULAR DISEASE

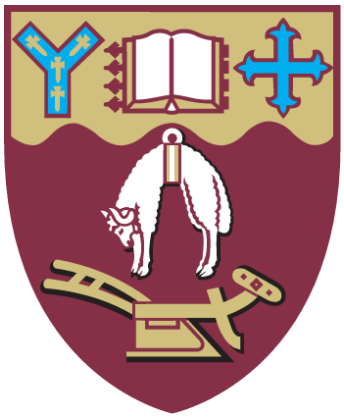

---

A thesis submitted in partial fulfilment of the requirements for the degree of Master of Science in Biochemistry.

School of Biological Sciences
University of Canterbury
New Zealand

---

Sean Cross
2016

# TABLE OF CONTENTS

# LIST OF FIGURES

## Introduction



## Methods



## Results

**OxLDL-induced cell death**



**OxLDL variability**

**OxLDL-induced oxidative stress**



**NADPH Oxidase (NOX)**



**Mitochondria**

## Discussion

# ACKNOWLEDGEMENTS

I really cannot believe that I have finally got to this point. This definitely has been the most challenging part of my life so far, but in return I have learnt so much more about myself and my field of study.

First of all I would like to express my love to my family for their encouragement and support throughout my thesis, this thesis is for you. Thank you to my best friends/flatmates (Shane van Bergen, Brett Mckenzie, Benjamin Riley, Sarah Gilmour and Paddy Gibson) for being there till the end despite the all-nighters, my moodiness and frustrations when my experiments were playing up.

I would like to give a huge thank you to my supervisor, Associate Professor Steven Gieseg. Thank you for all the help, without you this thesis would not have been possible. Thank you for always being there for me throughout the good and bad times, you will always be someone that I look up to. Thank you to my co-supervisor Barry Hock for his input and advice.

Thank you to Craig Galilee for being our wonderful 4$^{th}$ floor lab technician. He did an amazing job of being a health and safety role model and being a wonderful father figure throughout my time here.

A special thank you to the members of the Plaques and Recreation team, in particular Hannah Prebble, Greg Parker (who is only mentioned as a formality), Anthony Yeandle, Joe Healy, Nina Steyn, Izani Othman and Shane Reeves for sharing their knowledge and support. An enormous thank you to you guys for having to listen to my cell culture rants and helping me through when my experiments weren't working.

I'd like to thank all the amazing people that donated blood that was used for the isolation of LDL and Justin Roake of the Christchurch Vascular Surgery Department.

Lastly, a special thank you to my fellow Masters crew (Hayley Schoch, Olivia Steel, and Courtney Burn) for the lunch dates, late night study and gossip sessions, this could not have been done without you guys.

# ABBREVIATIONS

| | |
|---|---|
| **7-KC** | 7-Keto cholesterol |
| **7,8-NP** | 7,8-Dihydroneopterin |
| **ACN** | Acetonitrile |
| **ANOVA** | Analysis of variance |
| **Apocynin** | 4’-hydroxy-3’-methoxyacetophenone |
| **ATP** | Adenosine triphosphate |
| **BCA** | Bicinchoninc acid |
| **BSA** | Bovine serum albumin |
| **$Ca^{2+}$** | Calcium ion |
| **$CaCl_2$** | Calcium chloride |
| **$Cl^-$** | Chloride ion |
| **$CO_2$** | Carbon dioxide |
| **$CuCl_2$** | Copper chloride |
| **DHE** | Dihydroethidium |
| **DMSO** | Dimethyl sulphoxide |
| **DNA** | Deoxyribonucleic acid |
| **ECM** | Extracellular matrix |
| **EDTA** | Ethylenediaminetetraacetic acid |
| **ER** | Endoplasmic reticulum |
| **ETC** | Electron transport chain |
| **FAD** | Flavin adenine dinucleotide |
| **FBS** | Foetal bovine serum |
| **GAPDH** | Glyceraldehydes-3-phosphate dehydrogenase |
| **GSH** | Glutathione |
| **GTP** | Guanosine triphosphate |
| **$H_2O_2$** | Hydrogen peroxide |
| **HCl** | Hydrochloric acid |
| **HMDM** | Human monocytes-derived macrophage |
| **HOCl** | Hypochlorous acid |
| **HPLC** | High performance liquid chromatography |
| **IMM** | Inner mitochondrial membrane |

| | |
|---|---|
| **IMS** | Inter-membrane space |
| **INF-γ** | Interferon-gamma |
| **KBr** | Potassium bromide |
| **LDL** | Low density lipoprotein |
| **$LD_{50}$** | Lethal dose to 50% of the population |
| **MPO** | Myeloperoxidase |
| **MTT** | 3-[4,5-Dimethylthiazol-2-yl]-2,5-diphenyl-tetrazolium bromide |
| **$NADP^+$** | Nicotinamide adenine dinucleotide phosphate |
| **NaCl** | Sodium chloride |
| **$NaH_2PO_4.H2O$** | Sodium dihydrogen phosphate monohydrate |
| **NaOH** | Sodium hydroxide |
| **NADPH** | Reduced nicotinamide adenine dinucleotide phosphate |
| **NO** | Nitric oxide |
| **NOX** | NADPH oxidase |
| **$O_2$** | Molecular oxygen |
| **$O_2\cdot^-$** | Superoxide anion |
| **OH·** | Hydroxyl radical |
| **OMM** | Outer mitochondrial membrane |
| **OxLDL** | Oxidized LDL |
| **PBS** | Phosphate buffered saline |
| **Phox** | Phagocytic oxidase |
| **PI** | Propidium iodide |
| **PMA** | Phorbol 12-myristate 12-acetate |
| **rpm** | Revolutions/minute |
| **RPMI-1640** | Roswell Park Memorial Institute 1640 |
| **NaSCN** | Sodium thiocyanate |
| **SEM** | Standard error of the mean |
| **SOD** | Superoxide dismutase |
| **TAT** | Trans-Activator of Transcription |
| **U937** | U937 monocyte-like cell line |
| **VLDL** | Very low density lipoprotein |
| $^{V}/_{V}$ | Volume/Volume |
| $^{W}/_{V}$ | Weight/Volume |

# ABSTRACT

Atherosclerosis is characterized by chronic inflammation of the arterial wall through the accumulation of lipid-loaded macrophages. Cell death within this region causes the progression of the fatty streak into an advanced atherosclerotic lesion with a characteristic necrotic core, consisting of cholesterol, calcium deposits, dead cells and other cellular debris. The oxidation of low-density lipoprotein (LDL) to form oxidized LDL (oxLDL) is a crucial event in the development of the atherosclerotic lesion resulting in death to a range of cell types within the intima. OxLDL is cytotoxic to macrophages through a rapid induction of intracellular oxidative stress, resulting in oxidative damage to essential biomolecules causing cell death that contributes to the development of the necrotic core.

This study investigated the source of the cytotoxic oxidative stress triggered by the presence of oxLDL in U937 monocyte like cells. The research investigated whether NADPH oxidase, myeloperoxidase or uncoupled mitochondria generated intracellular oxidants in response to oxLDL.

Specific NOX inhibitors, (gp91ds-tat and apocynin), provided insight on the involvement of NOX in the oxLDL-induced oxidative stress mechanism. Increasing concentrations of gp91ds-tat significantly decreased intracellular superoxide generation in U937 cells but did not prevent cell viability loss. The competitive inhibitor, gp91ds-tat, did not completely inhibit the complex, allowing for residual superoxide to be generated. Apocynin treated plaque sections showed a significant reduction in 7,8-dihydroneopterin (7,8-NP) oxidation. This study also measured the U937 intracellular 7,8-NP oxidation by cellular oxidants in response to oxLDL. The addition of apocynin significant reduced the oxLDL-induced 7,8-NP oxidation. This suggested that NOX was the major source of intracellular oxidative stress in both *in vivo* and *in vitro* research.

Myeloperoxidase was shown to not be involved in the *in vitro* mechanism, as inhibition of hypochlorite production through MPO inhibitors (ABAH & thiocyanate) did not restore cell viability, nor did it reduce the intracellular oxidative stress when

U937 cells were incubated with oxLDL. This suggests that MPO is not involved in the U937 cell death mechanism as a result of oxLDL exposure.

OxLDL induced a significant depolarization of the mitochondria membrane potential after 6 hours exposure and the addition of 7,8-NP did not protect the membrane depolarization. However, the data that was collected was deemed inconclusive due to fundamental problems occurring within the JC-1 assay.

Our results suggest that NOX is the major source of oxidative stress causing significant cell death and progression of the plaque necrotic core. It was shown that myeloperoxidase has no involvement in the oxidative stress mechanism and that the mitochondria appears to play a role.

# 1. INTRODUCTION

## 1.1 Overview

Atherosclerosis is a complex disease that results from the thickening of the arterial wall from a build-up of cellular debris and lipids to form a complex plaque that restricts the blood flow (Libby 2002). Low-density lipoprotein (LDL) is a lipid-carrying particle that distributes cholesterol, phospholipids and triglycerides around our body (Brown 1986). These particles can accumulate underneath the arterial wall, forming a fatty streak and promoting inflammation. Macrophages play an important role in the inflammatory process and are recruited to the site to resolve the inflammatory response initiated by trapped LDL. Macrophages release oxidants into the environment that can oxidize the LDL particles (Aviram 1996). The formation of oxidized LDL (oxLDL) is a significant driving factor in the disease, as it drives the transition of a fatty streak into an advanced complex plaque by initiating cell death to the immune cells present (Gieseg 2010 A). Death of the cell results in cell debris, cytokines and more oxidants to be released into the artery intima contributing to further inflammation and progression of a plaque. Eventually the necrotic core can rupture, releasing all of the trapped content into the artery and the formation of a blood clot causes a blockage downstream of the plaque, resulting in a heart attack or stroke (Libby 2002, Douglas 2014). Acute oxLDL toxicity causes intracellular oxidative stress by an overproduction of oxidants in HMDM and U937 cells (Gieseg 2010 B, Katouah 2015). Experimental research indicates that there is a strong relationship between an overproduction of intracellular oxidants and subsequent cell death as a result of oxLDL exposure (Chen 2012, Katouah 2015). It is currently unknown the source of intracellular oxidative stress, however, NADPH oxidase (NOX-2), mitochondria and myeloperoxidase are all known sites to produce oxidants. 7,8-Dihydroneopterin (7,8-NP) is synthesized by activated macrophages at sites of inflammation, however, its cellular purpose is undetermined. 7,8-NP has been shown to protect cells against an oxLDL induced cell death and reduce the intracellular oxidative stress generated by oxLDL (Gieseg 2001 A, Chen 2012). Therefore this research will investigate the three possible sources of oxLDL-induced intracellular oxidative stress and directly measure the intracellular oxidation of 7,8-NP in U937 cells.

# 1. 2 Atherosclerosis

## 1.2.1 Cardiovascular disease and atherosclerosis

According to the World Health Organization (WHO), cardiovascular diseases (CVD) are the number one cause of death globally, accounting for approximately 30% of all global deaths (Santulli 2013). CVD includes coronary heart disease, strokes and peripheral vascular disease that all involve the underlying process of atherosclerosis.

Atherosclerosis is a chronic inflammatory disease that involves endothelial dysfunction, inflammation of the arterial wall, immune cell recruitment and thickening of the arterial intima through a build-up of cellular debris, lipids, cholesterol and calcium deposition (Bobryshev 2006). Modifications to the arterial wall results in large occlusions called plaques that restrict the blood flow, causing abnormalities and reduced oxygen supply to essential organs. Progression of the atherosclerotic plaque makes the lesion unstable and vulnerable to rupturing. Plaque rupture releases the content into the blood stream triggering a thrombus (blood clot) formation, which lodges in smaller capillary beds, restricting or completely blocking the blood supply (Falk 1983). This can result in a myocardial or cerebral infarction (heart attack or stroke respectively) depending on the location of the plaque (Libby 2002, Hansson 2011). There are a series of risk factors which influence the severity and likelihood of developing the disease, which include genetic predisposition, age, obesity, gender, cigarette smoking, physical inactivity, excessive alcohol consumption, hypertension, type II diabetes and hyperlipidemia (Meyer 2000, Libby 2002).

## 1.2.2 Initiation and progression of atherosclerosis

The exact details on the initiation of atherosclerosis remain controversial, however, a number of theories have been proposed to explain the early stages of plaque formation.

The response to injury hypothesis states that the lesion is formed through chronic injury occurring to the arterial endothelial layer at a branched point in the artery due to high blood pressure or mechanical shear stress. These events promote an inflammatory cascade to recruit leukocytes to the area of inflammation, to resolve the stress and promote healing. This results in the migration and adherence of monocytes

to the inflamed endothelium. As a result of the damaged endothelial layer, Low-Density Lipoprotein (LDL) particles are able to enter into the arterial intima layer. Aggregation or oxidative modifications occur to the LDL due to the vascular wall or the immune cells release oxidants into the environment. The LDL receptor mediates the endocytosis of cholesterol into hepatic or macrophage cells, removing it from the circulatory system. This is a highly regulated process and the LDL receptor is down regulated once cholesterol levels get too high, preventing further absorption of LDL (Zhao 2006) The LDL receptor recognizes specific amino acid residues on the LDL's apolipoprotein B100 (ApoB100) protein such as lysine, arginine and histidine. Oxidative degradation of the ApoB100 causes extensive fragmentation to the protein, forming smaller peptides and derivatization of positive lysine residues on the LDL molecule, preventing the LDL receptor from recognizing the particle (Esterbauer 1990, Obama 2007, Levitan 2010). When modifications have occurred to the LDL particle, it permits a rapid, unregulated uptake of modified LDL by the macrophages scavenger receptors, located on the membrane of the cell. This leads to excessive cholesterol accumulation and the differentiation into a lipid-loaded foam cell (Steinbrecher 1991, Bobryshev 2006, Jayaraman 2007) which is an early sign of atherosclerosis (Ross 1977, Sun 2000).

The response to retention hypothesis indicates that the initiation of the atherogenic properties is caused by LDL diffusing beneath the sub-endothelial layer and binding (with high affinity) to proteoglycans chain present on the muscle layer (Williams 1995). Proteoglycans contain long carbohydrate side chains of glycosaminoglycans (GAGs), which are covalently attached to a core protein via a glycosidic linkage. GAGs have repeating disaccharide units, with negatively charged sulfate or carbohydrate groups. Majority of the GAGs are produced by fibroblasts as a part of the extracellular matrix (Borén 1998, Evanko 1998, Williams 1998, Alvarez 2006). Once LDL moves through the sub-endothelial layer, the positively charged lysine residues present on the ApoB100 protein have a high affinity for the negatively charged sulfate proteoglycans, causing the LDL to stick to the GAG matrix (Evanko 1998, Libby 2009). LDL itself is non-toxic to the macrophages until it is caught by proteoglycan chains and undergoes oxidation by oxidants produced by vascular cells or macrophages. Scavenger receptors, present on the macrophage, uncontrollably uptake oxLDL to form lipid-loaded foam cells.

Aspects from the previous hypothesizes are plausible, however, the oxidative modification hypothesis is the commonly accepted theory to explain the events occurring in the initial stages of plaque development. The oxidative modification theory proceeds via the LDL particles enter into the arterial intima layer where the trapped LDL is oxidatively modified by cellular oxidants produced by endothelial or smooth muscle cells (**Figure 1.1**). The endothelial cells produce proinflammatory cytokines, adhesion molecules, chemotactic proteins to promote recruitment and migration of monocytes to the inflammation area within the intima space. Activated monocytes roll, via cell adhesion proteins, along the surface of lumen endothelial layer in response to the endothelial cells releasing the proinflammatory signal. The monocytes move through the layer and undergo differentiation into macrophages in response to the inflammatory cytokines (**Figure 1.1**). The macrophages produce oxidants such as superoxide, hydrogen peroxide and hypochlorite via the NADPH oxidase (NOX) complex and myeloperoxidase (MPO) respectively, in attempt to oxidize the pathogenic threat. Further lipid and protein oxidation occurs to the minimally oxidized LDL, forming oxidized LDL (oxLDL) (**Figure 1.1**) (Steinbrecher 1991, Stocker 2004, Bobryshev 2006, Libby 2009). Macrophages are immune cells that specialize in removing cellular debris or modified proteins from the body via phagocytosis. This is initiated by various scavenger receptors that are expressed on the cell's surface and these receptors are unregulated.

There is an abundant amount of experimental evidence that supports scavenger receptor CD36 in the pathology of atherosclerosis. Research performed by Rahaman (2006) demonstrated CD36-null mice showed a significant 70 – 80% inhibition of foam cell formation (Rahaman 2006). Additionally, Nozaki (1995) showed a 40% reduction of oxLDL uptake in CD36-null human macrophages (Nozaki 1995). Suggestions have been made that CD36 binds to the positively charged lysine residues that are present on the apoB100 and the oxidized phospholipids on the oxLDL particle (Boullier 2001). Scavenger receptors have uncontrolled uptake of modified lipoproteins, causing an accumulation of oxLDL within the macrophage (Silverstein 2009). A combination of increased oxLDL uptake and the reduced oxLDL efflux causes the macrophage to differentiate into a lipid-loaded foam cell (**Figure 1.1**). The accumulation of lipids induces ER stress (**Section 1.3.2**) and subsequent cell death, driving the development of the necrotic core (Park 2014).

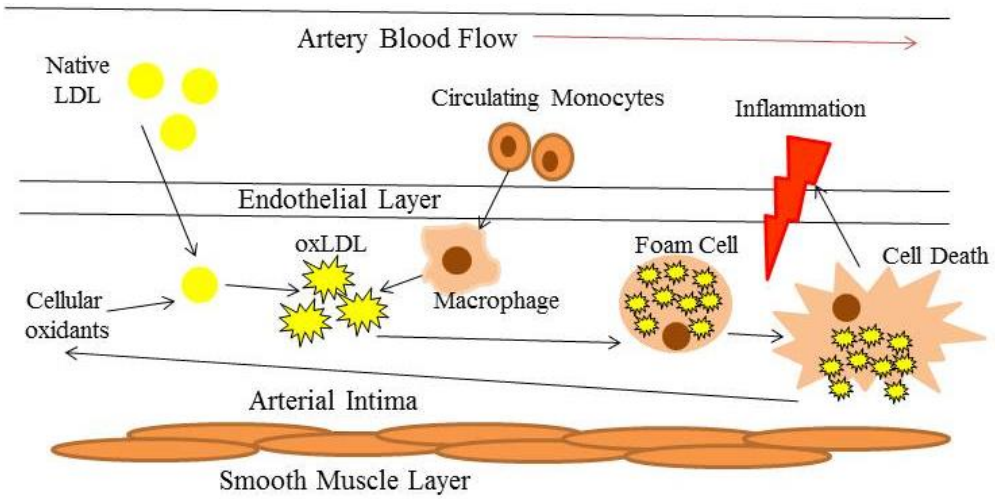


**Figure 1.1 Early atherosclerotic plaque development**

Native LDL can enter into the intima space and undergo oxidation by cellular oxidants by the endothelial, macrophage or smooth muscle cells. The presence of oxLDL recruits macrophage differentiated monocytes to the site of inflammation. OxLDL is taken up by the macrophage via the scavenger receptor CD36, forming lipid-loaded foam cells. Death of the foam cells results in the intracellular content to be released back into the environment, further propagating the inflammation in the intima space.

OxLDL induces extensive damage to cells and causes the cells to undergo apoptosis or necrosis. The cell's intracellular content (cellular debris, oxidants, chemotactins and cytokines) is released into the environment, contributing to the further inflammation and progression of the necrotic core (**Figure 1.2**). (Madamanchi 2005, Gieseg 2009, Libby 2009). Inflammatory cells play a crucial role in the destabilization in the plaque's fibrous cap, resulting in the plaque rupture. Inflammatory cytokines (interleukin-1 (IL-1), tumour necrosis factor (TNF), CD140 and CD-40) can stimulate an up-regulation of matrix metalloproteinases (MMP) in macrophages and vascular smooth muscle cells (Mach 1997, Libby 1998). These enzymes is responsible for remodelling the extracellular matrix and degrading the fibrous cap, making the plaque more prone to rupturing (Galis 1994, Geng 1995). Dysfunction of the expression of MMP enzymes is believed to be responsible for the rupture of the atherosclerotic plaques (Kim 2004). Once the plaque ruptures, it will form an acute thrombosis upstream, flow down and get lodged in smaller capillaries. This restricts or completely blocks the blood supply resulting in nutrient deprivation and tissue death. The progression of this will often manifest itself as a heart attack or stroke (Libby 2002, Bobryshev 2006).

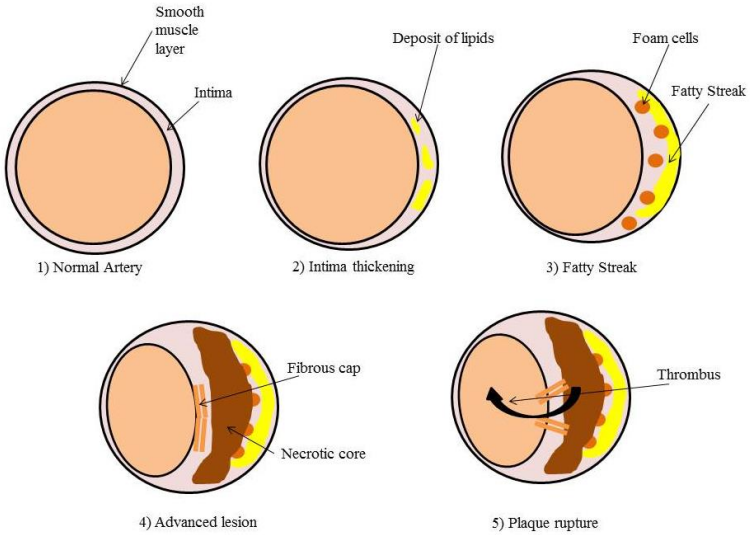


**Figure 1.2 The progression of atherosclerosis on the artery wall**

The different stages of atherosclerotic plaque development, depicting deposition of lipids (**2**), the formation of the fatty streak (**3**), formation of the necrotic core and fibrous cap (**4**) and rupturing of the plaque, forming a thrombus.

OxLDL has been shown to induce cytotoxic effects in a variety of cell types including macrophages (Gieseg 2010 B), smooth muscle cells (Hsieh 2001), endothelial cells (Henriksen 1979), U937 (Katouah 2015) and THP-1 cell lines (Baird 2004). The mechanism by which oxLDL exerts its toxicity is still under investigation, but it appears that oxLDL induces a variety of mechanisms depending on the cell type. Research performed by Ermak (2010) compared the LDL hypochlorite oxidation with copper-ion oxidation. The results showed that HOCl oxidized LDL (predominately forms protein oxidative products and some lipid oxidative products) and copper oxidized LDL (combination of both protein and lipid oxidation products) was just as toxic as each other to U937 cells. This suggests that the toxicity of oxLDL is predominately from advanced protein oxidation rather than lipid oxidation (Ermak 2010). Previous researchers claimed that oxysterols, especially 7-ketocholesterol (7-KC), were the main cytotoxic component of oxLDL (Larsson 2006). However, further investigation of 7-KC toxicity showed that U937 cells that had been treated with modified oxLDL, enriched with 7-KC, did not increase the toxicity of oxLDL, suggesting that 7-KC is not the toxic component (Rutherford 2012). This suggests that protein oxidation of the ApoB100 is inducing the cytotoxic effect.

Other effects observed in U937 and HMDM cells have seen an increase of intracellular oxidative stress with a subsequent decrease in cell viability with prolonged exposure to oxLDL (Gieseg 2010 B, Chen 2012, Katouah 2015). The intracellular oxidative stress reduces the activity of essential glycolytic enzymes

involved in metabolic processes, such as a reduced activity of GAPDH, aconitase and lactate dehydrogenase. (Gieseg 2010 B, Chen 2012, Katouah 2015). Significant oxidative damage to the cell with lack of ATP results in necrosis which is a key characteristic of oxLDL induced damage (Golstein 2007). This indicates that oxLDL-induced oxidative stress is the most likely the main initiator of the death cascade.

## 1.3 Types of cell death

When different cell lines are exposed to oxLDL, it can induce different biochemical pathways, resulting in the various cell death mechanisms explained below.

### 1.3.1 Apoptosis and necrosis

Apoptosis, also known as programmed cell death is a highly regulated cell death mechanism and occurs during development, aging and as a homeostatic mechanism to maintain cell populations in tissue. Apoptosis also occurs as a defence mechanism such as in immune reactions or when disease or chemical agents damage cells. Apoptosis involves a series of intracellular signalling cascades for controlled shutdown of the cell. These include maintaining ion homeostasis and intact organelles to sustain the ATP production throughout the cell death, as apoptosis cannot occur without ATP. Features of apoptosis involve morphological changes such as cell shrinkage, plasma membrane blebbing, chromatin condensation, DNA fragmentation and apoptotic body formation. Typical biochemical changes comprise of cytochrome c release from mitochondria resulting in the activation of caspases and labelling of the cell for clearance by phagocytes through exposure of phosphatidylserine on the surface of the cell. Biochemical changes during apoptosis involve the release of cytochrome c from the mitochondria and a redistribution of phosphatidylserine to the outside surface of the plasma membrane, signalling the apoptotic bodies (small membrane bound vesicles) for phagocytosis. Phagocytes then engulf the apoptotic bodies to entirely remove the cell (Vicca 2003, Vindis 2005, Elmore 2007).

Necrosis is a unregulated form of cell death mechanism that does not follow the apoptotic signal transduction pathway but rather various receptors are activated that result in the loss of cell membrane integrity and an uncontrolled release of cellular contents into the intracellular space (Golstein 2007). Morphological characteristics include cell membrane swelling due to complete loss of control over ion homeostasis,

degradation of organelle structure resulting in disruption of internal organelles, nuclear membrane disruption, rupturing of the plasma membrane and release of the intracellular content into the extracellular space (Majno 1995, Golstein 2007). Necrotic cells release denatured proteins, fragmented DNA, cytokines and cell debris into the environment, inducing an inflammatory response (Tabas 1997). Secondary necrosis can occur when the apoptotic bodies membrane rupture, resulting in the cellular content to pour out into the extracellular space.

### 1.3.2 Endoplasmic reticulum (ER) stress

The endoplasmic reticulum (ER) is involved in intracellular signalling by acting as a major store of intracellular calcium, initiating the signalling transduction. Additionally, it is involved in protein folding and post translational modifications (Koch 1990). If there is significant disruption to the ER, the stress response pathway called the unfolded protein response (UPR) can activate. Three ER chaperone proteins: PKR-like endoplasmic reticulum kinase (PERK), inositol requiring enzyme 1 (IRE1) and activating transcription factor 6 (ATF6) function as primary sensors of ER stress and can sense the accumulation of unfolded proteins within the lumen. Chronic accumulation of unfolded proteins results in an up regulation of C/EBP homologous protein (CHOP) and after a prolonged elevation can cause a release of intracellular calcium which starts the apoptotic signalling transduction, activating the caspase pathway, condemning the cell to an apoptotic cell death mechanism (Tabas 2010). ER stressors that are present within advanced plaque lesion include: oxidative stress, oxysterols, high levels of intracellular cholesterol and saturated fatty acids. These stressors can lead to chronic activation of the UPR pathway and lead to calcium release and the activation of apoptosis (Tabas 2010, Oh 2012). Cholesterol is transported out of the cell, onto High-Density Lipoprotein (HDL) ApoA1 proteins via ATP binding cassette A1 (ABCA1) and ABCG1 transporters (Gieseg 2009). 7-KC is an abundant substituent in oxLDL and has been shown to impair the ABCA1 transporter, preventing the transport of free cholesterol out of the cell. This leads to membrane vesicles, filled with cholesterol esters, to accumulate in the cytoplasm (Brown 1999, Gieseg 2009). A combination of uncontrolled oxLDL uptake and the impairment of cholesterol efflux, cause the formation of lipid-loaded foam cells (Brown 2000, Gieseg 2009). As the ER membrane is low in free cholesterol, it is

sensitive to large quantities of free cholesterol. The movement of free cholesterol into the ER membrane triggers the UPR by stiffening of the ER membrane, causing the phospholipids to become more organized and tighter packing. This process causes dysfunction of the ER integral membrane proteins and induces UPR. The UPR activates signalling pathways that promote apoptosis cell death through the activation of specific caspases (**Section 1.3.1**) or CHOP (Tsukano 2010, Oh 2012). Cells that die within the atherosclerotic plaque release the cholesterol back into the environment, contributing to further inflammation of the plaque (Feng 2003, DeVries-Seimon 2005)

# 1.4 Oxidative stress

## 1.4.1 Oxidants

The generation of oxidants is a normal physiological process as a result of exercise, metabolism and immune system defence against pathogens. Radicals are highly reactive molecules that are formed as a result of incomplete electron transfer to another molecule, to form an oxidative species. These are capable of oxidizing biochemical molecules, causing further damage (Banerjee 2003). Species such as superoxide radical ($O_2^{\bullet-}$), hydrogen peroxide ($H_2O_2$), hydroxyl radical ($^{\bullet}OH$) and hypochlorite (HOCl) are all generated from biochemical processes (**Figure 1.4**) and if not utilized in the correct function then they can be extremely damaging to other biomolecules (Sies 1997, Hemnani 1998, Al Ghouleh 2011). Oxidative stress is an imbalance of oxidants generated in the body and the inability of the biological system to detoxify the reactive species resulting in damage to all components of the cell such as proteins, lipids and DNA (Evans 1997, Hemnani 1998).

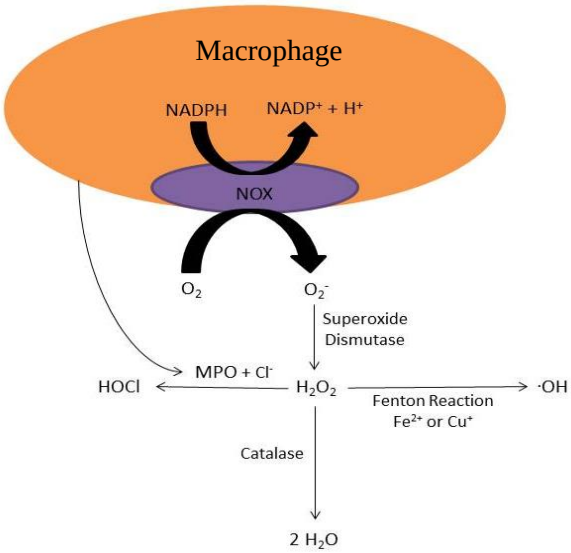


**Figure 1.3 Oxidative mechanism of macrophages against pathogens**
Macrophages generate superoxide anions via NADPH oxidase that can be rapidly dismutated to hydrogen peroxide by superoxide dismutase (SOD). Hydrogen peroxide can either: breakdown into hydroxyl radicals via the fenton reaction, form hypochlorite via myeloperoxidase or breakdown into water via catalase.

In extreme cases of oxidative stress, cell death occurs through inactivation of essential enzymes by oxidation of the essential amino acid side chains in the active site or damage to the plasma membrane (Liu 2006). Cell damage will result in failure of cellular processes and will undergo either apoptosis or necrosis explained in **Section 1.3**. Oxidative damage can occur to cell membrane receptors through oxidation at the phosphorylation sites and preventing ligands from recognizing the binding sites. Oxidative damage to ion channels in the plasma membrane prevents ions from properly flow in and out of the cell. This creates an imbalance of the distribution of water due to an influx of calcium ions will move into the cell, causing swelling of the cell and triggering necrosis (Matsuura 2006). Oxidants are naturally removed by cellular antioxidant systems, which include vitamins (C, E), antioxidant enzymes (glutathione) or cellular generated antioxidants such as 7,8-dihydroneopterin (**Section 1.5**). Antioxidants function by reacting with the oxidant faster than the oxidant can react with biomolecules. Antioxidants have a π conjugated ring motif that enables delocalization of unpaired electrons, stabilizing the molecule and preventing it from further reacting with other biomolecules. (Sies 1997, Valko 2007) Inflammation of the tissue is a complex biological response in which the immune system releases numerous different oxidants into the environment in an attempt to alleviate the harmful stimulus such as pathogen or irritant. Inflammatory diseases are a result of the immune system generating a wide array of oxidants into the site of inflammation creating an oxidative stress environment that causes excessive tissue damage which in turn exacerbates the inflammation (Libby 2002).

### 1.4.2 Oxidative stress and atherosclerosis

Oxidants can cause oxidative damage to the lipid and protein components of the LDL particle, transforming the particle into the high uptake form (oxLDL) and inducing the differentiation of macrophages into foam cells (Fu 1998). Additionally, oxidative stress can cause cell death, contributing to the necrotic core and driving the transition of early plaque development into an advanced plaque (Tabas 1997). OxLDL has been shown by researchers to be cytotoxic to a variety of different cell lines, initiating an oxidative stress response in HMDM and U937 cells (Gieseg 2010 B, Katouah 2015). It has been shown by Katouah (2015) that not only are the macrophages producing oxidants into the environment, causing tissue damage and LDL oxidation, but the oxLDL is causing an overproduction of intracellular oxidative stress after 3 hours. Intracellular oxidative stress has been shown to deplete intracellular glutathione levels, inactivate essential glycolytic enzymes such as GAPDH, aconitase, causing a loss of ATP and the cell is unable to control the cell death, resulting in necrosis (Gieseg 2010 B, Katouah 2015). Several enzymatic systems have been viewed as potential sources of intracellular oxidant production: these include xanthine oxidase, lipooxygenases, cyclooxygenases, cytochrome P450, nitric oxide synthase, uncoupled enzymes of the mitochondria electron transport chain (**Section 1.6**) and NADPH oxidase (**Section 1.7**) (Ballinger 2005, Madamanchi 2007, Al Ghouleh 2011). As NOX's major role is to produce superoxide anions to eliminate pathogens in inflammatory sites, it is considered to be the predominant source of intracellular oxidative stress when cells are exposed to oxLDL (Madamanchi 2005, Brandes 2010).

# 1.5 7,8-Dihydroneopterin (7,8-NP)

## 1.5.1 Biosynthesis of 7,8-NP

Macrophages, monocytes, dendritic cells and fibroblasts are the only known cell types to produce substantial amounts of 7,8-NP in physiological conditions. The biopterin pathway begins with a two-step synthesis with the cleavage of guanosine-5'phosphate (GTP) by GTP-cyclohydrolase-I, yielding 7,8-dihydroneopterin (7,8-NP) triphosphate. The biosynthetic pathway is shown in **Figure 1.4**, representing the two possible branch points to either 7,8-dihydroneopterin or tetrahydrobiopterin from the precursor 7,8-NP triphosphate (Werner-Felmayer 1990, Thony 2000, Walter 2001, Fuchs 2009).

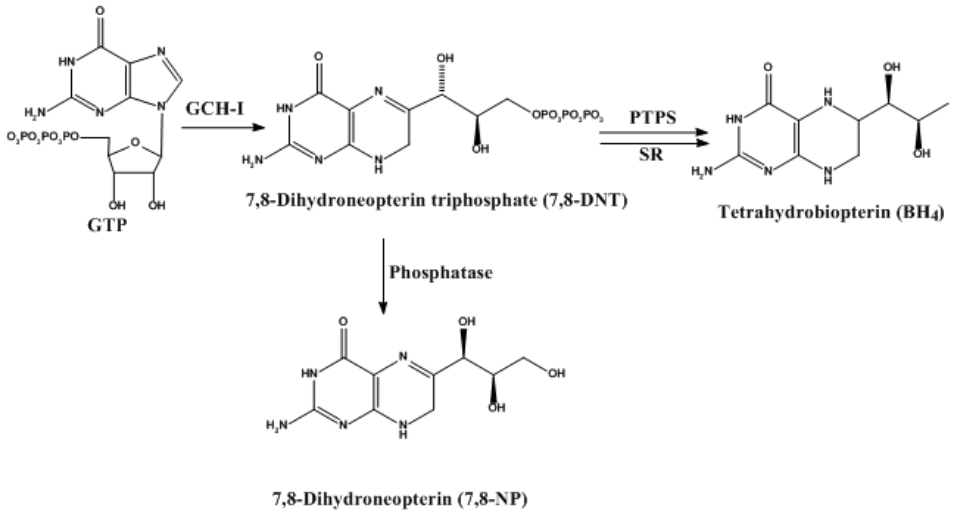


**Figure 1.4 The pterin biosynthetic pathway**

The 7,8-NP biosynthesis pathway involves the conversion of GTP to 7,8-dihydroneopterin triphosphate (7,8-DNT) via GTP cyclohydrolase-I (GCH-I). The accumulation of 7,8-DNT in myelocytic cells drives the flux to dephosphorylation of 7,8-DNT to 7,8-dihydroneopterin (7,8-NP) as they have insufficient 6-pyruvonyltetrahydropterin synthase (PTPS). Alternatively, non-myelolytic cells have functional PTPS, driving the flux to tetrahydrobiopterin ($BH_4$). Diagram was taken from Parker (2015) and permission was received.

Tetrahydrobiopterin ($BH_4$) is an essential cofactor in multiple biological processes, including inducible nitric oxide synthase (NOS) (Channon 2004) and plays an essential role in various aromatic amino acid hydroxylations (Walter 2001, Leitner 2003, Fuchs 2009). 7,8-Dihydroneopterin (7,8-NP) triphosphate is generated by two subsequent enzymes, 6-pyruvonyltetrahydropterin synthase (PTPS) and sepiapterin reductase (SR), producing $BH_4$ (**Figure 1.4**). Human macrophages and related cell types produce insufficient amounts of $BH_4$ and large quantities of 7,8-NP due to the

fact that PTPS activity is considerably low in these cell types owing to a specific exon 3 skipping in PTPS pre-mRNA causing a premature stop codon (Leitner 2003). Non-macrophage cell types possess fully functional PTPS, producing large amounts of BH4 (Leitner 2003). 7,8-NP is product that is produced from the precursor 7,8-NP triphosphate and has been shown to provide antioxidant properties in *in vitro* research (Gieseg 1995, Gieseg 2001 A). In human macrophages and related cell types, there is higher concentrations of 7,8-NP triphosphate available, driving the flux towards 7,8-NP production. This is achieved by non-specific phosphatases cleave the triphosphate off 7,8-NP triphosphate to produce 7,8-dihydroneopterin (7,8-NP) (**Figure 1.4**). 7,8-NP is readily oxidized by oxidants to produce a series of oxidative products including: neopterin, xanthopterin, dihydroxantopterin as seen in **Figure 1.5**.

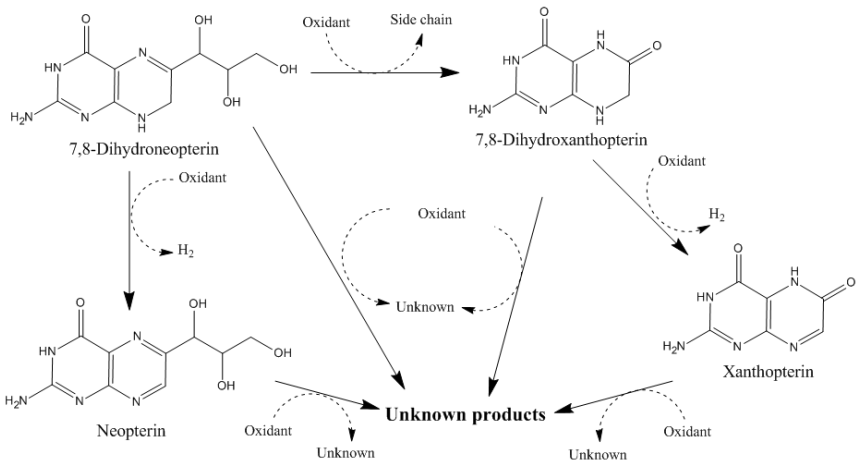


**Figure 1.5 Oxidative mechanisms of 7,8-dihydroneopterin**
Breakdown products are depicted as 7,8-NP reacting with an oxidant into neopterin, 7,8-dihydroxanthopterin and xanthopterin that can oxidize further into an unknown product. Diagram was taken from Parker (2015) and permission was received.

In *in vitro* studies, 7,8-NP is oxidized to a highly fluorescent product called neopterin and is utilized as a clinical marker for immune cell activation. Patients suffering from cardiovascular disease have been shown to have significantly elevated levels of neopterin in their plasma (Schumacher 1992) and in their atherosclerotic plaques (Schumacher 1997, Gieseg 2008). During inflammation, macrophages are stimulated by a pro-inflammatory cytokine, interferon gamma (γ-INF) derived from activated T-cells. This stimulant up regulates GCH-I and induces the breakdown of GTP to produce large quantities of 7,8-NP. (Werner-Felmayer 1990, Andert 1992, Fuchs 2009).

### 1.5.2 Antioxidant properties of 7,8-dihydroneopterin on cell viability

As explained above, primate macrophages lack the enzyme required to produce tetrahydrobiopterin causing the flux of intracellular 7,8-dihydroneopterin to increase and leak into the extracellular environment. The exact reason for this is currently unknown although γ-INF (a pro-inflammatory cytokine) up regulates the production of 7,8-NP which suggests that 7,8-NP role is to protect the human macrophage from oxidative stress environments (Andert 1992, Gieseg 1995, Gieseg 2001 A). 7,8-NP is a potent antioxidant which has been shown in numerous studies to inhibit oxidation of low-density lipoprotein, linoleic acid, lysis of red blood cells and oxidation of tyrosine residues (Gieseg 1995, Gieseg 2001 A). Others studies found 7,8-NP to protect U937 cells from AAPH derived peroxyl radicals (Baird 2005) and protect against the secondary protein hydroperoxide formation from copper and AAPH mediated lipid oxidation (Gieseg 2003). Research carried out by our laboratory have shown oxLDL to be extremely toxic to U937 cells after 3 hours, demonstrating a concentration dependent increase of intracellular oxidative stress followed by a loss of GSH and enzymatic activity of GAPDH and aconitase. Addition of 7,8-NP inhibited the intracellular oxidative stress generated within the cell reducing the GSH loss and enzyme inactivation (Baird 2005, Katouah 2015). Incubation of human monocyte derived macrophages (HMDM) with oxLDL and increasing concentrations of 7,8-NP showed a significant concentration dependent increase in cell viability of up to 80% at 200μM 7,8-NP (Gieseg 2010 B). This suggests that 7,8-NP is scavenging the intracellular oxidants produced by oxLDL and protecting the biomolecules within the cell and restoring the cell viability.

## 1.6 Mitochondria

The mitochondrion is a multi-layer structure consisting of the outer mitochondrial membrane (OMM), intermembrane space, inner mitochondrial membrane (IMM) and the matrix (**Figure 1.6**). Its main function is to generate ATP through oxidative phosphorylation within the respiratory chain where the electron transport chain (ETC) is coupled to the production of ATP from ADP (Madamanchi 2005, Yu 2014). The ETC complex consists of 5 smaller complexes: Complex I (NADH-ubiquinone dehydrogenase), Complex II (succinate cytochrome c reductase), Complex III (ubiquinone cytochrome c reductase), Complex IV (cytochrome c oxidase), and

Complex V (ATP synthase) (**Figure 1.6**). NADPH and $FADH_2$ are both produced from the Krebs cycle (previous metabolic process) and NADPH transfers electrons onto complex I and $FADH_2$ transfers electrons to complex II. Electrons are then passed to ubiquinol via an electron carrier, coenzyme Q10, which passes the electrons on to complex III. Cytochrome c accepts the electrons and passes them on to complex IV, which transfers the electrons on to molecular oxygen, forming water. Whilst electrons are being passed along the complexes, complex I, III and IV are establishing an electrochemical gradient by passing hydrogen ions from the matrix, through the inner membrane, into the inner membrane space. Complex V (ATP synthase) utilizes this hydrogen electrochemical gradient to cross the inner membrane space to get back to the matrix with the synthesis of ATP from ADP and an inorganic phosphate. The hydrogen re-entry moves through complex V, generating the movement of the complex to synthesize ATP (**Figure 1.6**) (Madamanchi 2007). As a result, energy production produces oxidants as a byproduct from the movement of electrons through the complexes onto oxygen molecules (Liu 2002). Complex I and III have been considered to be the primary sites for electron leakage to generate oxidants, contributing up to 4% of molecular oxygen consumed by the mitochondria (**Figure 1.6**) (Lenaz 2002, Madamanchi 2007).

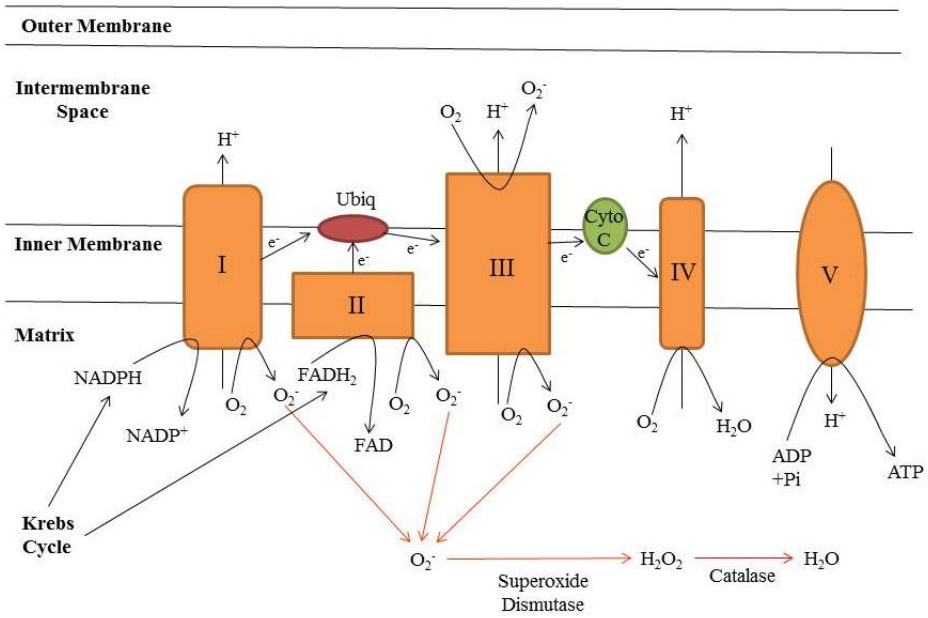


**Figure 1.6 The mitochondrial electron transport chain**

An illustration of the mitochondria electron transport chain, displaying the order of complexes, leakage of electrons onto molecular oxygen and the formation of oxidative products.

Significant literature has suggested that the mitochondria has an intimate relationship in development of atherosclerosis (Ballinger 2005, Madamanchi 2007, Wang 2014). The mitochondria is an essential organelle as it is involved in the energy production and death of the cell. As a result it has been linked as a potential source and primary target of oxidative stress (Murphy 2009). If significant damage has occurred to the mitochondria and is unable to produce ATP, the reverse electron transport phenomenon can occur. The electrons derived from $FADH_2$ via complex II can reversely flow back to complex I and has the potential to generate oxygen radicals (Liu 2002, Han 2003). Superoxide that is generated in the mitochondrial matrix is converted into hydrogen peroxide by superoxide dismutase (SOD), which then can be converted into water by glutathione peroxidase (**Figure 1.6**). Transition metals are capable of reducing hydrogen peroxide into hydroxyl radicals via the Fenton reaction (Mao 1993, Turrens 2003, Madamanchi 2007). Superoxide has the potential to react with nitric oxide (NO) to produce peroxynitrite, which can inactivate enzymes, oxidize DNA and cause mitochondria dysfunction (Ballinger 2000, Turrens 2003). All of oxidants produced are able to react with biomolecules present within the mitochondria, contributing to the oxidative damage and further dysfunction of the enzymes (Liu 2002, Turrens 2003). There is a lot of speculation of the role the mitochondria has in atherosclerosis. Studies have indicated that the cellular oxidative stress generated from NOX could act as a possible feedback, causing an increased production of radicals from the dysfunction mitochondria (Brandes 2005). In addition, a loss of ATP production through oxidative damage would cause an increase of oxidant production through reverse electron transport from complex I, enhancing the cell-mediated oxidant production (Liu 2002, Hort 2014).

# 1.7 NADPH oxidases (NOX)

## 1.7.1 NOX structure and Activation

NADPH oxidase (NOX) is a membrane-bound complex that is present in phagocytic cells such as neutrophils, macrophages and dendrites. Its primary function is to catalyze the production of superoxide anion radical from the reduction of NADPH and molecular oxygen in the presence of pathogens. Cytochrome *b*558 is a membrane bound heterodimer consisting of two catalytic subunits, $gp91_{phox}$ and $p22_{phox}$ (**Figure 1.7**). Phosphorylation of the $P47_{phox}$ subunit induces the translocation of the cytosolic

components (consist of $p47_{phox}$, $p67_{phox}$ and Rac-GTPase) to the membrane-bound component (Cytochrome *b*558). This allows the transfer of electrons from NADPH to molecular oxygen resulting in the production superoxide anions (**Figure 1.7**) (Vignais 2002, Lardy 2005, Bedard 2007).

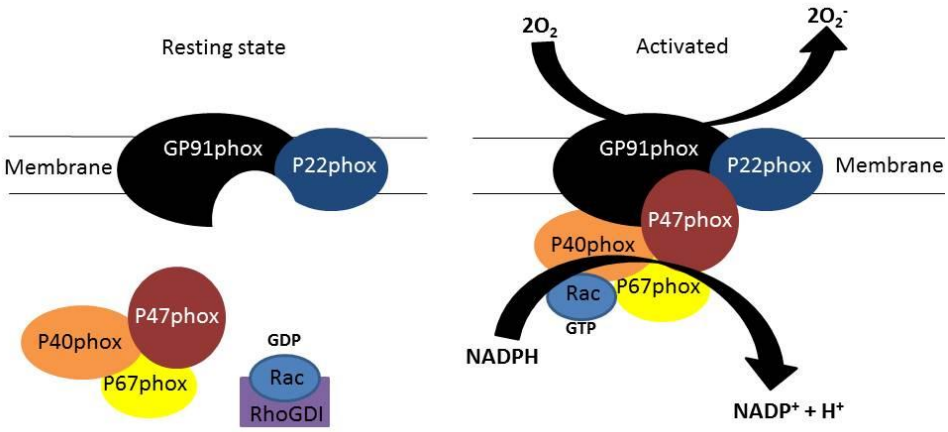


**Figure 1.7 The structural components of NOX-2 at resting and activated states**

Assembly of NADPH oxidase through the translocation of P47phox, P40phox, P67phox and a small GTP protein (Rac) to the membrane bound complex, gp91phox and p22phox. This activates the complex that causes the transfer of electrons from NADPH to molecular oxygen to produce superoxide anions.

Six homologs of neutrophil NOX-2 have been found in non-phagocytic mammalian cells, all displaying conserved regions of NADPH and FAD binding sites. NOX-1, NOX-3 and NOX-4, all have similar structures to NOX-2; while the others have N-terminal extensions, containing two calcium binding EF hands for NOX-5 and have additional peroxidase domains for DUOX 1 & 2 (Bánfi 2001, Bánfi 2003, Lardy 2005). NOX-1 is found mainly in colon epithelium cells and has been proposed to regulate cell growth and participate in cell defence, NOX-4 in kidney cortex and mediates oxygen sensing, or DUOX-1, 2 which is involved in thyroid hormone synthesis (Bánfi 2001, Bánfi 2003, Brandes 2010). NOX-5 is found in lymphoid organs and testis and similar to NOX-2, generates large amounts of superoxide in response to an increase in cytosolic calcium. NOX-1 and 4 generates very little superoxide unless it is stimulated by $P67_{phox}$ and $P47_{phox}$ (Bánfi 2001, Takeya 2003, Bedard 2007). However, NOX-2 is the homolog of interest as it is the only known NOX to be in activated phagocytic cells. Once stimulated, the complex generates large amounts of superoxide anions in response to foreign pathogens (Bellavite 1988, Cross 2004).

### 1.7.2 NOX and its role in atherosclerosis

NOX has been described throughout the literature as the major superoxide generator in phagocytic cells in response to a foreign stimulus. In the past 10 years, the literature is escalating the importance of NOX in inflammatory diseases such as atherosclerosis. OxLDL, the major cytotoxic agent in the progression of atherosclerosis, has been suggested to activate NOX-2 and generate an overproduction of oxidative stress within HMDM and U937 cells (Gieseg 2010 B, Katouah 2015). It was demonstrated in human atherosclerotic plaque, there was an increase of NOX-2 expression, parallel with the atherosclerotic plaque development (Goncharov 2015). Additionally, the NOX-4 expression remained constant through plaque development (Sorescu 2002). However, it was shown in human aortic smooth muscle cells (HASMC) that there was increased NOX-4 protein expression with 7-KC exposure. As NOX-4 predominately generates hydrogen peroxide rather than superoxide, it was shown that 7-KC induced up-regulation of NOX-4 expression, accompanied with higher intracellular hydrogen peroxide levels (He 2013). It is currently unclear how oxLDL interacts with the NOX complex. Studies have suggested that oxLDL can activate NOX via the CD36 scavenger receptor in smooth muscle cells (SMC) (Sukhanov 2006, Pongnimitprasert 2009). Excessive generation of superoxide in smooth muscle cells caused a significant loss of GAPDH activity, causing the cell to undergo necrosis as it was unable to generate ATP (Morgan 2002). The loss of GAPH activity was prevented by the use of NOX inhibitors (Sukhanov 2006) and 7,8-NP (Katouah 2015). Oxidant production and GAPDH loss has been shown to be prevented by anti-CD36 antibodies in SMCs. This suggests that NOX can be activated through oxLDL binding to CD36 scavenger receptor (Sukhanov 2006).

### 1.7.3 NOX inhibitors

A large number of studies are attempting to elucidate the role NOX has in the oxLDL-induced oxidative stress mechanism by the use of NOX inhibitors. Gp91ds-tat and apocynin are considered to the most relevant inhibitors for NOX-2 (**Figure 1.8**).

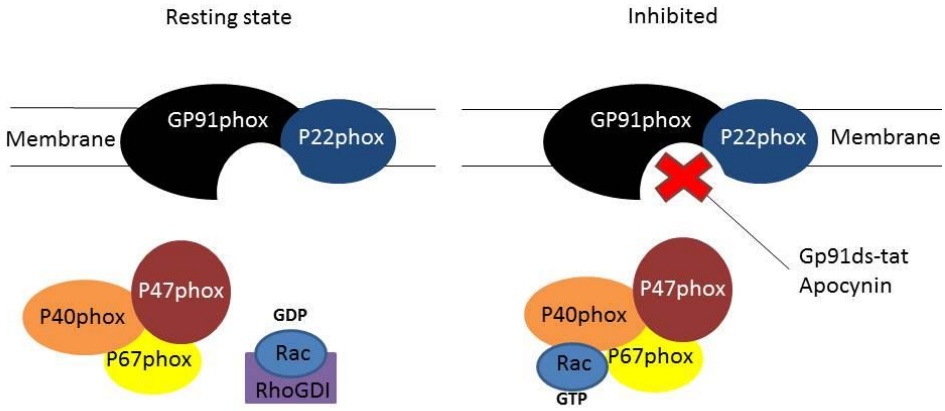


**Figure 1.8 Inhibition of NOX through peptide and non-peptide inhibitors.**

Apocynin and gp91ds-tat inhibitors prevent the translocation of P47phox subunit to the gp91phox subunit, preventing the activation of the complex and subsequent electron transfer.

#### 1.7.3.1 Apocynin

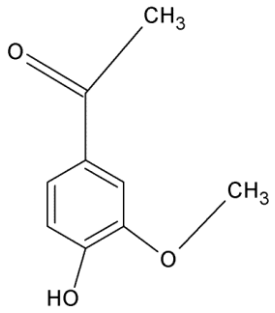


**Figure 1.9 Chemical structure of apocynin**

Apocynin (4,hydroxyl-3methoxy-acetophenone) (**Figure 1.9**) is originally isolated from Picroria *kurroa* plant and has been greatly studied for its role as a potent inhibitor of superoxide generation in activated neutrophils and vascular smooth muscle cells (VSMC) (Stolk 1994, Van den Worm 2001, Williams 2007). The exact mechanism of how apocynin inhibits NOX is currently unclear but it is thought to prevent the assembly of NOX by interfering with the translocation of $P47_{phox}$ to the membrane bound component seen in **Figure 1.8**) (Williams 2007, Kanegae 2010).

Apocynin is a pro-drug that needs to be activated or oxidized before it is a potent inhibitor of NOX. Apocynin is oxidized in the presence of myeloperoxidase (MPO) and hydrogen peroxide, which is abundant in phagocytic cells (neutrophils). The active metabolite forms dimers and trimer derivatives resulting in diapocynin formation. Diapocynin is then thought to react with thiol groups that are essential in the assembly of NOX, preventing the translocation of $P47_{phox}$ and $gp91_{phox}$ (Stolk 1994, Touyz 2008). These properties indicate that apocynin is only activated at sites of inflammation (Stolk 1994). Convincing data from *in vitro* studies show that activated apocynin produced from phagocytic cells can effectively reduce superoxide production in endothelial cells, vascular smooth muscle cells, and adventitial fibroblasts through inhibition of NOX complex (Stolk 1994, Van den Worm 2001, Touyz 2008, Kanegae 2010). All of the previous *in vitro* studies demonstrated that apocynin effectively inhibited NOX complex, thus inhibiting superoxide generation, although research performed by Heumueller et al (2008) highlighted that phagocytic cells and non-phagocytic cells have different apocynin mechanisms. Non-phagocytic cells (HEK293 cells) do not possess MPO, therefore activated apocynin cannot be formed and cannot inhibit NOX activation or superoxide generation. However, they demonstrated that apocynin can act as an antioxidant by scavenging radicals formed, especially hydrogen peroxide (Lapperre 1999, Heumüller 2008, Touyz 2008) Apocynin has also been shown to act as an antioxidant by enhancing intracellular glutathione synthesis through increasing the activity of gamma-glutamylcysteine synthase in A549 cells by activating the transcription factor AP-1, however, an over production of GSH can cause the cell to go into reductive stress (Lapperre 1999).

Similar results were observed in U937 cells, as apocynin reduced the intracellular oxidative stress induced from oxLDL but caused a subsequent increase of intracellular glutathione and providing little cell viability protection. This indicated that the U937 cells were undergoing reductive stress as a result of apocynin (Katouah 2015).

### 1.7.3.2 Gp91ds-*tat*

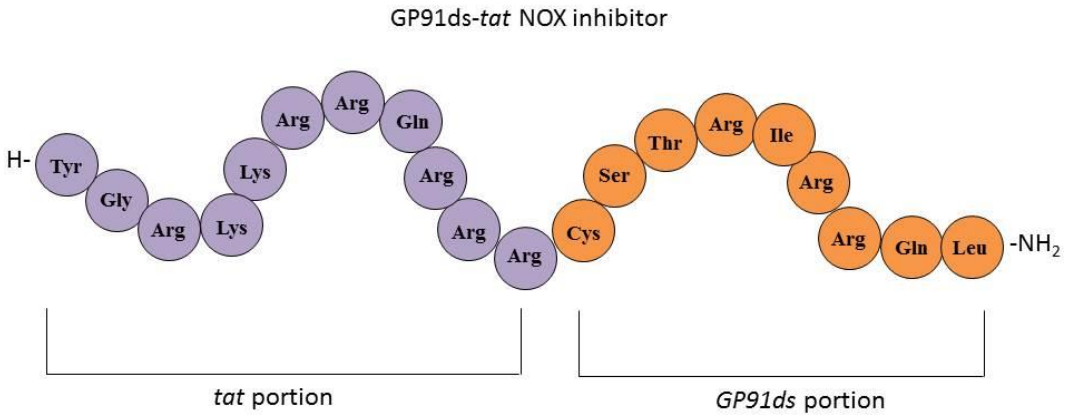


**Figure 1.10 Structure of gp91ds-tat NOX inhibitor**

Gp91ds-*tat* ($gp91_{phox}$ docking sequence – *Trans-Activator of Transcription*) has an inhibitory effect on NADPH Oxidase by preventing the assembly of the $gp91_{phox}$ with $P47_{phox}$, therefore stopping the transfer of electrons from NADPH to oxygen to produce superoxide (**Figure 1.8**). The peptide sequence specifically binds to $P47_{phox}$, mimicking the region of $gp91_{phox}$ and preventing the assembly and activation of NOX (Rey 2001, Williams 2007, El-Benna 2010). Rey et al. (2001) identified the gp91phox sequence from a mouse homolog, calling it $gp91_{phox}$ ds and later added the a translocating peptide domain (*tat*) to the end, forming a 20 amino acid long sequence, gp91ds-tat (**Figure 1.10**) (Rey 2001, Williams 2007). When using peptide inhibitors, the main obstacle is getting the peptide across the plasma membrane lipid bilayer in living intact cells to inhibit NOX. This is accomplished by using cell-penetrating peptide (CPP) or protein transduction domains (PTD) attached to the inhibiting protein. *TAT* (Trans-Activator of Transcription) is a CPP domain and is derived from the human immunodeficiency virus (HIV1). This peptide's function is to deliver biomolecules that is naturally impermeable to the cell, across the plasma membrane into the extracellular space to achieve a desired effect (Debaisieux 2012). The gp91ds-*tat* peptide inhibitor has a *tat* CPP domain attached to the end of the peptide to allow bioavailability into the cell to inhibit NOX from generating super oxide anions (**Figure 1.10**) (Rey 2001, El-Benna 2010). Studies have shown gp91ds-tat to be a highly specific competitive inhibitor of NOX so far. Research performed *in vitro* assays indicated that gp91ds-tat inhibited the assembly of NOX, significantly

decreasing oxidase activity and superoxide generation in neutrophils and mouse aorta (Rey 2001). It was shown that in cell free assays, the peptide inhibitor significantly decreased the oxidases activity of up to 80% (Rey 2001). Although gp91ds-tat is effective in reducing superoxide production in animals and cell systems, Rey (2001) states that when administered orally, it has a relatively low bioavailability, limiting the clinical application (Rey 2001). Gp91ds-tat is effective in the NOX homologs that contain the $gp91_{phox}$ and $P47_{phox}$ subunits (NOX1 and NOX2) and unlikely to be effective in homologs that are significantly different (NOX4 and NOX5) (Williams 2007).

# 1.8 Myeloperoxidase (MPO)

## 1.8.1 Biology of MPO

Activated neutrophils are a highly effective defence against foreign microorganisms, as they provide the necessary cytotoxic agents to kill the microbes that invade the human body (Hampton 1998, Prokopowicz 2012). Myeloperoxidase (MPO) is a peroxidase enzyme, which is secreted by activated neutrophils and is released in conjunction with hydrogen peroxide (generated indirectly from NOX complex), for antimicrobial activity. Hydrogen peroxide is generated from the reaction of superoxide anions and hydrogen via superoxide dismutase (**Reaction 1**).

**Reaction 1** $2\ O_2^{\bullet-} + H_2 \rightarrow O_2 + H_2O_2$

**Reaction 2** $H_2O_2 + Cl^- + H^+ \rightarrow HOCl + H_2O$

As hydrogen peroxide is only toxic at high concentrations and NOX generated superoxide does not kill the bacteria directly, MPO generates a potent secondary oxidant (hypochlorite) from hydrogen peroxide and a chloride anion during the respiratory burst (**Reaction 2**) (Hampton 1998, Brennan 2001, Exner 2004, Prokopowicz 2012). Majority of the oxygen consumed from the immune respiratory burst can be accounted in the hydrogen peroxide generated by the dismutation of superoxide radical (Hampton 1998, Brennan 2001, Davies 2011). The reaction mechanisms of MPO can be seen in **Figure 1.11**. Ferric myeloperoxidase ($MP^{3+}$) reacts with hydrogen peroxide to form the intermediate compound I. This enables compound I to oxidize either a chloride ions to produce hypochlorite and restoring the enzyme back to its $MP^{3+}$ state. Compound I can also oxidize organic substances (RH) involving an electron transfer, converting intermediate compound I into compound II.

When superoxide anions are present, compound II can be recycled back to the native enzyme state ($MP^{3+}$). Poor substrates or if superoxide is not present then the MPO enzyme is trapped as the compound II intermediate, inhibiting the hypochlorite production. Superoxide can convert the native state into compound III which further reacts with superoxide to compound I which may oxidize chloride ions or react with organic substrates (Hampton 1998, Malle 2007, Davies 2011).

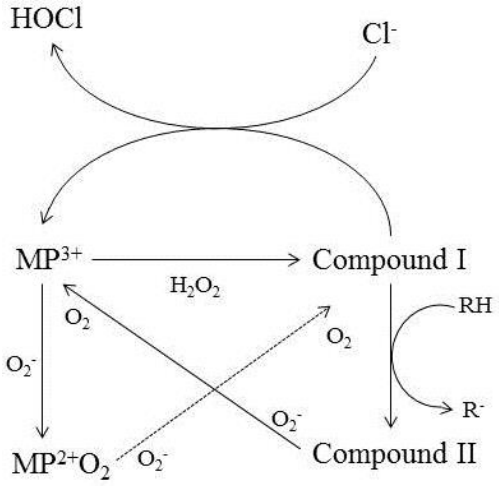


**Figure 1.11 Reaction mechanisms of myeloperoxidase**

The reaction mechanism shows the enzymatic intermediates of the enzyme myeloperoxidase, utilizing hydrogen peroxide and chloride ions to produce hypochlorite. Illustration adapted from Hampton (1998).

## 1.8.2 Role of MPO in Atherosclerosis

Hypochlorite (HOCl), is a strong oxidizing agent that primarily attacks the ApoB100 on the LDL particle, forming protein chloramines and leading to the atherogenic effects seen in cardiovascular disease (Brennan 2001, Yang 2012 A). High concentrations of HOCl kills human monocyte derived macrophages by oxidizing and causing a necrotic cell death (Yang 2012 A). It has been previously observed that hypochlorite can oxidize 7,8-NP with high efficiency, generating large quantities of neopterin (Widner 2000, Gieseg 2001 B, Parker 2015). Additionally, both MPO and its oxidative products have been found within atherosclerotic lesions (Hazen 1997). These findings has led to the theory that hypochlorite forms the basis of neopterin formation during inflammation (Widner 2000). This implies that hypochlorite generated during inflammation may be responsible for the neopterin observed in plasma and urine during immune system activation (Fuchs 1989, Schumacher 1997, Fuchs 2009, Parker 2015).

## 1.8.3 MPO Inhibitors

### 1.8.3.1 ABAH

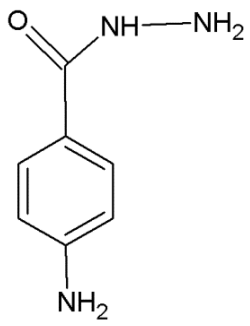


**Figure 1.12 Chemical structure of 4-aminobenzoic acid hydrazide (ABAH)**

ABAH (4-aminobenzoic hydrazide) (**Figure 1.12**) is a potent MPO inhibitor which functions by irreversible inhibition of MPO. Myeloperoxidase oxidizes ABAH to a radical form which in turn reduces the native enzyme into a ferrous intermediate. The ferrous MPO can rapidly react with oxygen to form compound III ($MP^{2+}O_2$) which can lead to turn over to the native enzyme. In the absence of oxygen, the ferrous MPO can react with hydrogen peroxide and it's haem groups were rapidly destroyed, leaving the enzyme irreversibly inactivated (Kettle 1997). ABAH has been studied as a potential inhibitor for MPO to help elucidate the role MPO has in the inflammatory process in cardiovascular disease. It was observed in a study that ABAH irreversibly inhibited hypochlorite production by 90% in stimulated neutrophils treated with phorbol myristate acetate (PMA) (Kettle 1995).

### 1.8.3.2 Thiocyanate

Humans naturally obtain $SCN^-$ through the consumption of plant material and human plasma levels vary between 10 – 140 µM (Xu 2009, Chandler 2012). Thiocyanate ions are important in a biological context for multiple reasons: It can limit harmful accumulations of hydrogen peroxide by an enzymatic reaction with lactoperoxidase (LPO) (**Figure 1.13 Reaction 1**). The enzyme catalyzes the oxidation of $SCN^-$ while consuming hydrogen peroxide, forming $OSCN^-$ which is tissue innocuous or nontoxic to human cells (**Figure 1.13 Reaction 2**), but is an effective antimicrobial agent (Tahboub 2005, Xu 2009, Chandler 2012). Secondly $SCN^-$ has been shown to effectively compete as a substrate against $Cl^-$ ions for myeloperoxidase, reducing the production of hypochlorite (Xu 2009). Thiocyanate can also rapidly reduce hypochlorite, producing $OSCN^-$ and leaving $Cl^-$ ions as a product, without the

requirement of catalysis (**Figure 1.13 Reaction 3**). Previous research from Xu (2009) showed that LPO catalyzed the oxidation of thiocyanate ions, protecting a human lung endothelial cell line by reducing the hydrogen peroxide induced damage. The study also showed that MPO has a higher affinity for $SCN^-$ ions than $Cl^-$ ions, producing $OSCN^-$ and suppressing hypochlorite production (van Dalen 1997, Xu 2009).

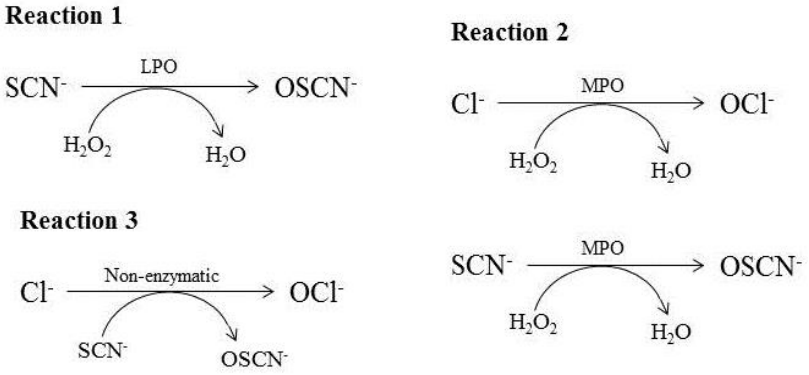


**Figure 1.13 The enzymatic reaction of MPO and the antioxidant properties of SCN- ions**
The illustration shows the antioxidant properties of thiocyanate ions by competing against chloride ions to prevent the formation of hypochlorite. Diagram adapted from Xu (2009).

# 1.9 Objective of research

Cell death is a major event in the progression of the necrotic core and oxLDL has been implicated as the cytotoxic agent (Colles 2001). Previous research has shown oxLDL to increase the oxidative stress inside U937 cells, resulting in a depletion of intracellular glutathione. The oxidative stress inactivates essential metabolic enzymes such as GAPDH and aconitase, causing the death of the cell from metabolism failure (Chen 2012). It is currently unknown the source of intracellular oxidative stress, however, NADPH oxidase (NOX-2), mitochondria and myeloperoxidase are all known sites to produce oxidants.

In this study it is hypothesized that oxLDL can activate the NOX complex and trigger an overproduction of intracellular superoxide, resulting in subsequent cell death. It is thought that NOX is the primary source of intracellular oxidative stress, to validate this hypothesis, *in vitro* research will determine if the oxLDL-induced oxidant generation can be reduced by a NOX specific inhibitor (gp91ds-tat).

Secondly, gp91ds-tat and apocynin will be used in PMA-activated plaque sections to determine if the inhibition of NOX will prevent 7,8-NP oxidation. If the inhibition of NOX reduces the intracellular oxidant production and prevents 7,8-NP oxidation, then it will implicate NOX as the major oxidant producer in both *in vivo* and *in vitro* research. The second part to this thesis will investigate the mitochondria as a potential source of intracellular oxidative stress as a result of oxLDL. Previous research have detected increased mitochondrial superoxide generation in response to oxLDL exposure (Chen 2012).

This study will determine what time frame is oxLDL inducing mitochondrial dysfunction by using a mitochondria specific dye and determine if the mitochondria dysfunction can be saved by a potent antioxidant, 7,8-dihydroneopterin. The timing of mitochondria dysfunction will be compared to the generation of cytosolic oxidative stress to determine if oxLDL is directly damaging the mitochondria or generation of intracellular oxidative stress is damaging the mitochondria.

The third part of this thesis will investigate myeloperoxidase as a potential source of intracellular oxidative stress as a result of oxLDL exposure. The aim of this section is to determine if hypochlorite is causing oxidative extensive damage to cell causing subsequent cell death. This will be validated by the use of two myeloperoxidase inhibitors (thiocyanate ions and ABAH) to determine if hypochlorite is causing U937 cell death as a result of oxLDL exposure.

This research will aid in the understanding of the mechanism of the oxLDL induced oxidative stress and determine if the inhibition of oxidative stress will restore the U937 cell viability.

# 2. MATERIALS & METHODS

## 2.1 Reagents, media and buffers

### 2.1.1 Reagents

All reagents were of analytical grade. All solutions were prepared with deionized water purified with a Milli-Q ultrafiltration system (Millipore, Massachusetts, USA). This water is referred to as Nano-pure water in this thesis.

| | |
|---|---|
| 7,8-Dihydroneopterin (7,8-NP) | Schircks Laboratory, Switzerland |
| 7,8-Dihydroxanthopterin (7,8-DXP) | Schircks Laboratory, Switzerland |
| Acetic acid (glacial) | Scharlau Chemie S.A., Barcelona, Spain |
| Acetonitrile (ACN) | J.T. Baker, NJ, USA |
| Ammonium phosphate dibasic ($AmPO_4$) | Sigma-Aldrich Co. LLC, New Zealand |
| Apocynin | Sigma Chemical Co., Missouri, USA |
| Argon gas | BOC Gases, Auckland, New Zealand |
| Bovine serum albumin (BSA) | Sigma-Aldrich Co. LLC, New Zealand |
| Chelex®100 resin | Bio-Rad Laboratories, California, USA |
| Cholesterol reagent | Roche Diagonostics, USA |
| Copper Chloride ($CuCl_2$) | Sigma Chemical Co., Missouri, USA |
| Ethylene-diamine-tetra-acetic acid (EDTA) | Sigma-Aldrich Co. LLC, New Zealand |
| Dihydroethidium | Invitrogen., Oregon, USA |
| Dimethyl suoxide (DMSO) | BDH Lab Supplies Ltd, Poole, England |
| Ethanol | BDH Lab Supplies Ltd, Poole, England |
| Flow Cytometry chemicals | BD Accuri Cytometers, Ann Arbor, MI, USA. |
| Hydrochloric acid (HCl) | BDH Lab Supplies, Poole, England |
| JC-1 | Invitrogen, Oregon, USA |
| Methanol | Merck, Darmstadt, Germany |
| Nitrogen gas | BOC Gases, Auckland, New Zealand |
| Neopterin | Schircks Laboratory, Switzerland |
| Phorbol 12-myristate 12-acetate | Sigma Chemical Co., Missouri, USA |
| Phosphoric acid | Sigma-Aldrich Co. LLC, New Zealand |
| Potassium chloride (KCl) | Merck, Darmstadt, Germany |
| Propidium iodide (PI) | Invitrogen., Oregon, USA |
| Sodium chloride (NaCl) | BDH Lab Supplies Ltd, Poole, England |

| | |
|---|---|
| Sodium dihydrogen orthophosphate | Merck, Darmstadt, Germany |
| Sodium hydroxide (NaOH) | Merck, Darmstadt, Germany |
| Sodium Thiocyanate (NaSCN) | Sigma-Aldrich Co. LLC, New Zealand |
| Tetramethylrhodamine, methyl ester (TMRM) | Invitrogen., Oregon, USA |
| Triton X100 | Sigma-Aldrich Co. LLC, New Zealand |
| Trypan blue solution (0.4%) | Sigma-Aldrich Co. LLC, New Zealand |
| Tween-20 | Sigma-Aldrich Co. LLC, New Zealand |

## 2.1.2 Media

| | |
|---|---|
| Penicillin/Streptomycin solution, 1000 U of Penicillin G & 1000 µg of Streptomycin/mL | Invitrogen, Life Technologies, New Zealand |
| Roswell Park Memorial Institute 1640: | |
| - RPMI 1640 media, with phenol red | Sigma-Aldrich Co. LLC, New Zealand |
| - RPMI 1640 media, without phenol red | Sigma-Aldrich Co. LLC, New Zealand |

## 2.1.3 General solutions and buffers

### A) Roswell Park Memorial Institute 1640 (RPMI 1640)

RPMI1640 with and without phenol red powder was supplied by Sigma- Aldrich Co. LLC, New Zealand. The media was prepared according to the manufacturer's instructions. Schott bottles were acid washed by adding 50mL of 65% nitric acid and rinsed 3 times with distilled water and autoclaved for 15minutes at 121°C and 15 psi. The media was prepared by dissolving the RPMI1640 powder in nano-pure water, followed by the addition of sodium bicarbonate (2g/L). The pH was adjusted to 7.2 – 7.4 by 37% fuming hydrochloric acid or 10M sodium hydroxide. The media was filter-sterilized through a 0.22µm membrane MillexR-GP filter/ a 0.20µm Sartolab®-P20 filter (Sartorius AG, Goettingen, Germany) using a pump (CP-600, Life Technologies) into sterilized 500mL bottles.

### B) Phosphate buffered saline (PBS)

PBS solution contained 150mM sodium chloride (NaCl) and 10mM sodium dihydrogen orthophosphate ($NaH_2PO_4$) at pH 7.4. The solution was prepared by mixing 50 mL of 3M NaCl, 40mL of 250 mM $NaH_2PO_4$, pH 7.4 and 910 mL of nano-pure water. PBS that is required for sterile cell culture experiments was vacuum filtered through a 0.45 µm membrane (Phenomenex).

## C) Ammonium dihydrogen phosphate ($AmPO_4$)

A 20mM $AmPO_4$ solution for HPLC was prepared by weighing 2.64g of powder and added to 900 ml of nano-pure water while magnetic stirring. The pH was then adjusted to 2.5 using concentrated orthophosphoric acid and made up to 1 litre. The solution was then filtered through a 0.45μm membrane (Phenomenex) into a 1-litre schott bottle under vacuum.

## D) 7,8-Dihydroneopterin solution

A 2mM 7,8-dihydroneopterin (7,8-NP) (Schircks Laboratories, Switzerland) stock solution was prepared in RPMI 1640 media, in a 15mL screw top centrifuge tube (Greiner, Greiner Bio-one, Neuburg, Germany). The solution was sonicated for 10 minutes to dissolved before sterilized through a syringe 0.22μm PES syringe filter (Membrane Solution, USA) if added to cell culture. The 7,8-NP solution was kept on ice at all times and used immediately after preparation.

## E) 50% acetonitrile & 0.5% Triton X100 solution

A 1% triton X100 solution was prepared by weighing out 1 g ($^{W}/_{V}$) in a schott bottle, and dissolved in 99 ml of nano-pure water before sonication to ensure the detergent had dissolved. A 100mL 1:1 ratio of 100% ACN : 1% triton X100 was vortexed briefly and placed on ice before being used.

## F) Propidium Iodide solution

A 1 mg/mL stock solution of propidium iodide (Sigma-Aldrich Co. LLC, New Zealand) dye was prepared in nano-pure water and was kept in a sterilize schott bottle, wrapped in tin foil at 4°C.

## G) D-Neopterin

Neopterin stock solution (100μM) was prepared by dissolving D-neopterin powder (Schircks Laboratories, Switzerland) in AmPO4 pH6 by sonicating. The solution was stored at -20°C in 200μL aliquots.

## H) Apocynin solution

An apocynin stock solution was prepared by dissolving apocynin powder (Sigma-Aldrich) in RPMI 1640 without phenol red to give a concentration of 2mM. The

solution was then filter-sterilized through a 0.22μM PES syringe filter (membrane Solutions, USA) and stored at 4°C.

### I) Sodium Thiocyanate solution

A sodium thiocyanate stock solution was prepared by dissolving sodium thiocyanate powder (Sigma-Aldrich) in RPMI 1640 without phenol red to give a concentration of 2mM. The solution was then filter-sterilized through a 0.22μM PES syringe filter and stored at 4°C.

### J) Phorbol 12-myristate 12-acetate (PMA)

The PMA stock solution was prepared by dissolving PMA powder in DMSO to produce a 5mM solution. 20μL aliquots were pipetted into 1.7mL centrifuge tubes and stored at -20°C.

### K) Acidic Iodide & ascorbic acid

Powdered iodine (2.7g) and potassium iodide (5.4g) were dissolved into 35mL of nano-pure water. Concentrated HCl (4.37mL) was added to make the final volume up to 50mL. The solution contains 5.4% I2 / 10.8% KI in 1M HCl forming triodide ($I_3^-{}_{aq}$) equilibrium. The reaction proceeds via: $I_3^- \leftrightarrow I^-_{(aq)} + I_{2(aq)}$

A 0.6M ascorbic acid solution was prepared by dissolving 1.057g in 10mL of nano-pure water. The solution was prepared fresh each day and wrapped in aluminium tin foil to avoid light exposure as it can oxidize easily.

# 2.2 Methods

## 2.2.1 Cell Culture based research

All cell culture was performed under aseptic conditions in a Class II biological safety cabinet (Clyde-Apex BH 200). All instruments and plasticware were either brought sterilized (Greiner, Greiner Bio-one, Neuburg, Germany) or been sterilized by autoclaving (15 min, 121°C, 15 psi). All media and solutions added to cells were sterilized by autoclaving or by filtration through a 0.22μm membrane filter (Membrane Solutions, USA). The cells were kept at 37°C in a humidified atmosphere calibrated to 5% carbon dioxide: 95% air (Sunnyo Electric Co. Ltd, Japan). All items were sprayed with 70% ($^v/_v$) ethanol (diluted in distilled water) before being placed in

the Class II cabinet. Viable cells stained with trypan blue (1 part stain to 1 part cell solution) and counted on a haemocytometer slide using a light microscope.

### 2.2.1.1 Cell Culture media

Penicillin G (100units/mL), streptomycin (100μg/mL) and 5% ($^{v}/_{v}$) foetal bovine serum (FBS) were combined with RPMI-1640 with glutamine media (with phenol red) for normal cell culture maintenance.

### 2.2.1.2 U937 cell line preparation

The U937 cell line was originally isolated from the pleural fluid of a 37-year old patient with generalized histiocytic lymphoma (Sundstrom and Nilsson, 1976). This cell line was chosen to study atherosclerosis as they adopt the morphology and characteristics of monocytes. The U937 cells used were a gift from the Haematology Research Laboratory at the Christchurch School of Medicine, University of Otago. A cryo-vial of cell culture was removed from liquid nitrogen storage and defrosted in a 37ºC water-bath until almost thawed. The cell suspension was gently poured into a 50mL centrifuge tube containing 20mL RPMI1640 and centrifuged at 1500 rpm for 5minutes to remove the DMSO freezing media. The supernatant was discarded and the cell pellet was resuspended in 10 mL of RPMI 1640 media with FBS and penicillin/streptomycin and transferred to a 25cm$^2$ tissue culture flask at 37°C in a 5% $CO_2$ humidified incubator. The cells were monitored daily and the density was counted via a haemocytometer to ensure the population was maintained between 0.3 – 1.5 x 10$^6$ cells/mL by passaging in Cellstar® 75cm$^2$ tissue culture flasks (Greiner Bio-one) every 2-3 days.

### 2.2.1.3 Cell experiment procedures

The cells experiments were performed using Cellstar® 12 or 24-well suspension culture plates (Greiner Bio-one), which prevent cells from sticking to the plate surface. Before each experiment, viable cells were counted using a haemocytometer, light microscope and the trypan blue exclusion assay to predict the cell density in the flask. The required quantity of cells for the experiment was pelleted by centrifugation at 500g for 5 minutes at room temperature and re-suspended in a calculated amount of RPMI-1640 (with or without phenol red) at 37ºC, to achieve a final concentration of 5 x 10$^5$ cells/mL. Cells were pipetted into wells with any reagent specific to the

experiment, maintaining the cell concentration per mL. Every experiment, unless stated otherwise, was performed in RPMI-1640 without phenol red and FBS to remove background colour interference with fluorescent techniques.

#### 2.2.1.4 Collection of human serum for culture media

Donated blood was kept at room temperature for two hours for clotting to occur. The blood was then kept at 4ºC overnight to settle and to allow the human serum to separate from the clot. The serum was then transferred to 50mL centrifuge tubes using a 20mL syringe. The serum was centrifuged at 1000g for 15 minutes to pellet the red blood cells. The clear serum was then transferred to a new centrifuge tube, avoiding the transfer of any pelleted red blood cells. If the red blood cells were transferred over, the pelleting procedure was repeated. The serum was stored in 20mL aliquots at -80ºC for long-term storage, the aliquots were used up within 6 months.

## 2.2.2 Low-density lipoprotein preparation & oxidation

### 2.2.2.1 Blood collection and plasma preparation

Collection of blood from donors and preparation of LDL from plasma was carried out under ethics approval Ethics Committee (CTY/98/07/069). The blood was collected by venipuncture from consenting healthy donors after an overnight fast. 200 mL of blood was collected from each donor into 50 mL tubes containing 0.5 mL of 100mg/mL ethylene-diamine-tetra-acetic acid (EDTA). The tubes were centrifuged for 20 minutes at 4 ºC in a swing-out rotor at 2350 g. Plasma was transferred to 50 mL round bottomed centrifuge tubes and centrifuged for 30 minutes at 11,000 g with slow acceleration/deceleration in a fixed angle rotor to remove any remaining cells. Plasma from all donors (5-6 at a time) was pooled to minimize the inter-individual variation (Gieseg 1994). The plasma was stored in 32 mL aliquots at -80 ºC for a maximum of 6 months.

### 2.2.2.2 LDL purification from pooled plasma

A 32 mL frozen tube of human plasma was left to defrost in running cold water and centrifuged at 47,000 rpm for 10 minutes at 4ºC to pellet any fibrinogen that had formed. The plasma supernatant was emptied into a 50 mL beaker and placed on ice.

11.4g of potassium bromide (KBr) was slowly added to the plasma with gentle stirring with a magnetic flea. The final plasma density was 1.24 g/ml. The plasma was constantly kept on ice under argon gas until ultracentrifugation. Eight mL of 1mg/mL EDTA (pH 7.4) solution was added to 8 x OptiSeal$^{TM}$ polyallomer centrifuge tubes (Beckman Coulter, USA). Using a long luer-fitting needle attached to a 10 ml syringe, 4 ml of KBr-Plasma was placed in the bottom of the centrifuge tubes, underneath the EDTA solution.. The centrifuge tubes were balanced within 1% (0.01g) of each other and transferred to the NVTi-65, Beckman Near Vertical rotor and centrifuged at 60,000 rpm for 2hours at 10ºC with slow acceleration/deceleration in OptimaTM L-90K Preparative Ultracentrifuge (Beckman Coulter Inc, Fullerton, California). After centrifugation, a distinct layer of LDL appears in the density range of 1.019 - 1.063 g/ml. LDL was extracted using a 90º needle attached to a 20 ml syringe. The extracted LDL was pooled into a 15 ml screw top centrifuge tube and flushed with argon gas and kept at 4ºC to prevent oxidation.

### 2.2.2.3 LDL concentration determination and washing

The LDL concentration was determined by measuring the total cholesterol content through an enzymatic reaction. The assay involves incubating 10µL of LDL with 1 mL of cholesterol reagent (CHOL$^{TM}$, Roche Diagnostics, Auckland, New Zealand) at room temperature for 10 minutes. The absorbance was read at 500nm against a blank containing cholesterol reagent. The LDL concentration was calculated from the absorbance, which is based on the estimate that cholesterol accounts for 31.69% of the entire LDL particle by weight and having a molecular weight of 2500 kDa. The LDL concentration value in the present study is the total mass of the apolipoprotein B (protein component of LDL) as 5:1 (Gieseg 1994).

**Calculating the LDL concentration**

Absorbance x 14.9 = [cholesterol] (mM)

[cholesterol] (M) x 386.64 g/mol = [cholesterol] (g/L)

[cholesterol] (g/L) x 100/31.69 = [LDL] (mg/mL)

The LDL was buffer exchanged and concentrated using Amicon® Ultra-15 filter tubes (Millipore, USA). The tubes were prepared by rinsing out with nano-pure water, followed by centrifugation for 2 minutes with PBS to remove excess ethanol from the

tubes. The LDL was split equally between the two tubes, topped up with PBS and centrifuged at 3000 g for 30 minutes at 4ºC (fast acceleration/deceleration). Further centrifugation or addition of PBS was required to adjust the LDL concentration to ~10mg/mL (total mass).

### 2.2.2.4 Dialysis tubing preparation

The dry dialysis tubing (Medical International, UK) with 14.4 mm width and 14,000 Dalton molecular weight cut off were cut into 25 cm sections. The sections were boiled in a beaker with 5% ($^{w}/_{v}$) $NaHCO_3$ and 1mM EDTA for 20 minutes. The sections were washed with nano-pure water and stored in 50% ethanol at 4ºC. Dialysis tubing was prepared by thoroughly rinsing with distilled water, followed by PBS.

### 2.2.2.5 LDL oxidation

Oxidized LDL (oxLDL) was prepared using the method of Gerry (2008). Concentrated LDL at ~10 mg/mL (total mass) was transferred into a section of the washed dialysis tubing. LDL was mixed with 0.5mM copper chloride ($CuCl_2$) and the tubing was knotted on both ends with a 1.7mL centrifuge tube to prevent it from unraveling. The dialysis tubing was placed in a 2L bottle of 37ºC PBS containing 0.5mM $CuCl_2$ final concentration. The final volume of the PBS was adjusted according to the amount of LDL in the dialysis tubing, with 1L of PBS per 10mg of LDL protein. The bottle containing dialysis tubing was placed into an orbital shaker (Bioline, Edwards Instrument Company, Australia) at 37ºC for 24 hours. Incubating the yellow LDL solution with $CuCl_2$ turns the LDL colourless, confirming that the oxidation had taken place. At the end of the incubation time, the dialysis tubing was transferred into 1L of 4ºC PBS containing a teaspoon of washed Chelex-100 resin and a large magnetic flea. The oxLDL was dialysed for 2 hours at 4ºC, constantly stirring to remove the free copper ions in solution. The dialysis tubing was then transferred to a fresh bottle of PBS with chelex-100 and stirred for a further 2 hours. The tubing was then transferred to a third bottle and dialyzed overnight. The dialysed oxLDL was removed out of the dialysis tubing via a mixing cannula and syringe, filter sterilized through a 0.22μM membrane filter in the CII cabinet and stored at 4ºC.

## 2.2.3 Cell viability assays

### 2.2.3.1 Propidium iodide

The viability of U937 cells after treatment was measured using propidium iodide (PI) staining and flow cytometer (BD Accuri$^{TM}$ C6 flow cytometer, BD Biosciences, California, USA). PI intercalates between the DNA bases and fluoresces at an excitation wavelength of 535 nm and emission wavelength of 617 nm. PI is only able to intercalate the DNA of the cell when the cell membrane has been compromised during cell death. PI is used on the flow cytometer to evaluate cell viability and distinguish between necrotic, apoptotic and healthy cells. Analysis was performed using 250µL of the cell suspension incubated with 2µl of 1 mg/mL PI and mixing by gently inverting before incubating for 10 minutes in the dark. A set volume (30µL) was used to assess for cell viability on the flow cytometer using forward scatter (FSC) and the fluorescence filter FL-3 (FL-3). The cellular debris was excluded and the cell viability ratio (PI negative and PI positive cells) was compared with control and treatment samples.

### 2.2.3.2 Trypan blue exclusion assay

Trypan blue is a dye that selectively colours dead cells a distinctive blue by penetrating through the membrane. Viable cells have intact membranes and can actively pump out the dye so they are easily distinguishable from dead cells (Avelar-Freitas 2014). The assay was used to count viable cells in a 50 mL culture flask to assess the cellular density of the suspension. The flask was gently stirred and an aliquot of cell suspension was pipetted out of the flask into a 1.5 mL eppendorf tube. A 1:1 ratio of cell suspension: 0.4% trypan blue stain was added to the eppendorf and gently mixed with a pipette. The tube was left for 2 minutes to allow the dye to penetrate the cell membrane of any dead cells. A haemocytometer (Marienfeld, Germany) was used and a 10µL aliquot of the cell suspension with trypan blue. The ratio of stained and non-stained cells/mL of media was calculated to maintain the required density of cells in the flask otherwise cells were aliquoted from the flask and suspended in fresh media for an experiment.

## 2.2.4 Determination of protein concentration

The total cell lysate protein concentration was determined by using Pierce BCA Protein determination kit (Pierce, Illinosis, USA). This method utilizes the reduction of $Cu^{2+}$ to $Cu^{+}$ by proteins in an alkaline medium. Two molecules of bicinchoninic acid (BCA) chelate one $Cu^{1+}$ ion, to form a purple dye. This chemical complex exhibits a strong absorbance at 562 nm on the spectrophotometer and the formation of purple dye is proportional to the protein concentration. The working reagent was prepared by mixing Reagent A (sodium carbonate, sodium bicarbonate, bicinchoninic acid, and sodium tartrate in 0.1 M sodium hydroxide) and Reagent B (4% hydrated copper sulphate) at a 50:1 ratio.

Cell lysate samples were vortexed and diluted with nano-pure water by a factor of 2 and 50µL of the sample was added to 1 mL of the working reagent. Samples were incubated on a heating block at 60ºC with gentle shaking for 30 minutes. The reaction was stopped by immediately transferring the samples to cold running water before reading the absorbance at 562 nm against a water blank. The protein concentrations were determined from a bovine serum albumin (BSA) standard curve with known concentrations between 0 – 250 µg/ml in 1 ml of the working reagent. The standard curve was analyzed by Prism (GraphPad Software, version 6.0, USA).

## 2.2.5 Mitochondrial potential measurement with JC-1

5',6,6'-tetrachloro-1,1',3,3'-tetraethylbenzimidazolylcarbocyanine iodide, commonly known as JC-1 is a cationic dye which accumulates within the mitochondria membrane and enables quantification of mitochondrial function. Healthy mitochondria exhibit a high mitochondrial potential through red-aggregation of the dye, however, the dye forms green monomers at low membrane potential. Mitochondria that exhibit a strong red fluorescence have a high mitochondrial potential whereas mitochondria that have a high green fluorescence have a low mitochondrial membrane potential. The intensity ratio between red:green fluorescence allows a comparative measurement of membrane potential inside the mitochondria against a particular toxin or uncoupler and determine if the mitochondria is depolarized (Galluzzi 2007).

A regular cell control is compared against a carbonyl cyanide 3-chlorophenylhydrazone (CCCP) control that uncouples the proton gradient, depolarizing the mitochondria to allow standard compensation of the samples.

After an experiment, 1mL of cell suspension were transferred to 1.7 ml centrifuge tube and spun at 500g for 5 minutes at room temperature. The cell pellet was washed once with warm PBS, resuspended in 500µL of RPMI-1640 without phenol red and incubated for 20 minutes with 1 µM JC-1 dye. The cells were pelleted and washed once with warm PBS and run through the flow cytometer for 10,000 viable gated events. Analysis of the results using the flow cytometer recorded the ratio between red fluorescence (FL-2 filter) and green fluorescence (FL-1 filter) to determine the mitochondrial membrane potential.

## 2.2.6 Dihydroethidium (DHE)

Dihydroethidium (DHE) is used to detect intracellular superoxide anions as measure for oxidative stress. The dye functions by reacting with superoxide anions in the cytoplasm resulting in the formation of ethidium ($E^+$) which in turn binds to DNA and fluorescing red (excitation 510nm and emission 605nm). DHE (315.4 g/mol) 1mM stock solutions were prepared in DMSO and 50µL aliquots were pipetted into 1.7mL centrifuge tubes and stored at -20°C. After treatment, 400µL of cell suspension was centrifuged at 1500rpm for 5 minutes. The supernatant was discarded and the cell pellet was resuspended in 200µL of 10µM DHE. After 20-minute incubation, the samples were run through the flow cytometer and analysed using the FL-2 mean fluorescence filter for 10,000 viable gated events.

## 2.2.7 Plaque culture

### 2.2.7.1 Endarterectomy plaque and patient plasma collection

Plaque tissue (**Figure 2.1**) was collected from the Christchurch hospital, from patients undergoing a carotid endarterectomy procedure under the supervision of Prof. Justin Roake. The plaque samples were kept on ice until brought to the Free Radical Biochemistry laboratory. Under sterile conditions, (**section 2.2.1**) the plaque obtained was initially photographed (Canon EOS 76OD with an EFS 60mm f/2.8 macro USM lense) and cut into 2mm sections using a sterile scalpel blade. The plaque sections

were placed into 60 x 15mm polystyrene non-pyrogenic tissue culture dishes (**Figure 2.2**) (Becton Dickinson Labware, Franklin Lakes, NJ, USA) and the weights of the dishes were recorded before and after to determine the weight of the plaque sections alone.

**Figure 2.1 Atherosclerotic plaque excised from carotid endarterectomy**

## 2.2.7.2 Live plaque culture procedure

Under sterile conditions (**Section 2.2.1**), 2mL of RPMI 1640 with phenol red (10% human serum as discussed above in **section 2.2.1.4** and penicillin G (100units/mL), streptomycin (100μg/mL)) was added to each plate. Each dish was labelled according to the order in which the plaque sections were cut from the whole plaque and incubated for 24 hours at 37ºC. After the 24hour incubation, the media was removed using a 1mL pipette then stored in 1.7mL centrifuge tubes at -80 ºC with the appropriate incubation time. Plaque sections were incubated for a total of 96 hours, changing the media every 24 hours and storing the collected samples in the -80ºC for future analysis. After 96 hours, the plaque sections are removed from the dishes using forceps and stored in 1.7mL centrifuge tubes with parafilm around the cap and stored in the -80ºC freezer.

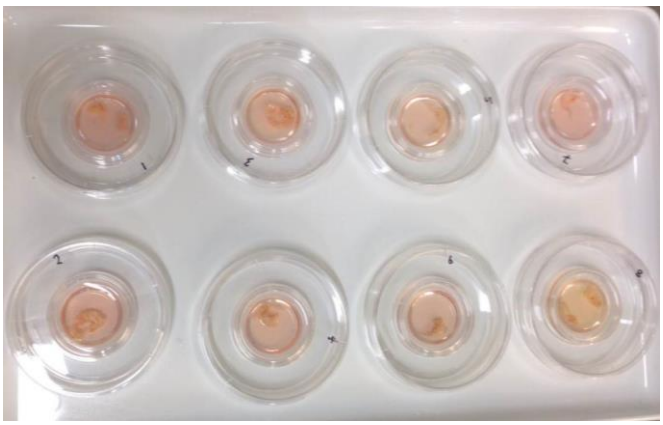

**Figure 2.2 Plaque Sections incubating in their corresponding plates**

### 2.2.7.3 PMA stimulation of live plaque

The plaque sections had been incubated for 24 hours to wash the plaque and remove excess clot. The media was removed and the plaque was incubated for a further 24 hours in media only to determine the baseline production of neopterin. The media was removed and stored in 1.7mL centrifuge tubes at -80 ºC. 20mL of fresh media containing 5μM PMA was aliqouted into the dish (2mL per dish) and incubated for a further 24 hours at 37 ºC. PMA was added 48 hours after the initial wash step and the media was kept and stored at -80ºC for future analysis.

## 2.2.8 Lactate assay

The lactate assay kit from Roche Diagnostics (Indianapolis, Indiana, USA) utilizes the concept of lactate oxidase (LOD), converting the substrate lactic acid into pyruvate and hydrogen peroxide. The peroxidase (POD) then catalyses the reaction of hydrogen peroxide and a hydrogen donor, in the presence of 4-aminoantipyrine (AAP), producing a purple chromogen. The intensity of the purple chromogen is directly proportional to the concentration of lactic acid present within the media. Live cells utilize glucose to produce lactic acid so the concentration of lactic acid in solution gives an indication of the metabolic state of the cells. The kit has two working reagents: Reagent 1 (R1) contains the hydrogen donor, ascorbate oxidase, buffers and preservatives, Reagent 2 (R2) contains AAP, lactate oxidase, horse peroxidase, buffers and preservatives. The assay total volume in this method has been reduced from the standard method volumes to allow for the reaction to take place in a 250μL 96 well plate. Reagent 1 (80uL) was combined with 20uL of sample or standard in a 1.7mL centrifuge tube and vortexed for 5 seconds. 150uL of R1 was

added to 35uL of R2 with 20uL of the diluted sample to give a 205uL total reaction volume. Each sample was run in duplicate and a microplate reader spectrophotometer (660nm absorbance wavelength) was used to analyse each sample.

### 2.2.8.1 Lactate standard curve preparation

The standard curve was prepared by diluting lactic acid with nano-pure water to seven standards between the 0.22 to 15.5mM kit detection limit. These standards were in duplicate using a 96 well plate along with two blanks, one blank with reagent 1 with nano-pure water and the other containing reagent 1 with RPMI and reagent.

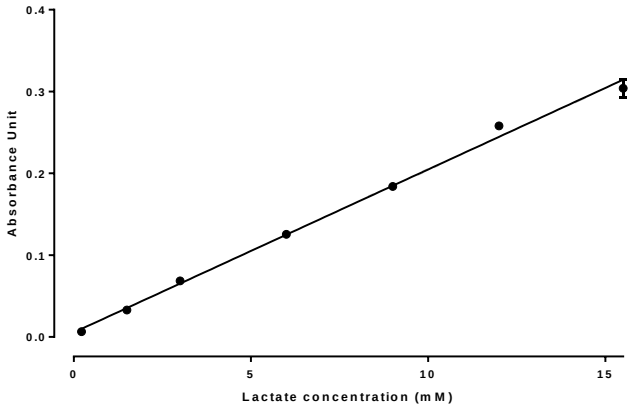


**Figure 2.3 Lactate standard curve**

## 2.2.9 Detection and analysis of pterin compounds

Pterin analysis was conducted by using isocratic cation exchange high performance liquid chromatography (HPLC) with detectors measuring both fluorescence and UV/Vis absorbance at Ex 353/Em 438 nm, and 254 nm respectively (Lindsay 2014). Peak height and were determined by using Shimadzu software Postrun Analysis ™ version 1.22SP1, with peak area only used in analysis. HPLC analysis was conducted using two similar machines from Shimadzu ™ Corporation, Japan.

**Shimadzu SCL 10A** was equipped with a SCL-10A VP controller, RF-10AXL fluorescence detector (xenon lamp), LC-10AD solvent delivery system, SPD-10A UV-Vis detector (deuterium lamp), SIL-10A autoinjector with a CTO-10A column oven and DGU-14A on-line degasser.

**Shimadzu CBM 20A** was equipped with a CBM-20A central bus module, LC-20AD solvent delivery module, SPD-M20A UV-Vis detector (deuterium lamp) detector, RF-

10AXL fluorescence detector (xenon lamp), SIL-20ACHT autoinjector with CTO-20A column oven and DG-20 As degasser

Ammonium phosphate buffer (pH 2.5) (**Section 2.1.3 C**) was run through a cation exchange LUNA $^{TM}$ SCX column (250 mm x 4.6 mm ID, 5µm column, Phenomenex, New Zealand) with 10% ACN as a mobile phase at 35ºC. The required concentration of 10% ACN (HPLC grade 100%) was mixed online at flow rate of 1mL/minute. The column utilizes the concept of cation exchange where the mobile phase passes over the stationary phase that is made up of negatively charged sulphonyl groups, which interact with positively charged molecules in the mobile phase at low pH. As 7,8-dihydroneopterin has little or no natural fluorescence, the pterin assay utilizes the highly fluorescent oxidized form, neopterin.

### 2.2.9.1 Preparation of cell culture samples for pterin assay

After the required cell preparation had been achieved, the cell pellet was washed twice with warm PBS and resuspended in 300µL of 50% acetonitrile/0.5% triton X100. The samples were left for 5 minutes on ice to allow the cells to lysis and centrifuged at 17900 rcf for 5 minutes at 4ºC to pellet the proteins. 100µL of the sample's supernatant was directly used for neopterin analysis while the 50µL of the remaining supernatant was left in the -20ºC freezer for BCA protein assay as mentioned above in **section 2.2.4 protein determination**.

### 2.2.9.2 Preparation of plaque samples for pterin assay

#### Neopterin

A 50:50 ratio of defrosted samples (100µL) and ACN (100µL) were added in to a 1.7mL centrifuge tubes and spun at 20,300g for 10 minutes at 4ºC. 100µL of the supernatant was loaded into HPLC vials and 10µL of this sample was injected into the HPLC for analysis. The same sample was injected twice to eliminate the machine error.

#### Total Neopterin

7,8-NP is oxidized to the fluorescent neopterin using tri-iodide before HPLC analysis of neopterin. 100µL of the defrosted plaque media and cell lysates samples were transferred into to a 1.7mL centrifuge tube followed by 100µL of 100% ACN. The

sample was vortexed for five seconds then centrifuged at 20,300g for 10 minutes at 4ºC. 40µL of acidic iodide solution was added, vortexed for five seconds and left to incubate at room temperature for 15 minutes. After the incubation time, 20µL of 0.6M ascorbic acid was added to reduce the iodine and stop the oxidation. This caused the sample to change from brown to clear. The samples were then centrifuged at 20,300g at 4ºC for 10 minutes before loading 100µL of sample into the HPLC vials. 10µL of the sample was injected into the HPLC for analysis. Each plasma sample was run in two separate duplicates to reduce error.

## 2.2.10 Statistical analysis

The results presented were graphed and statistically analysed by GraphPad Prism version 6.0 for Macintosh (GraphPad Software, San Diego, California, USA).

Significance is confirmed by either, one-way or two-way analysis of variance (ANOVA). Significance levels are indicated as: (*) $p \leq 0.05$, (**) $p \leq 0.01$ and (***) $p \leq 0.001$. Most results that are presented within this thesis are taken from a single experiment, which is representative of three separate experiments. The graphs are presented as the mean and the standard error of the mean (SEM) were calculated from triplicate samples in most cases.

# 3. RESULTS

## 3.1 Toxicity of oxLDL

### 3.1.1 The effect of oxLDL on the cell viability of U937 cells

The research commenced with an investigation of the oxLDL induced toxicity in U937 cells, confirming previous findings that oxLDL can cause significant cell death. The toxicity of oxLDL to U937 cells was investigated by using the technique propidium iodide (PI) staining to determine the ratio of alive cells (PI negative) and cells undergoing necrosis (PI Positive) (**Figure 3.1.1A**). Cells were incubated for 24 hours with increasing concentrations of oxLDL between 0.10mg/mL to 0.60mg/mL and cell viability was measured through PI staining. Results show that the median lethal dose to kill 50% of the cell population ($LD_{50}$) was 0.18 mg/mL (**Figure 3.1.1A**).

Changes in cell morphology after oxLDL treatment was examined through a light microscope (Leitz Wetzlab Germany) (**Figure 3.1.1B**). The U937 cells in the absence of oxLDL showed the typical spherical cell morphology. Cells treated with 0.10 – 0.20 mg/mL oxLDL showed a swelling of the plasma membrane with cellular debris present, signifying prominent cell death. OxLDL at 0.30 – 0.50 mg/mL caused significant cell death, displaying rupturing of the cells membrane and leaving behind remnants of cells.

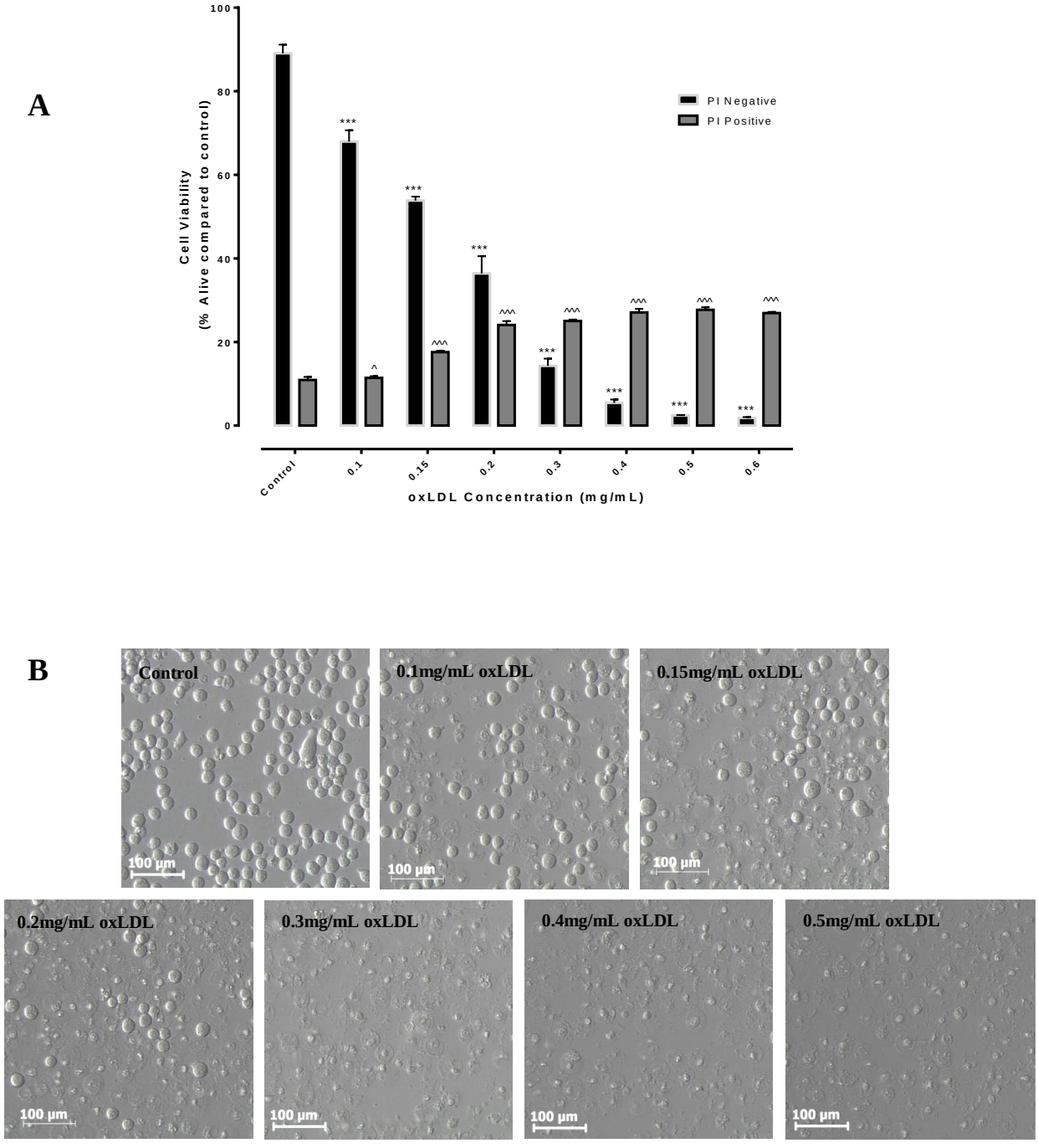


## Figure 3.1.1 Effect of oxLDL on U937 cell viability using the Propidium Iodide.

U937 cells ($0.5x10^6$ cells/mL) were treated with increasing concentrations oxLDL and incubated at 37ºC for 24 hours in non-phenol red RPMI-1640. **A**) Cell viability was measured by PI and the data was expressed as a percentage of the respective control (0mg/mL oxLDL). Results were analyzed by Flow Cytometry under the FL-3 filter. Significance is indicated from the cell only control. Results are displayed as mean ± SEM of triplicates from a single experiment, representative of three separate experiments. Significance levels are indicated as: (*) $p \leq 0.05$, (**) $p \leq 0.01$ and (***) $p \leq 0.001$. **B**) Cells treated with varying concentrations of oxLDL were viewed in tissue culture plates through an inverted microscope (20x magnification) after 24hours. Images were taken using a LEICA DMIL microscope with a LEICIA DFC290 camera.

### 3.1.2 7,8-NP protection against oxLDL toxicity

It has been previously shown by this laboratory that 7,8-dihydroneopterin (7,8-NP), a water-soluble antioxidant, can provide protection to U937 cells against oxLDL toxicity (Gieseg 2001, Baird 2005). This experiment was to confirm the previous findings of 7,8-NP protecting the U937 cells from oxLDL.

U937 cells were incubated with 0 – 200 μM 7,8-NP for 10 minutes before being incubated with oxLDL. The results (**Figure 3.1.2A**) showed that the PI negative cells treated with 200μM 7,8-NP had a significant increase in cell viability of up to 70% compared to cells that had been treated with 0 μM 7,8-NP (oxLDL only control) with a decrease of 45% from the control . The 200μM 7,8-NP treatment provided the most protection to PI negative cells compared to lower concentrations of 7,8-NP treatments. The cell morphology was also examined after 7,8-NP and oxLDL treatment, under the light microscope (**Figure 3.1.2B**). The images show a considerable amount of cellular debris present in the oxLDL only control compared to cell only control. OxLDL treated cells showed an increase in cell count and a reduction in cellular debris with increasing concentrations of 7,8-NP. These results support the hypothesis that 7,8-NP does have a protective, concentration dependent effect on U937 cells treated with oxLDL by scavenging the intracellular oxidants generated by oxLDL.

**A**

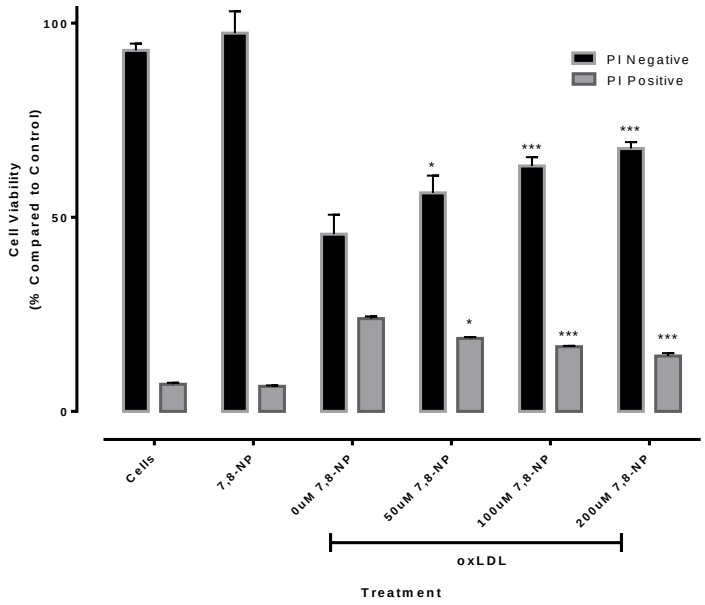


**B**

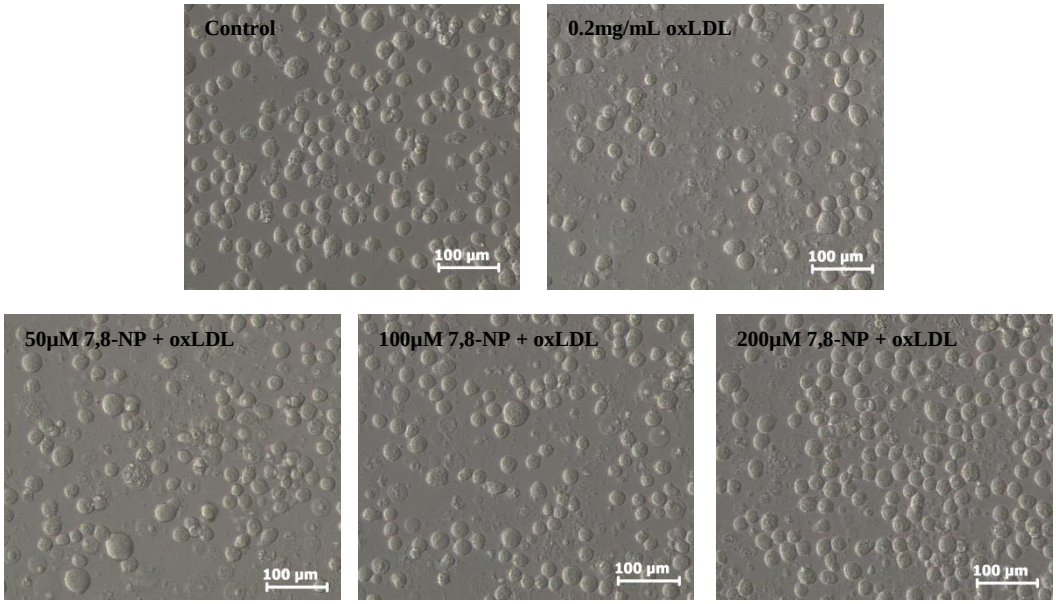


## Figure 3.1.2 Effect of 7,8-dihydroneopterin on oxLDL treated cells

U937 cells ($0.5x10^6$ cells/mL) were treated with increasing concentrations of 7,8-NP and 0.2mg/mL oxLDL and incubated at 37ºC for 24 hours in non-phenol red RPMI-1640. **A**) Cell viability was measured by PI and the data was expressed as a percentage of the respective control (0mg/mL oxLDL). Results were analyzed by Flow Cytometry under the FL-3 filter. Significance is indicated from the oxLDL control. Results are displayed as mean ± SEM of triplicates from a single experiment, representative of three separate experiments. Significance levels are indicated as: (*) $p \leq 0.05$, (**) $p \leq 0.01$ and (***) $p \leq 0.001$. **B**) Cells treated with various concentrations of 7,8-NP + oxLDL were viewed in tissue culture plates through an inverted microscope (20x magnification) after 24hours. Images were taken using a LEICA DMIL microscope with a LEICIA DFC290 camera.

## 3.2 Variability of oxLDL

OxLDL is an extremely potent cytotoxic agent to U937 cells (Katouah 2015). However, there is a large variability in the level of toxicity to U937 cells between different batches prepared. The toxicity of each batch prepared was tested to determine the median lethal dose ($LD_{50}$) and this concentration was used in subsequent experiments. The exact reason for this variability in toxicity is currently unknown, but is not due to varying levels of 7-ketocholesterol (Rutherford 2012).
The variability of oxLDL toxicity to U937 cells was examined by incubating cells with two separate batches of oxLDL for 24 hours. The results are consistent to what was seen in **Section 3.1**. Analysis of **Figure 3.2.1 A & B** show that the standard $LD_{50}$ was between 0.15 – 0.20mg/mL. Problems were encountered with the oxLDL toxicity changing from the predetermined value. An oxLDL batch was prepared and an $LD_{50}$ experiment was conducted, the oxLDL toxicity had decreased the following week (**Figure 3.2.2**). The graph showed the $LD_{50}$ for week 1 to be 0.05mg/mL however, the following week (week 2) the $LD_{50}$ was 0.18mg/mL. This suggests that the unknown cytotoxic agent had decayed over the week when left at 4ºC.

Further research investigated the effect of washing a batch of oxLDL and testing the $LD_{50}$ before and after the wash steps. This was achieved by preparing a fresh batch of oxLDL and using chelexed PBS (pH 7.4) to dilute the oxLDL to 50mL and using filtered centrifuge tubes to separate the PBS and oxLDL. The oxLDL's concentration was retested via the cholesterol assay, followed by a $LD_{50}$ retest. The results (**Figure 3.2.3**) show that before the oxLDL was washed, the $LD_{50}$ was 0.12mg/mL however, after the PBS washing the $LD_{50}$ concentration increased to 0.30mg/mL. This suggests that there are cytotoxic agents present in the oxLDL that can be removed through further PBS wash steps.

The results suggested that in this research, during the oxLDL washing steps, it is essential that good dialysis methods are used to effectively remove the cytotoxic agents that are formed during the oxidation step.

**A**

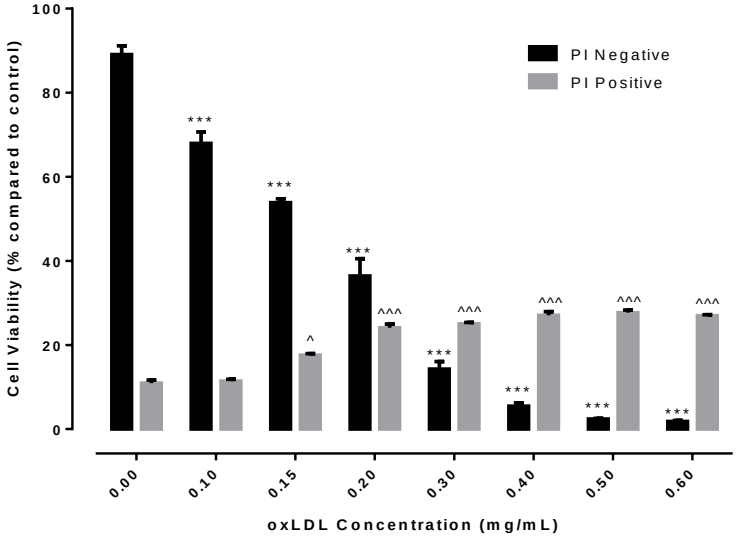


**B**

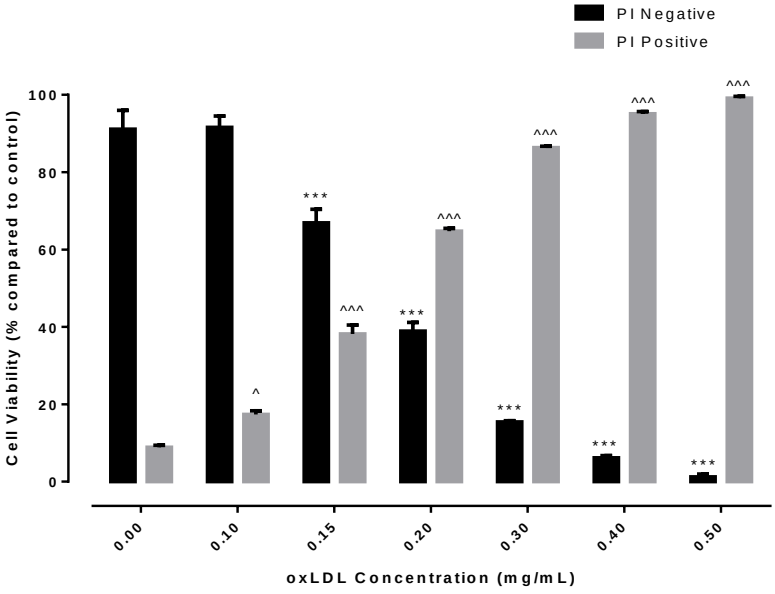


**Figure 3.2.1 Comparison of U937 cell viability between two separate oxLDL preparations**

**A**) OxLDL batch was prepared on 3.3.15 and **B**) a separate oxLDL batch was prepared on 29.9.15. U937 cells ($0.5x10^6$ cells/mL) were treated with increasing concentrations oxLDL from the corresponding batch and incubated at 37ºC for 24 hours in non-phenol red RPMI-1640. Cell viability was measured by PI and the data was expressed as a percentage of the respective control (0mg/mL oxLDL). Results were analyzed by Flow Cytometry under the FL-3 filter. Significance is indicated from the cell only control. Results are displayed as mean ± SEM of triplicates from a single experiment. Significance levels are indicated as: (*) $p \leq 0.05$, (**) $p \leq 0.01$ and (***) $p \leq 0.001$.

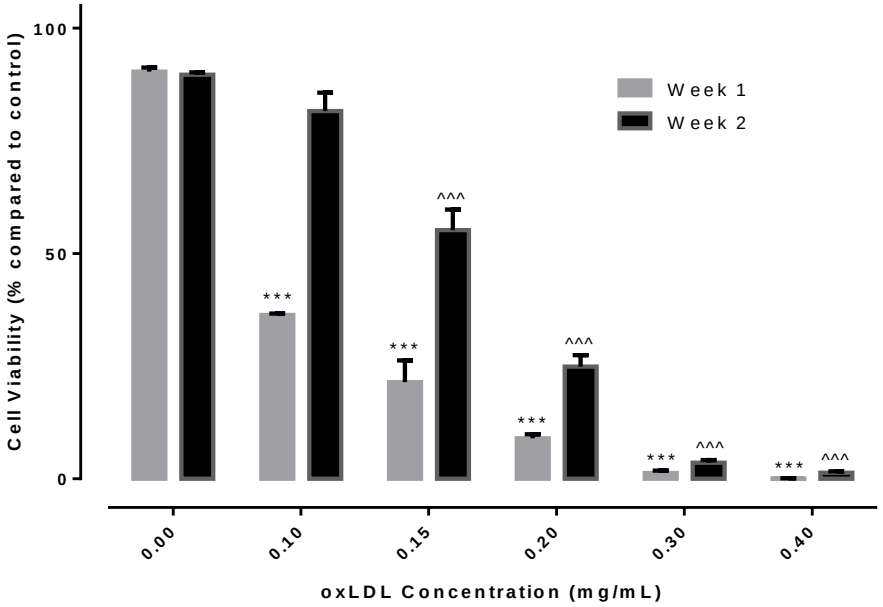


## Figure 3.2.2 Loss of oxLDL toxicity after over time

U937 cells ($0.5x10^6$ cells/mL) were treated with increasing concentrations oxLDL (prepared on 8.9.15) and incubated at 37ºC for 24 hours in non-phenol red RPMI-1640. Cell viability was measured by PI and the data was expressed as a percentage of the respective control (0mg/mL oxLDL). Results were analyzed by Flow Cytometry under the FL-3 filter. Significance is indicated from the cell only control. Results are displayed as mean ± SEM of triplicates from a single experiment Significance levels are indicated as: (*) $p \leq 0.05$, (**) $p \leq 0.01$ and (***) $p \leq 0.001$.

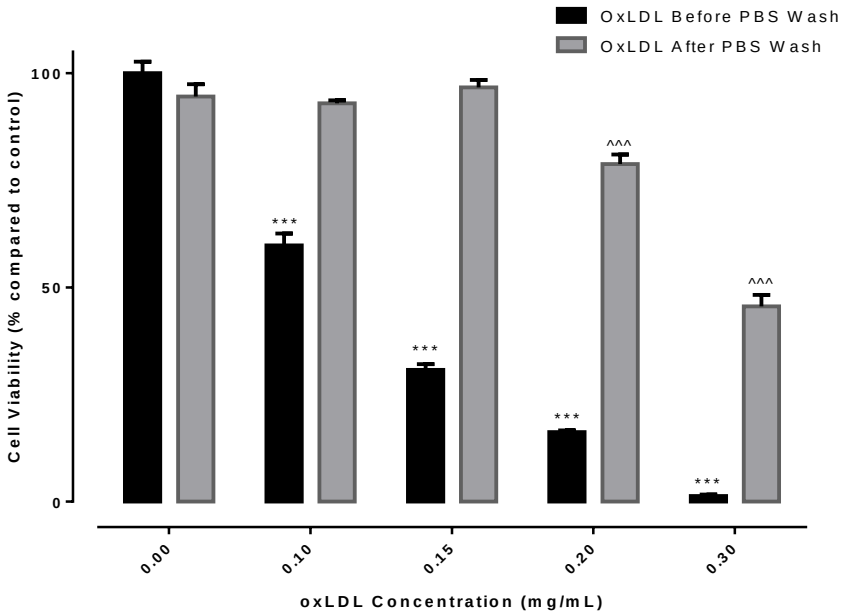


## Figure 3.2.3 Effect of PBS-washed oxLDL on U937 cell viability

U937 cells ($0.5x10^6$ cells/mL) were treated with increasing concentrations oxLDL (prepared on 10.2.16) and incubated at 37ºC for 24 hours in non-phenol red RPMI-1640. Cell viability was measured by PI and the data was expressed as a percentage of the respective control (0mg/mL oxLDL). Results were analyzed by Flow Cytometry under the FL-3 filter. Significance is indicated from the cell only control. Results are displayed as mean ± SEM of triplicates from a single experiment. Significance levels are indicated as: (*) $p \leq 0.05$, (**) $p \leq 0.01$ and (***) $p \leq 0.001$.

## 3.3 Oxidative stress induced by oxLDL

There is a substantial amount of evidence that implicates oxidative stress in the development and progression of atherosclerosis through an overproduction of oxidants generated within the cell (Madamanchi 2005, Goncharov 2015). Previously it has been found that oxLDL induces an over production of superoxide that results in a dramatic loss in glutathione (GSH) and cell viability (Gieseg 2010 B, Katouah 2015). In this section, the oxidative stress induced by oxLDL in U937 cells was investigated by using intracellular superoxide fluorescent probe, dihydroethidium (DHE). Additionally the oxLDL-induced oxidation of intracellular 7,8-NP was investigated through HPLC analysis.

### 3.3.1 The effect of oxLDL on intracellular oxidant production in U937 cells

A time course study was conducted to determine the effect of oxLDL on the intracellular oxidative stress in U937 cells when exposed to sub-lethal concentrations. The cells were treated with a sub lethal 0.20 mg/mL oxLDL followed by probing with DHE at 0, 1, 2, 3, 4 and 6 hours and the mean cellular fluorescence was analyzed via flow cytometry. The cells treated with oxLDL showed a gradual increase in mean cellular fluorescence between 0 – 6 hours, reaching a 50% increase from the 0 hour control (**Figure 3.3.1**). This confirms the finding that oxLDL is inducing a significant increase of intracellular superoxide, which is thought to cause significant damage to the cell resulting in cell death.

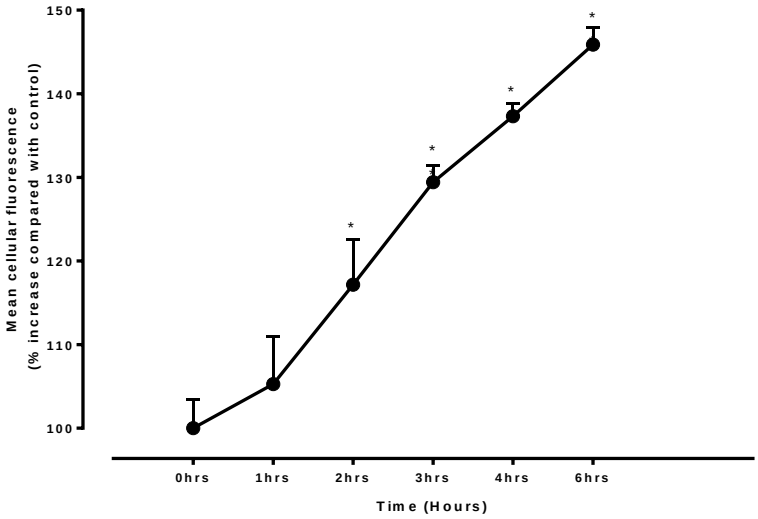


**Figure 3.3.1 Intracellular superoxide production in U937 cells when exposed to oxLDL.**

U937 cells ($0.5x10^6$ cells/mL) were treated with 0.20mg/mL of oxLDL and incubated at 37ºC in non-phenol red RPMI-1640. At various time points, the cells were washed and stained with DHE for 20minutes in the dark to measure the intracellular superoxide production from oxLDL. The cells were measured by Flow Cytometry under the FL2 filter and the data was expressed as a percentage increase of the 0 hour control. Significance is relative to the 0-hour control and results are displayed as mean ± SEM of triplicated from a single experiment, representative of three separate experiments. Significance levels are indicated as: (*) $p \leq 0.05$, (**) $p \leq 0.01$ and (***) $p \leq 0.001$.

As previously discussed in **section 3.1**, 7,8-NP has antioxidant properties that partially protect viable cells from undergoing cell death by scavenging the intracellular oxidants generated by oxLDL.

The hypothesis was further explored by using DHE probing on U937 cells exposed to both oxLDL and 7,8-NP, to confirm if the intracellular superoxide production would be reduced with the presence of 7,8-NP. The results (**Figure 3.3.2)** showed a 70% increase in mean cellular fluorescence of the oxLDL only treatment compared to the cell only control. The treatment with oxLDL and 200µM 7,8-NP showed a 15% increase in mean cellular fluorescence compared to the cell only control. The results show that treatments with 7,8-NP had a significantly lower DHE staining compared to oxLDL. This indicates that 7,8-NP is scavenging the intracellular superoxide anions produced when U937 cells are exposed to oxLDL.

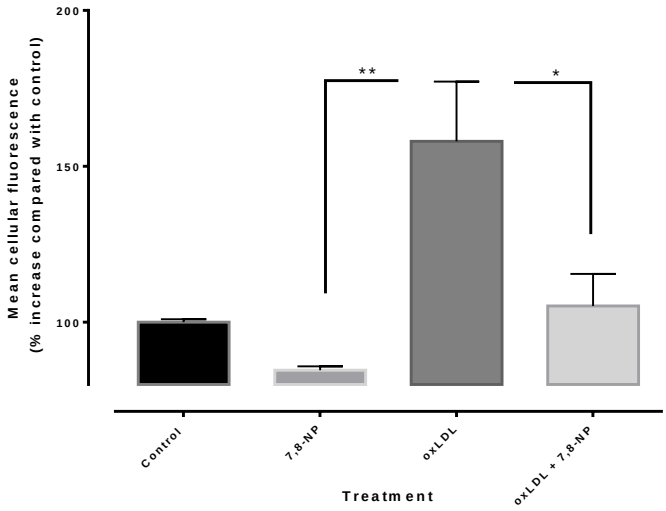


**Figure 3.3.2 Intracellular superoxide production in U937 cells when exposed to oxLDL and 200µM 7,8-NP.**

U937 cells ($0.5x10^6$ cells/mL) were treated with 0.2mg/mL of oxLDL + 200µM 7,8-NP and incubated at 37ºC in non-phenol red RPMI-1640. At the 6 hour time point, the cells were washed and stained with DHE for 20 minutes in the dark to measure the intracellular superoxide production from oxLDL. The cells were measured by Flow Cytometry under the FL2 filter and the data was expressed as a percentage increase of the 0 hour control. Significance is relative to the 0-hour control and results are displayed as mean ± SEM of triplicated from a single experiment, representative of three separate experiments. Significance levels are indicated as: (*) $p \leq 0.05$, (**) $p \leq 0.01$ and (***) $p \leq 0.001$.

Further research investigated the intracellular oxidation of 7,8-NP when U937 cells were incubated with oxLDL. Before this research could take place, appropriate experiments had to be carried out to determine the minimum concentration of triton X100 required for 100% of the cells to lyze and ensure the triton X100 detergent would not affect the neopterin elution time or the peak area. The minimum triton X100 concentration was determined by incubating various concentrations between 0 – 0.5% for 10 minutes then determining the cell viability through light microscope. Cell images (**Figure 3.3.3**) of the triton X100 treatments showed that 0.05% triton X100 was the minimum concentration required to lyze 100% of the viable cells.

Determining the effect of 50% acetonitrile in the injected sample (not the mobile phase) on the neopterin peak area was done by mixing a 100nM neopterin standard with either ammonium dihydrogen phosphate or 50% acetonitrile and injecting them into the HPLC. Ammonium dihydrogen phosphate is the standard media used in pterin analysis on the HPLC (**Section 2.2.6.1**), therefore acts as an effective reference point to determine whether the 50% acetonitrile in the sample was altering the peak area of the neopterin standard. According to **Figure 3.3.4**, there was no significant difference between ammonium dihydrogen phosphate or 50% acetonitrile neopterin peak area, indicating 50% acetonitrile as a suitable cell media for the HPLC.

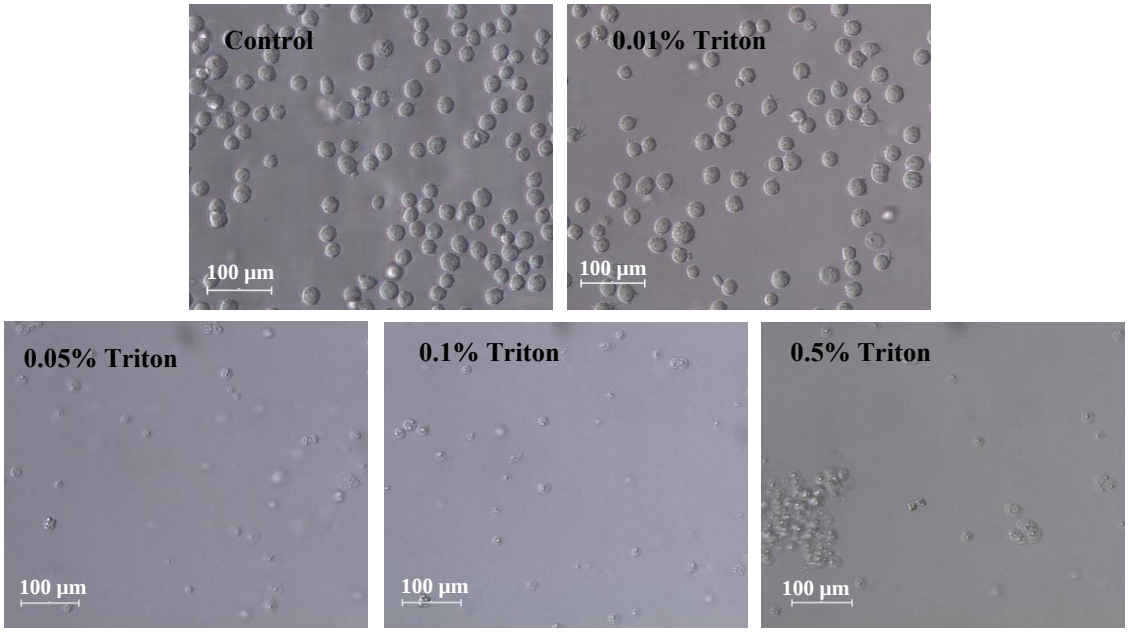


**Figure 3.3.3 Cell images of U937 cells incubating with 0 – 0.5% triton X100.**

U937 cells ($0.5x10^6$ cells/mL) were treated with 0 – 0.5% triton X100 and incubated at 37ºC in non-phenol red RPMI-1640 for 10 minutes. Cells were viewed in tissue culture plates through an inverted microscope (20x magnification). The images were taken using a LEICA DMIL microscope with a LEICIA DFC290 camera.

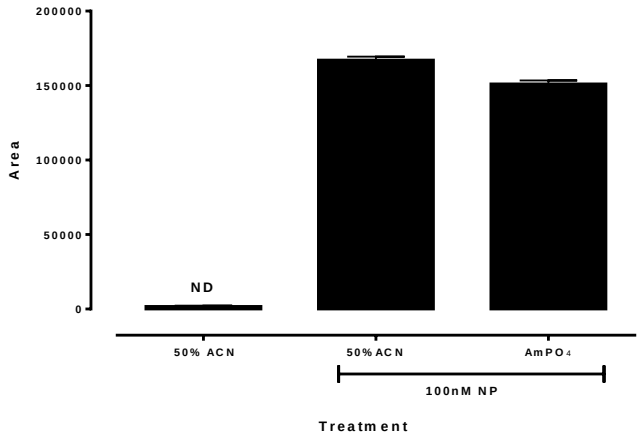


**Figure 3.3.4 Comparison of AmPO4 vs ACN Media on neopterin peak area using HPLC.**

100nM neopterin standard was made up in either 50% acetonitrile or 20mM ammonium phosphate dibasic ($AmPO_4$). Five samples of each treatment were run through the HPLC to determine the effect of the media on the neopterin peak area. Results are displayed as mean ± SEM and ND represents not detected.

The second experiment was to determine if the non-ionic detergent, triton-X100, would affect the neopterin peak area. A 100nM neopterin standard was mixed with 50% acetonitrile or 50% acetonitrile + 0.5% triton X-100. The results showed no notable difference in the elution time of neopterin (**Figure 3.3.5A)** or peak area (**Figure 3.3.5B**) between both treatments. This confirmed that the non-ionic detergent was not interfering with the column side-chains and altering the neopterin elution time or peak area. Therefore 0.5% triton X100 in 50% acetonitrile was used because it effectively lyzed and acetonitrile precipitated the soluble proteins in solution while not altering the neopterin standard's elution time or peak area.

**A**

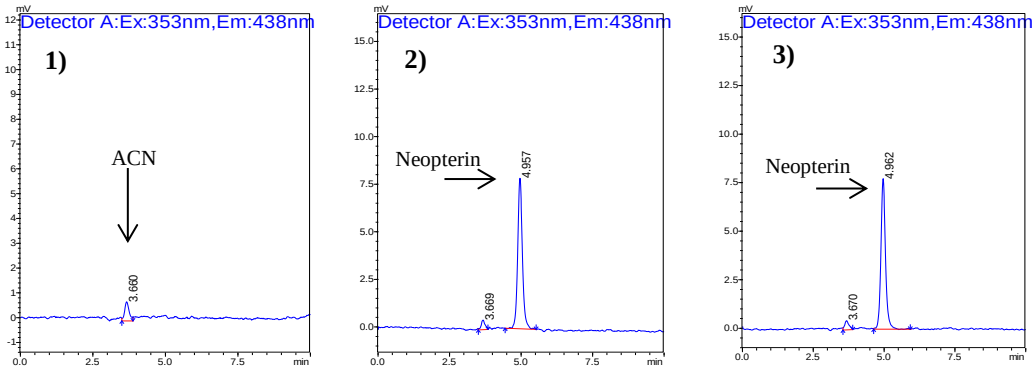


**B**

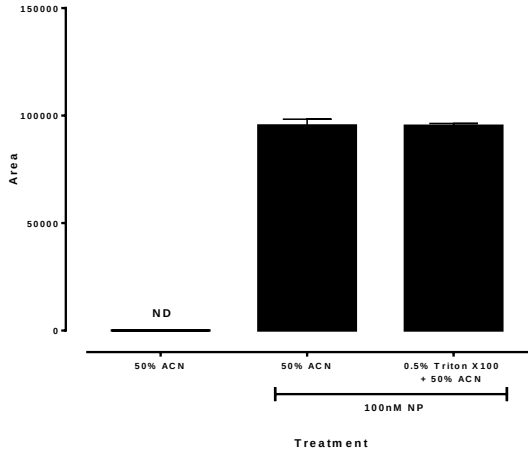


**Figure 3.3.5 The effect of 0.5% Triton-X100 on neopterin peak area using HPLC.**

Fluorescence (Ex 353/Em 438 nm) chromatograms (1, 2 & 3) of 100nM neopterin standards with either **1** (ACN only), **2** (100nM Neopterin + 50% ACN) or **3** (100nM Neopterin + 50% ACN + 0.5% Triton X100). A) Samples were run through the HPLC to determine the effect of triton x100 on the neopterin peak area. B) Results were displayed as mean ± SEM of the peak area which is directly proportional to the concentration. Samples were run in triplicate and ND represents not detected.

7,8-NP protection of U937 cells against oxLDL mediated oxidative stress has been extensively studied in our lab, however, *in vitro* neopterin production has not been investigated. This part of the study focused on measuring the intracellular neopterin produced when U937 cells were exposed to oxLDL. This was done by preloading U937 cells with 7,8-NP for 10 minutes before oxLDL exposure for 0, 1, 3, 6 and 12 hours. The treated cells were incubated with 0.5% triton X-100 and placed on ice for 10 minutes before addition of 50% acetonitrile. The cell lysates were injected into the HPLC for analysis for intracellular neopterin. The cell images were taken at 0 hours (**Figure 3.3.6A)** and after 12 hours exposure **(Figure 3.3.6B**). Prominent cell death was seen after 12 hours of oxLDL exposure, by the disturbance of the plasma membrane and cellular debris. The cells show a swelling of the cell membrane and do not show the typical nuclear condensation characteristic of apoptosis, suggesting the cells were undergoing a necrotic cell death. Analysis of the HPLC fluorescence chromatograms (Ex 353/Em 438 nM) shows a significant increase of intracellular neopterin peak area when cells had been incubated with oxLDL and 7,8-NP (6.7 nmoles/mg cell protein) for 12 hours (**Figure 3.3.7B**) compared to 0hr oxLDL treated cells (1.5 nmoles/mg cell protein) (**Figure 3.3.7A**). The cell lysate samples were run coincide with neopterin standards to ensure that the retention time of 5.4 minutes was neopterin. The third peak with an elution time of 7.1 (**Figure 3.3.7A**) and 6.5 (**Figure 3.3.7B**) is thought to be intracellular 7,8-NP. The results (**Figure 3.3.8**) show that oxLDL treated cells had a significantly higher neopterin production at 6 and 12 hours than the 7,8-NP only treatment. This confirms that oxLDL exposure generates intracellular oxidative stress that facilitates the oxidation of 7,8-NP into neopterin.

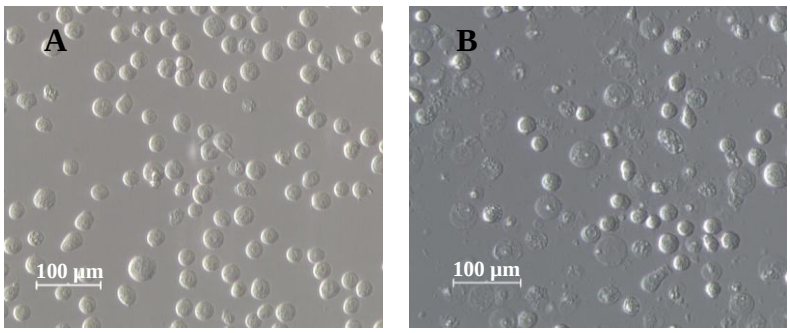


**Figure 3.3.6 Images of U937 cells after 0 and 12 hours of oxLDL treatment**

Images of U937 cells after incubation with 0.2mg/mL oxLDL for 0 hours (**A**) and 12 hours (**B**). The images were taken using a LEICA DMIL microscope with a LEICIA DFC290 camera. The population density is at 500,000 cells per mL. After 12 hours incubation (**B**) there is significant cell death and cellular debris present that is not seen at 0 hour.

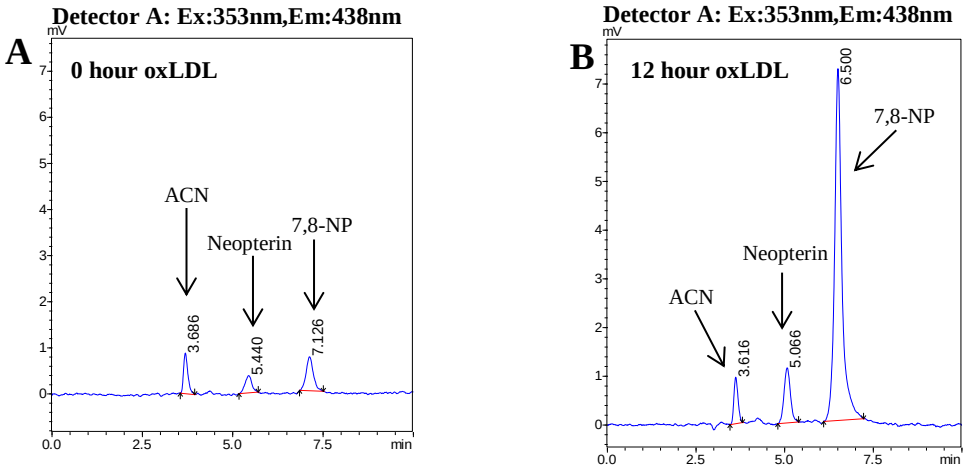


**Figure 3.3.7 Fluorescence chromatograms of intracellular neopterin peak generated from U937 cells with oxLDL for 12 hours.**

Fluorescence (Ex 353/Em 438 nm) chromatograms (**A**, **B**) of intracellular neopterin from U937 cells, preincubated with 200µM 7,8-NP before the addition of 0.2mg/mL oxLDL for 0 – 12 hours. **B** neopterin peak increases significantly compared to **A**, indicating that oxLDL is causing neopterin formation.

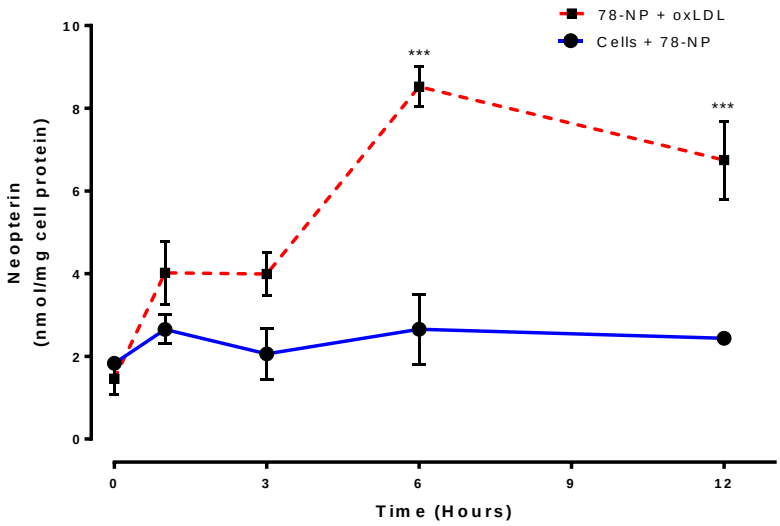


**Figure 3.3.8 Intracellular neopterin production in U937 cells incubated with 7,8-NP and exposed to 0.20mg/mL oxLDL.**

U937 cells ($500x10^3$ cells $mL^{-1}$) in RPMI were incubated with 200µM 7,8-NP, followed by addition (dotted line) or absence (filled line) of 0.2mg/mL oxLDL. Cell lysates were collected at indicated times and analyzed for intracellular neopterin via HPLC. Protein was determined via BCA assay. Results are displayed as mean ± SEM in triplicate and significance is indicated from the 7,8-NP baseline (filled line) from the corresponding time point. Significance levels are indicated as: (*) $p \leq 0.05$, (**) $p \leq 0.01$ and (***) $p \leq 0.001$.

NOX is thought to play a significant role in the production of intracellular oxidants when cells are exposed to oxLDL, apocynin was utilized as a tool to reduce the intracellular oxidation of 7,8-NP, through inhibition of NOX. This experiment was following on from the previous results of observing oxLDL-induced 7,8-NP oxidation. This was achieved by preincubating U937 cells with 200µM 7,8-NP and 20µM apocynin for 10 minutes before the addition of 0.20mg/mL oxLDL and incubated for 0, 1, 3, 6 and 12 hours. The treated cells were incubated with 0.5% triton X-100 and placed on ice for 10 minutes before addition of 50% acetonitrile. The cell lysates were injected into the HPLC for analysis for intracellular neopterin. The neopterin produced by the cell lysates were standardized via flow cytometry, to determine the amount of cells in each sample and to compensate for cell death or growth during the 12 hour incubation. The flow cytometry method was used in this experiment instead of the BCA protein assay due to the convenience and reduced the time taken for sample preparation.

Analysis of the HPLC fluorescence chromatograms (Ex 353/Em 438 nM) showed the significant increase of neopterin production in the oxLDL 12 hour treatment of 13.8 pmoles/500,000 cells (**Figure 3.3.9B**) compared to the control 12 hour treatment of 8.0 pmoles/500,000 cells (**Figure 3.3.9A**). Interestingly, the oxLDL + apocynin 12 hour treatment showed a decrease in neopterin production to 7.6 pmoles/500,000 cells (**Figure 3.3.9C**).

The results from **Figure 3.3.10** show a significant increase of intracellular neopterin in the oxLDL + 7,8-NP (red dotted line) treatment after 1 and 3 hours although the neopterin started to decrease after 6 hours and then plateaued at 12 hours. The oxLDL treatment showed a significant increase of intracellular neopterin compared to the 7,8-NP control (blue solid line). This confirms that oxLDL induces significant intracellular oxidative stress compared to basal level (**Figure 3.3.10)**. The oxLDL + 7,8-NP + apocynin (green dotted line) showed a significant decrease of intracellular neopterin after 6-12 hours. This suggests that the apocynin requires an incubation period to prevent the NOX complex assembly, thus reducing the 7,8-NP oxidation.

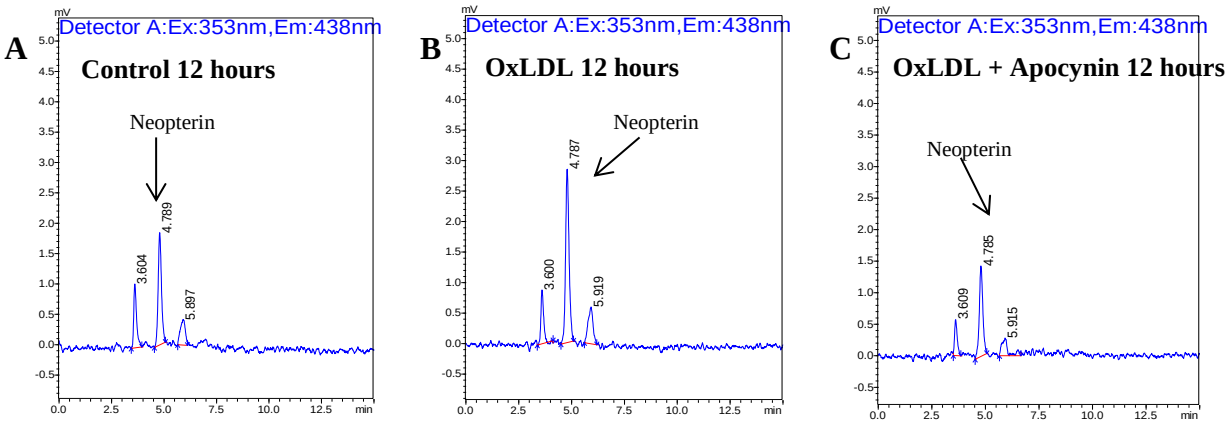


**Figure 3.3.9 Fluorescence chromatograms of intracellular neopterin peak generated from U937 cells with oxLDL and apocynin for 12 hours.**

Fluorescence (Ex 353/Em 438 nm) chromatograms (A, B and C) of intracellular neopterin from U937 cells, preincubated with 200µM 7,8-NP before the addition of 0.20mg/mL oxLDL or 20µM apocynin for 0 – 12 hours. B neopterin peak increases significantly compared to A and C, indicating that apocynin is preventing the formation of neopterin.

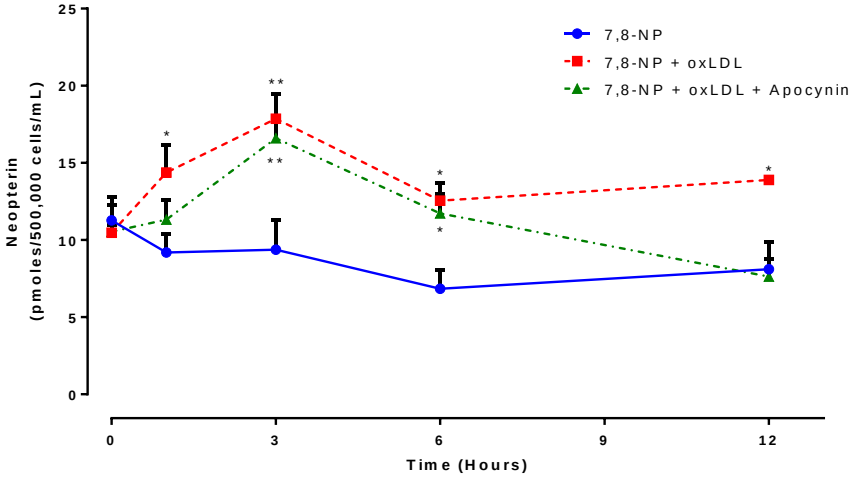


**Figure 3.3.10 Intracellular neopterin production in U937 cells exposed to oxLDL and apocynin.**

U937 cells ($100x10^4$ cells/mL) in RPMI were incubated with 200µM 7,8-NP, followed by addition (dotted red line), absence (filled blue line) of 0.20mg/mL oxLDL or 20µM apocynin + oxLDL (double dotted green line). Cell lysates were collected at indicated times and analyzed for intracellular neopterin via HPLC. Neopterin values were standardized by cell count performed on the Flow cytometer. Results are displayed as mean ± SEM in triplicate and significance is indicated from the 7,8-NP + oxLDL (dotted red line) from each corresponding time point. Significance levels are indicated as: (*) $p \leq 0.05$, (**) $p \leq 0.01$ and (***) $p \leq 0.001$.

# 3.4 NADPH Oxidase (NOX)

As previously shown in **section 3.2**, there was a significant increase of intracellular superoxide and a decrease of cell viability of U937 cells. Oxidant production and cell death are thought to be major driving factors of prolonged inflammation and progression of atherosclerotic lesions (Madamanchi 2005, Goncharov 2015, Katouah 2015). However, the major source of the intracellular oxidative stress and the mechanism by which the oxLDL is triggering the cell to produce an exaggerated amount of oxidants is currently unknown. NOX is a membrane bound enzymatic complex that is used by immune cells to generate superoxide anions to eliminate pathogens. It was hypothesized that NOX is the major contributor of oxidant production when U937 cells are exposed to oxLDL. The following studies were designed to implicate NOX in the oxLDL-induced oxidative stress and restore cell viability when the oxidative stress has been inhibited. The effect of gp91ds-tat (NOX inhibitor) on the superoxide production when U937 are exposed to oxLDL was extensively studied in this section.

## 3.4.1 The effect of gp91ds-tat on the cell viability of U937 cells

Initial experiments examined the concentration dependent effect of gp91ds-tat on the cell viability and ensure that cell death was not attributed to the inhibition of NOX. U937 cells were incubated with increasing concentrations of gp91ds-tat for 24 hours and cell viability (PI positive and PI negative stained cells) were measured via PI staining. The results (**Figure 3.4.1**) showed that 0 – 0.5µM gp91ds-tat did not significantly reduce the cell viability, implying that this concentration range did not induce a cytotoxic effect. The 1µM treatment showed no significant change in PI negative cells compared to the cell only control, however, there was a significant 3% increase of PI positive cells, suggesting a slight cytotoxic effect. The 2µM gp91ds-tat treatment showed a significant 15% reduction in PI negative cells and a significant 20% increase of PI positive cells, suggesting that the 2µM gp91ds-tat is inducing a cytotoxic effect on the cell viability. This was confirmed in the cell photos (**Figure 3.4.2**) of the 2µM treated cells showed cell blebbing and the presence of cellular debris.

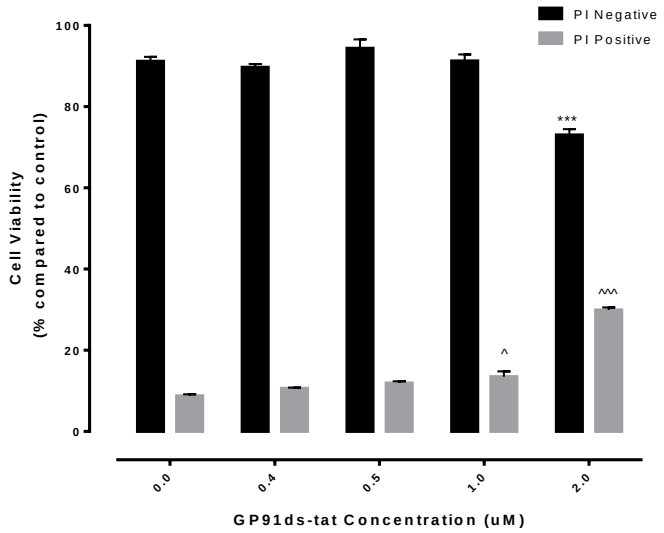


**Figure 3.4.1 The effect of increasing concentrations of gp91ds-tat (NOX-2 inhibitor) on PI cell viability in U937 cells.**

U937 cells ($0.5x10^6$ cells/mL) were treated with increasing concentrations of gp91ds-tat and incubated at 37ºC for 24 hours in non-phenol red RPMI-1640. Cell viability was measured by PI and the data was expressed as a percentage of the respective control (cell only control). Results were analyzed by Flow Cytometry under the FL-3 filter. Significance is indicated from the cell only control. Results are displayed as mean ± SEM of triplicates from a single experiment, representative of three separate experiments. Significance levels are indicated as: (*) $p \leq 0.05$, (**) $p \leq 0.01$ and (***) $p \leq 0.001$.

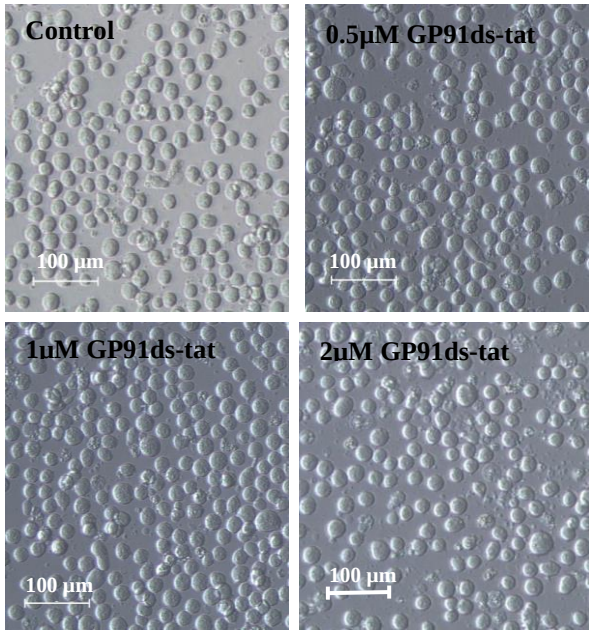


**Figure 3.4.2 Cell images of increasing concentration of gp91ds-tat**

Images of U937 cells after incubation with 0 – 2µM gp91ds-tat for 24 hours. The images were taken using a LEICA DMIL microscope with a LEICIA DFC290 camera. The population density is at 500,000 cells per mL.

### 3.4.2 The effect of gp91ds-tat on the superoxide production in U937 cells

The experiments in this section examined the effect of gp91ds-tat on the superoxide generation in oxLDL exposed U937 cells. Cells were incubated with different concentrations of gp91ds-tat for 1 hour before the addition of oxLDL, followed by DHE staining. Proceeding experiments investigated the effect of gp91ds-tat on the cell viability (PI positive and PI negative stained cells) when reducing the intracellular oxidative stress.

U937 cells treated with 0.25mg/mL oxLDL for 6 hours (**Figure 3.4.3**) showed a 35% increase of mean cellular fluorescence compared to the cell only control, distinctly showing that the oxLDL is inducing a significant oxidative burst within the cell. Cells that had been treated with 0.2, 0.4, 0.5µM gp91ds-tat and oxLDL showed a significant 15, 18 and 25% decrease in mean cellular fluorescence respectively. This suggests that NOX has a significant role in the oxidant generation, largely contributing to the cytosol oxidative stress initiated by oxLDL. However, the inhibitor did not restore the cell viability as expected (**Figure 3.4.4**). This suggests that the remaining 10% of oxidative stress is causing the decrease in cell viability or another mechanism is occurring parallel to the oxidative stress mechanism, initiating cell death. It may also suggest that the DHE probe is significantly under measuring the level of intracellular oxidant generation.

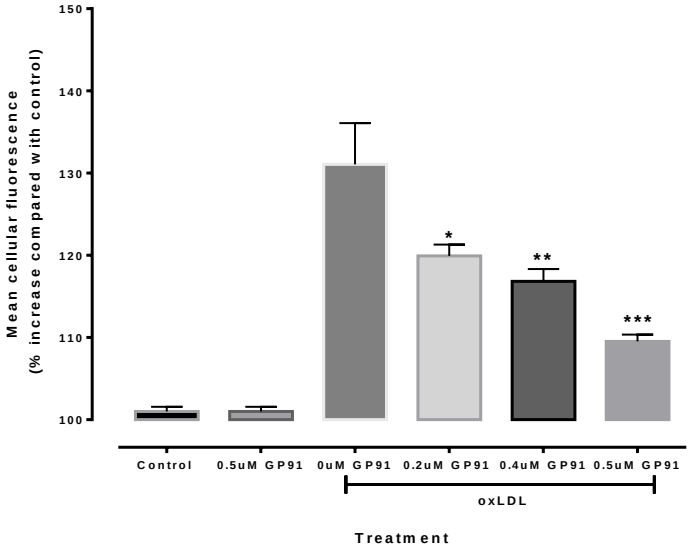


**Figure 3.4.3 Oxidant production in U937 cells when exposed to 0.25mg/mL oxLDL and gp91ds-tat.**

U937 cells ($0.5x10^6$ cells/mL) were treated with 0.25mg/mL of oxLDL and incubated at 37ºC in non-phenol red RPMI-1640. At 6 hour time point, the cells were washed and incubated with 10µM DHE for 20minutes in the dark to measure the intracellular superoxide production from oxLDL. The cells were measured by Flow Cytometry under the FL2 filter. The data is displayed in triplicate mean ±SEM and as a percentage increase of the cell only control. Significance is a two-way ANOVA, relative to the 0µM gp91 + oxLDL control. Significance levels are indicated as: (*) $p \leq 0.05$, (**) $p \leq 0.01$ and (***) $p \leq 0.001$.

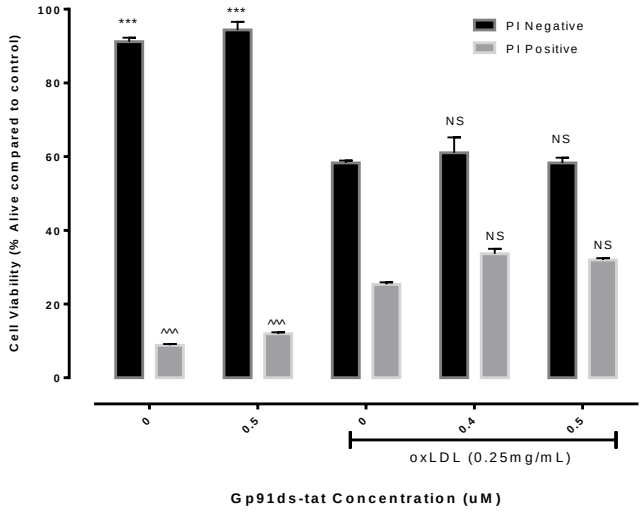


**Figure 3.4.4 The effect of oxLDL and increasing concentrations of gp91ds-tat on cell viability in U937 cells.**

U937 cells ($0.5x10^6$ cells/mL) were treated with increasing concentrations of gp91ds-tat and incubated with 0.25mg/mL oxLDL for 24 hours in non-phenol red RPMI-1640. Cell viability was measured by PI and the data was expressed as a percentage of the respective control (cell only control). Results were analyzed by Flow Cytometry under the FL-3 filter. Significance is indicated from the oxLDL only control (0µM gp91). Results are displayed as mean ± SEM of triplicates from a single experiment, representative of three separate experiments. NS = not significant. Significance levels are indicated as: (*) $p \leq 0.05$, (**) $p \leq 0.01$ and (***) $p \leq 0.001$.

U937 cells were incubated with the same concentrations of gp91ds-tat for 1 hour before the addition of lethal concentration of oxLDL (0.40mg/mL), followed by DHE staining. The results (**Figure 3.4.5**) showed a significant 85% increase in mean cellular fluorescence compared to the cell only control. Treatments with 0.2 – 0.5µM gp91ds-tat + oxLDL showed a significant decrease in mean cellular fluorescence, with the same trend as seen in **Figure 3.4.3**. Cells treated with 0.2, 0.4 and 0.5µM gp91ds-tat showed a 25%, 45% and 55% (respectively) reduction in mean cellular fluorescence compared to the oxLDL only control. This suggests that increasing gp91ds-tat concentrations are inducing a significant reduction in superoxide generation.

Cells with the same concentrations of gp91ds-tat and 0.40mg/mL oxLDL were incubated for 24 hours and the cell viability were measured by PI flow cytometry assay. Results (**Figure 3.4.6**) showed that gp91ds-tat provided no protection of the cell viability at a higher oxLDL concentration. There was a 85% decrease of PI negative cells and a 70% increase of PI positive cells in all of the oxLDL treatments. This suggests that even at the highest gp91ds-tat concentration (0.5µM) the U937 cells are still exposed to a remaining 30% oxidative stress (**Figure 3.4.5**) with significant cell death occurring (**Figure 3.4.6**). These results are in agreement to what was observed in **Figures 3.4.3 and 3.4.4**.

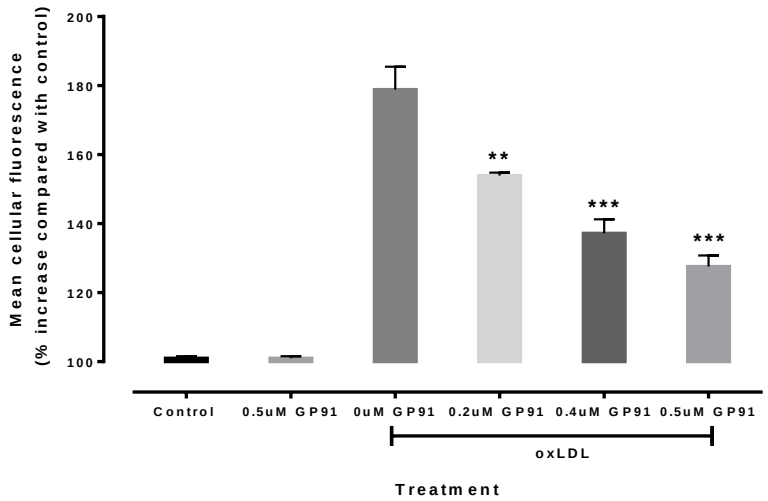


**Figure 3.4.5 Oxidant production in U937 cells when exposed to 0.40mg/mL oxLDL and gp91ds-tat.**

U937 cells ($0.5x10^6$ cells/mL) were treated with 0.4mg/mL of oxLDL and incubated at 37ºC in non-phenol red RPMI-1640. At 6 hour time point, the cells were washed and incubated with 10µM DHE for 20 minutes in the dark to measure the intracellular superoxide production from oxLDL. The cells were measured by Flow Cytometry under the FL2 filter. The data is displayed in triplicate mean ±SEM and as a percentage increase of the cell only control and significance is a two-way ANOVA, relative to the 0µM gp91 + oxLDL control. Significance levels are indicated as: (*) $p \leq 0.05$, (**) $p \leq 0.01$ and (***) $p \leq 0.001$.

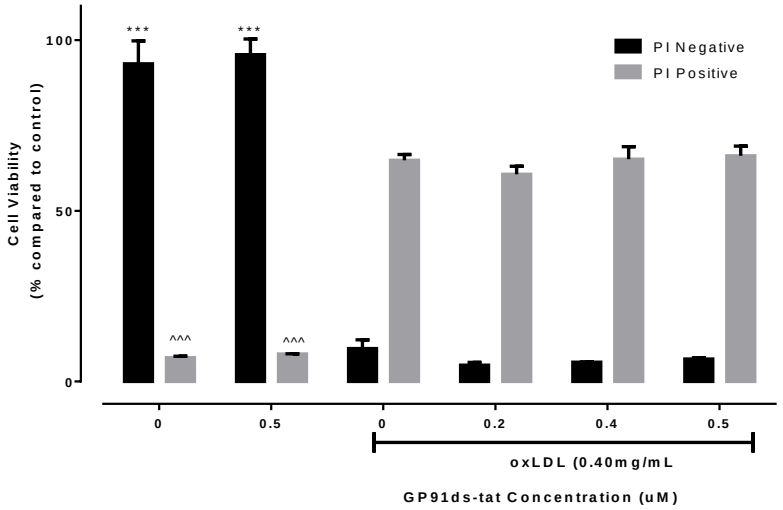


**Figure 3.4.6 The effect of oxLDL and increasing concentrations of gp91ds-tat (NOX-2 inhibitor) on cell viability in U937 cells.**

U937 cells (500,000 cells/mL) were incubated with 0.4mg/mL oxLDL and increasing concentrations of gp91ds-tat (0, 0.4, 0.5µM) for 24 hours to determine the effect on the cell viability. Cell viability was measured by PI and the data was expressed as a percentage of the control. The different treatments were aliquoted into centrifuge tube and PI stain was added and incubated for 10 minutes in the dark. Results were analyzed by Flow Cytometry under the FL-3 filter. The data is displayed in triplicate ±SEM. Significance was a two-way ANOVA and is indicated from the oxLDL control (0µM gp91). Significance levels are indicated as: (*) $p \leq 0.05$, (**) $p \leq 0.01$ and (***) $p \leq 0.001$.

# 3.5 Mitochondria

The mitochondria has been implicated as a potential source of oxidative stress when U937 cells are exposed to oxLDL. It is unknown if oxLDL is directly causing the mitochondria to release superoxide into the cell or if other sources of oxidative stress are damaging the mitochondria causing a secondary source of superoxide. This research focused on investigating this theory by utilizing a mitochondrial specific fluorescent dye called JC-1 and investigating the mitochondria membrane potential when U937 cells were incubated with oxLDL. Further research looked at using 7,8-NP as a tool to determine if the loss in in membrane potential was a result of oxidative stress. The JC-1 technique measures the fluorescence measured from two filters, red (FL2) and green (FL1). The results were displayed as a ratio of red:green fluorescence and a significant reduction in the ratio indicates a loss in mitochondrial membrane potential. A control treatment incubated with carbonyl cyanide m-chlorophenyl hydrazine (CCCP) was used to equalize the membrane potential, establishing the lowest potential the membrane can dissipate to.

## 3.5.1 The effect of oxLDL on U937 cells mitochondrial membrane potential

Initial research investigated the effect of oxLDL on the mitochondria membrane potential by treating U937 cells with 0.20mg/mL oxLDL for 0, 2, 4, 6 and 8 hours followed by JC-1 staining. The FL2:FL1 ratio (**Figure 3.5.1A**) showed a small decline in membrane potential at 2 and 4 hours (3 & 15% respectively) and a significant depolarization at 6 and 8 hours (38 & 44% respectively). The $LD_{50}$ concentration (0.20mg/mL) showed a slow, gradual decrease in membrane potential over the course of 8 hours. The decrease in membrane potential at 6 hours suggests the oxLDL is inducing a cytotoxic effect to the mitochondria; however, the difference between the 8-hour treatment and the CCCP control suggests the oxLDL is inducing a cytotoxic effect, but not completely damaging the mitochondrial membrane.

**A**

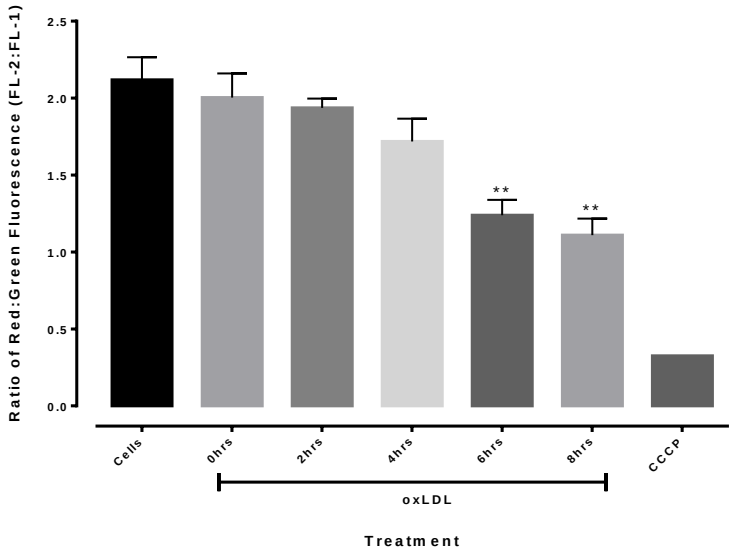


**B**

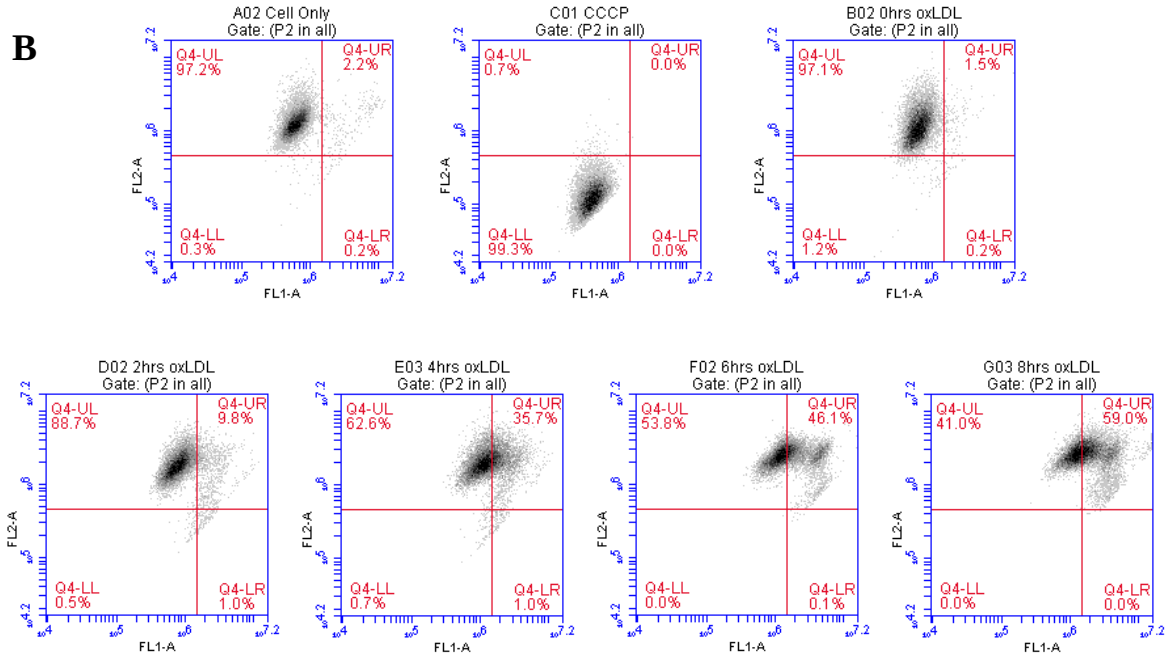


**Figure 3.5.1 The effect of the mitochondrial membrane potential on U937 cells when exposed to 0.20mg/mL oxLDL for 0, 2, 4, 6, and 8 hours.**

U937 cells (1,000,000 cells/mL) were incubated with 0.25mg/mL oxLDL and samples were taken after 0, 2, 4, 6 and 8 hours. Cells were washed and incubated with 100µM JC-1 for 20minutes. Results were analyzed by Flow Cytometer using the FL1,FL2 filter. **A**) Results are presented as a ratio of Red:Green fluorescence and in triplicate ±SEM. Significance was a one-way ANOVA and is indicated from the 0 hour oxLDL exposed control. Significance levels are indicated as: (*) $p \leq 0.05$, (**) $p \leq 0.01$ and (***) $p \leq 0.001$. **B**) Represents the dot plots of 10,000 individual gated cells treated with JC-1.

The next experiment focused on the effect of a higher concentration (0.40mg/mL) of oxLDL on the membrane potential by incubating with oxLDL for 0, 1, 3, 6 and 24 hours followed by JC-1 staining. Due to **Figure 3.5.1** yielding a small cytotoxic effect to the mitochondrial at 0.25mg/mL, the mitochondria was subjected to a more lethal concentration of oxLDL (0.40mg/mL).

The results (**Figure 3.5.2A**) showed a more prominent cytotoxic effect occurring, resulting in a loss of membrane potential over the 24-hour period. There was a slight decrease in membrane potential at 3 hours (36%), followed by a significant depolarization at 6 and 24 hours (56 & 69% respectively) compared to the 0 hour control. There was a small difference between the 24-hour treatment and the CCCP control, suggesting that 24-hour oxLDL exposure caused extensive membrane potential dissipation. Interestingly, there was a substantial 26% decrease in membrane potential between the cell only control and the 0-hour oxLDL exposure. There was virtually no difference between the cell only or the 0 hour oxLDL control groups except a 30 minute oxLDL exposure before analysis. This suggests that at high oxLDL concentrations, there is an instantaneous decrease in mitochondrial membrane potential indicating a fast mechanism occurring.

**A**

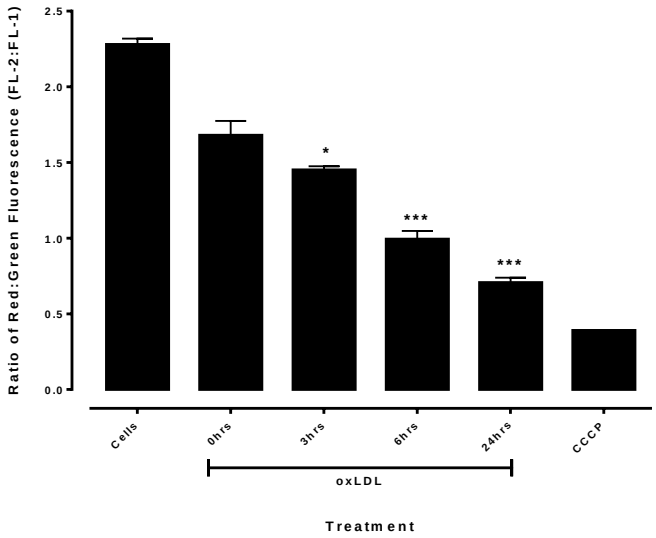


**B**

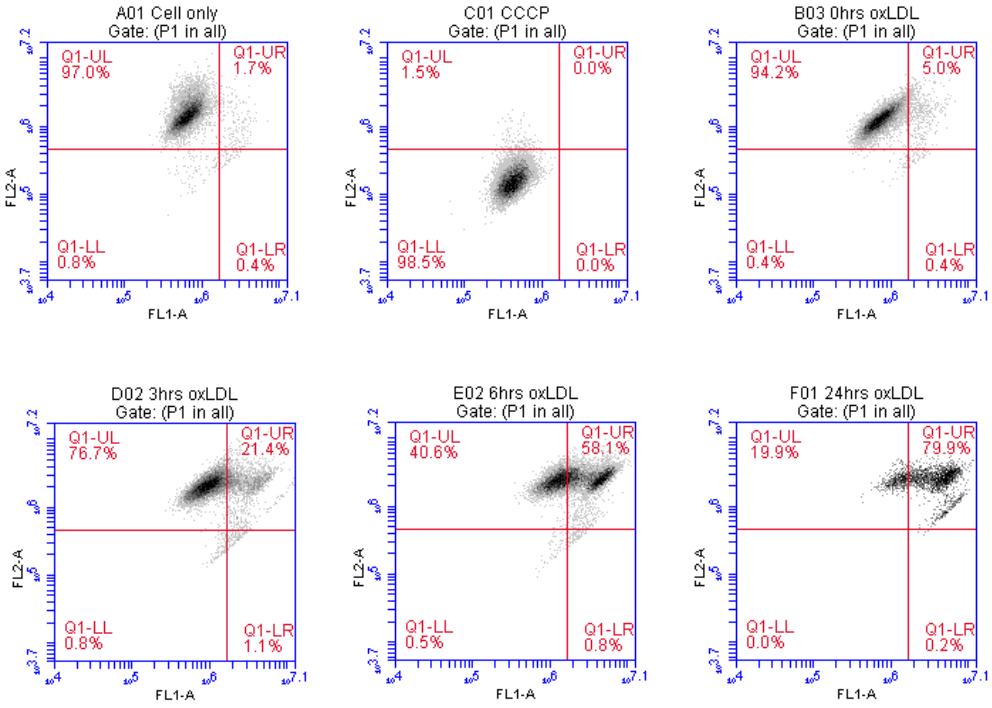


**Figure 3.5.2 The effect of the mitochondrial membrane potential on U937 cells when exposed to 0.40mg/mL oxLDL for 0, 3, 6 and 24 hours.**

U937 cells (1,000,000 cells/mL) were incubated with 0.4mg/mL oxLDL and samples were taken after 0,3,6 and 24 hours. Cells were washed and incubated with 100µM JC-1 for 20minutes. **A**) Results are presented as a ratio of Red:Green fluorescence and in triplicate ±SEM. Significance was a one-way ANOVA and is indicated from the 0 hour oxLDL exposed control. Significance levels are indicated as: (*) $p \leq 0.05$, (**) $p \leq 0.01$ and (***) $p \leq 0.001$. **B**) Represents the dot plots of 10,000 individual gated cells treated with JC-1.

### 3.5.2 The effect of increasing oxLDL concentration on U937 cells mitochondria membrane potential

Previously it was seen that 6-hour oxLDL exposure induced a significant decrease in membrane potential, therefore this research investigated the effect of increasing oxLDL concentration on the mitochondrial membrane potential at 6 hours exposure. U937 cells were incubated with 0 – 0.50mg/mL oxLDL for 6 hours and the membrane potential was analyzed. The results (**Figure 3.5.3A**) showed no decrease in membrane potential when incubated with 0 – 0.20mg/mL oxLDL, however, there was a significant decrease occurring at 0.30, 0.40 and 0.50mg/mL oxLDL (26, 33 and 52% respectively). This suggests that there is a proportional decrease in mitochondria membrane potential with increasing concentrations of oxLDL. In comparison to the CCCP and cells only control, the state of the mitochondria membrane potential was still relatively intact as the 0.50mg/mL treatment did not depolarize to the CCCP baseline. Further research investigated the effect on cell viability (**Figure 3.5.4)** of increasing oxLDL concentrations by PI staining. The 0.40mg/mL treatment showed 85% PI negative cells remaining with an 18% increase of PI positive cells. Contrasting with 0.50mg/mL oxLDL showed a 60% decrease of PI negative cells and a 50% increase of PI positive cells. This suggests that significant cell death is occurring when there is significant decrease in mitochondrial membrane potential.

**A**

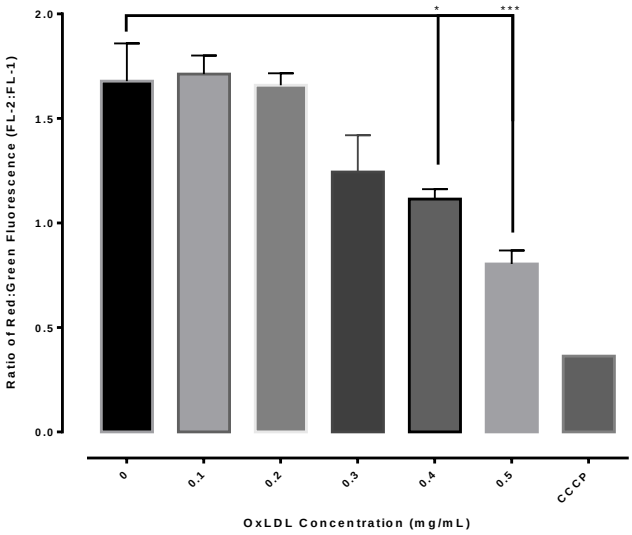


**B**

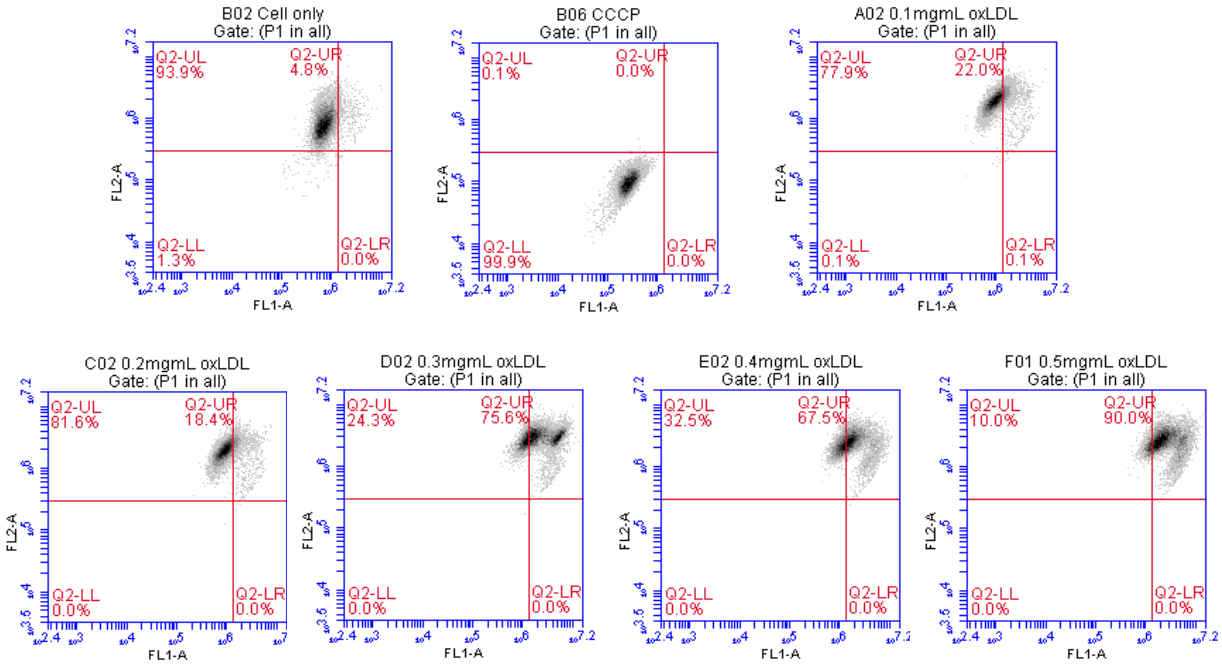


**Figure 3.5.3 The effect of mitochondrial membrane potential on U937 cells when exposed to increasing concentrations of oxLDL for 6 hours.**

U937 cells (1,000,000 cells/mL) were incubated with 0-0.5mg/mL oxLDL for 6 hours. Cells were washed and incubated with 100µM JC-1 for 20 minutes. **A**) Results are presented as a ratio of Red:Green fluorescence and in triplicate ±SEM. Significance was a one-way ANOVA and is indicated from the 0 hour oxLDL exposed control. **B**) Represents the dot plots of 10,000 individual gated cells treated with JC-1. Significance levels are indicated as: (*) $p \leq 0.05$, (**) $p \leq 0.01$ and (***) $p \leq 0.001$.

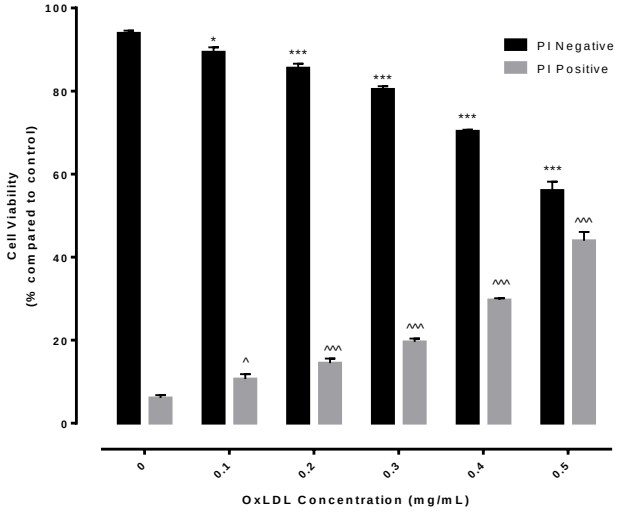


**Figure 3.5.4 The effect of increasing oxLDL concentration on cell viability**

U937 cells (1,000,000 cells/mL) were incubated with 0-0.5mg/mL oxLDL for 6 hours. Cell viability was measured by PI and the data was expressed as a percentage of the control with no oxLDL. The different treatments were aliquoted into centrifuge tube and PI stain was added and incubated for 10minutes in the dark. Results are presented as mean ± SEM. Significance was a one-way ANOVA and is indicated from the 0 hour oxLDL control. Significance levels are indicated as: (*) $p \leq 0.05$, (**) $p \leq 0.01$ and (***) $p \leq 0.001$.

## 3.5.3 The effect of 7,8-NP on U937 cells mitochondria membrane potential

It is currently unknown what causes the significant reduction in mitochondrial potential when U937 cells are exposed to oxLDL. It is hypothesized that there is a link between the oxLDL induced oxidative stress mechanism and reduction in membrane potential. This was investigated by preincubating U937 cells with 0 - 200µM 7,8-NP and exposed the U937 cells to oxLDL (0.20mg/mL) for 6 hours to determine if the 7,8-NP would prevent the reduction of the membrane potential. The results (**Figure 3.5.5A**) showed the oxLDL only treatment (0µM 7,8-NP) exhibited a significant 25% depolarization of membrane potential compared to the cell only control. Treatments with 100 & 200µM 7,8-NP + oxLDL exhibited a significant 25% reduction in membrane potential after 6 hours incubation compared to the cell only control. However, there was no significant difference between the oxLDL only or any of the 7,8-NP treatments, suggesting that 100 – 200µM 7,8-NP had no effect on the oxLDL induced membrane depolarization. The 200µM 7,8-NP only control had a significantly higher membrane potential than the cell only control indicating that 7,8-NP is scavenging the basal level of mitochondria oxidative stress. However, when oxLDL is introduced there is no restorative effect occurring to the membrane potential suggesting that the mitochondria depolarization is not an oxidative stress mechanism in U937 cells.

**A**

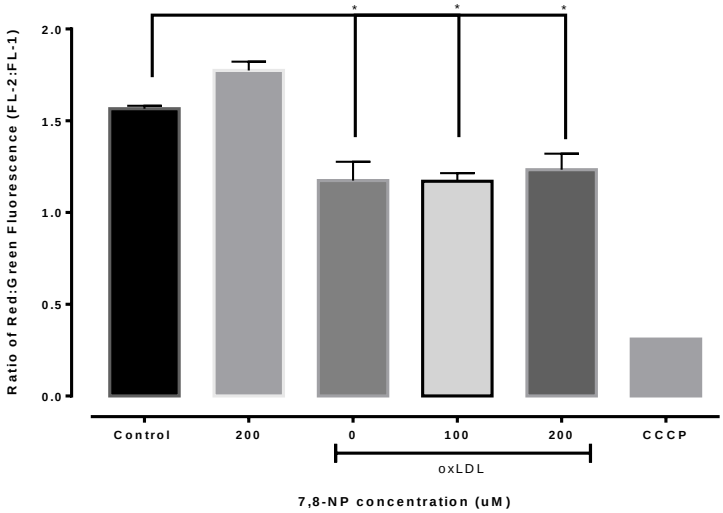


**B**

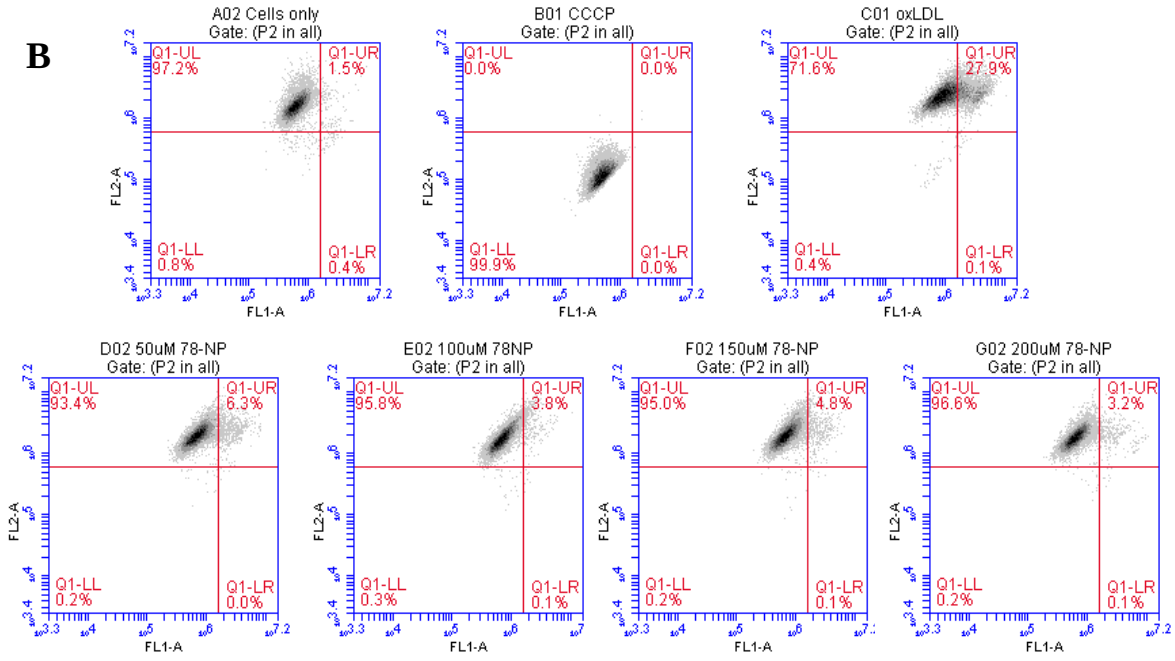


**Figure 3.5.5 The mitochondrial membrane potential in U937 cells when exposed to low oxLDL concentration and increasing concentrations of 7,8-NP at 6 hours.**

U937 cells (500,000 cells/mL) were incubated with 0.20mg/mL oxLDL and varying concentrations of 7,8NP (100 and 200µM) for 6 hours. Cells were washed and incubated with 100µM JC-1 for 20 minutes. **A**) Results are presented as a ratio of Red:Green fluorescence and in triplicate ±SEM. Significance was a one-way ANOVA and is indicated from the 0 hour oxLDL exposed control. Significance levels are indicated as: (*) $p \leq 0.05$, (**) $p \leq 0.01$ and (***) $p \leq 0.001$. **B**) Represents the dot plots of 10,000 individual gated cells treated with JC-1.

The effect of a higher oxLDL concentration was investigated when U937 cells were treated with increasing concentrations of 7,8-NP. U937 cells were treated with 0.50mg/mL oxLDL for 6 hours with 0, 50, 100, 150 and 200µM 7,8-NP to determine if the higher oxLDL concentration would induce a greater mitochondrial depolarization that was not observed in **Figure 3.5.5A** and determine if increasing concentrations of 7,8-NP would mitigate the oxLDL-induced depolarization. The results showed that 0.50mg/mL oxLDL produced a significant 74% decrease in membrane potential in the oxLDL only treatment compared to the cell only control. All 7,8-NP treatments (50, 100, 150 and 200µM) and oxLDL showed a significant 70% decrease in membrane potential compared to the cell only control, regardless of the 7,8-NP concentration (**Figure 3.5.6A**). This suggests that the decrease in mitochondrial membrane potential is not due to oxidative stress but infact could be a result of the cell undergoing a cell death. This idea is backed up in **Figure 3.5.7** as it represents the cell viability from the same experiment. The results showed that there was a 50% decrease of PI negative cells after 6 hour oxLDL exposure, representing significant cell death in all of the oxLDL treatments, regardless of increasing concentrations of 7,8-NP. There was no statistical difference between the oxLDL only treatment and increasing concentrations of 7,8-NP. However, 7,8-NP did not protect against oxLDL induced cell death as shown earlier in **Figure 3.1.2** at $LD_{50}$ oxLDL concentration. This suggests that higher oxLDL concentration induces considerable damage to the cell, resulting in a significant reduction in membrane potential and condemning the cell to death.

**A**

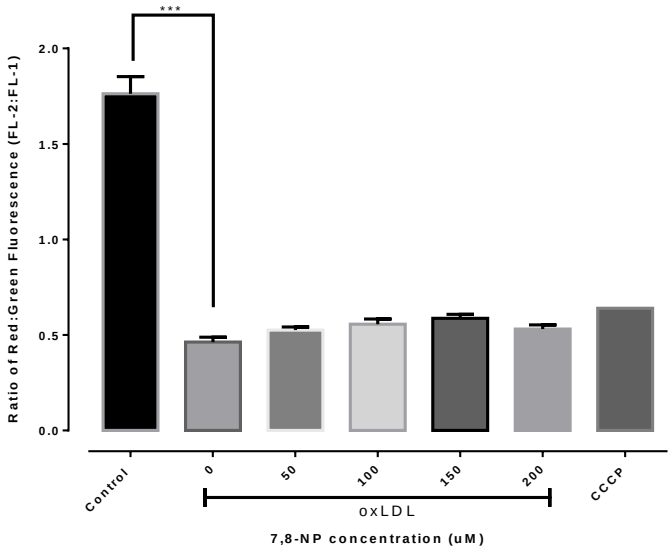


**B**

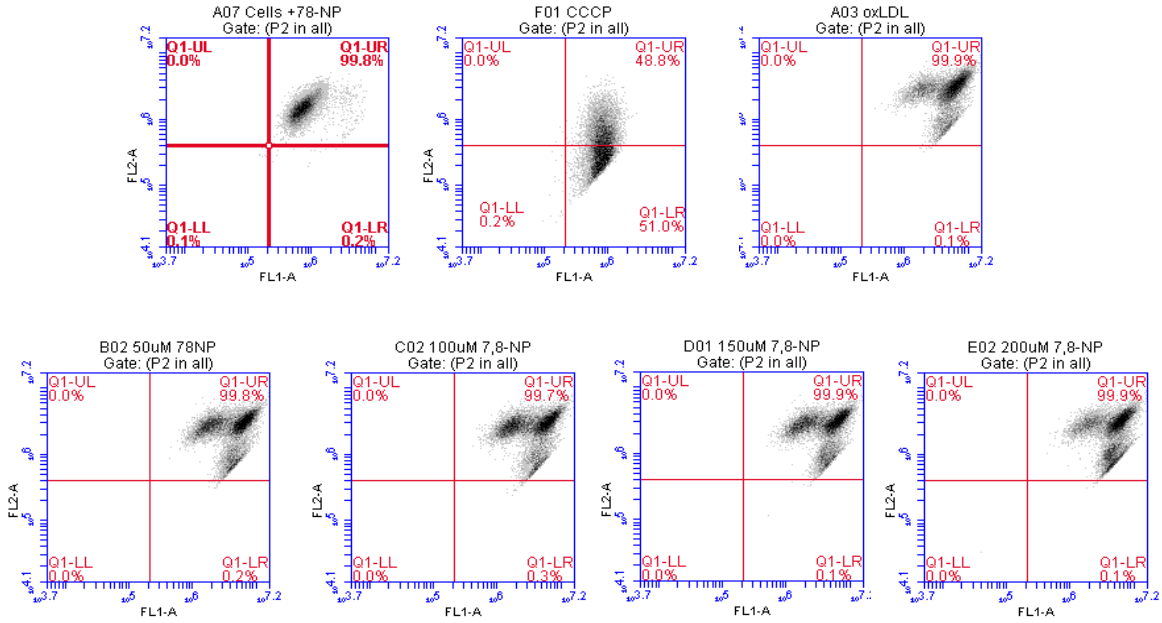


**Figure 3.5.6 The mitochondrial membrane potential in U937 cells when exposed to high oxLDL concentration and increasing concentrations of 7,8-NP at 6 hours.**

U937 cells (1,000,000 cells/mL) were incubated with 0.50mg/mL oxLDL and varying concentrations of 7,8NP (0, 50, 100, 150 and 200µM) for 6 hours. Cells were washed and incubated with 100µM JC-1 for 20 minutes. Results were analyzed by Flow Cytometer using the FL1,FL2 filter. **A**) Results are presented as a ratio of Red:Green fluorescence and in triplicate ±SEM. Significance was a one-way ANOVA and is indicated from the 0 hour oxLDL exposed control. Significance levels are indicated as: (*) $p \leq 0.05$, (**) $p \leq 0.01$ and (***) $p \leq 0.001$. **B**) Represents the dot plots of 10,000 individual gated cells treated with JC-1.

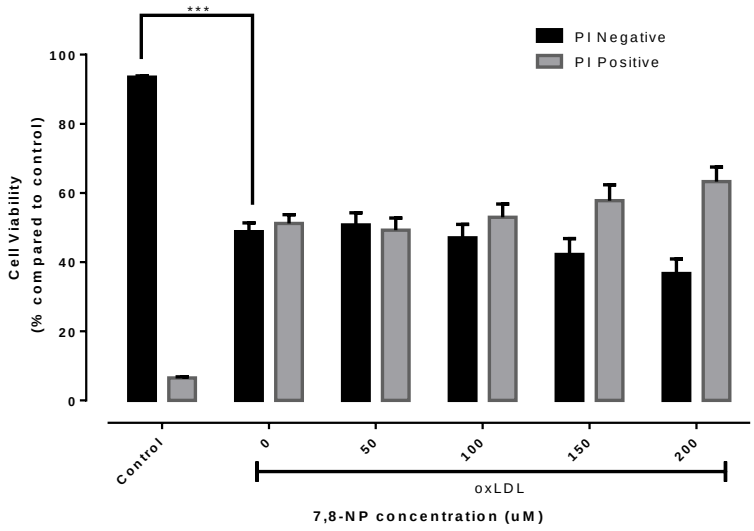


**Figure 3.5.7 The cell viability of U937 cells when exposed to high oxLDL concentration and increasing concentrations of 7,8-NP for 6 hours.**

U937 cells (1,000,000 cells/mL) were incubated with 0.50mg/mL oxLDL and varying concentrations of 7,8-NP (0, 50, 100, 150 and 200µM) for 6 hours. Cell viability was measured by PI and the data was expressed as a percentage of the control with no oxLDL. The different treatments were aliquoted into centrifuge tube and PI stain was added and incubated for 10minutes in the dark. Results were analyzed by Flow Cytometry under the FL-3 filter. Results are presented as mean ± SEM. Significance was a one-way ANOVA and is indicated from the respective control (0 µM 7,8-NP). Significance levels are indicated as: (*) $p \leq 0.05$, (**) $p \leq 0.01$ and (***) $p \leq 0.001$.

The JC-1 dot plots (**Figures 3.5.1B, 3.5.2B, 3.5.3B, 3.5.5B and 3.5.6B**) all express the similar trend of an increase in FL1 fluorescence in the oxLDL treatments, with no subsequent decrease of FL2 fluorescence. The cell only control exhibits a high FL2 with a low FL1 and contrasting to the opposite end of the spectrum, the CCCP control displays a low FL2 fluorescence and a high FL1 fluorescence. It was expected that both the dot plots and the FL2:FL1 ratio would display similar trends however, the JC-1 dot plot oxLDL treatments do not display the intermediate transition between these two extremes and only display an increase of FL1 fluorescence with no decrease in FL2. This is not in concert when the same data is displayed as a ratio of FL2:FL1 (**Figures 3.5.1A, 3.5.2A, 3.5.3A, 3.5.5A and 3.5.6A**), which effectively displays the transition between the positive and negative control.

## 3.6 Myeloperoxidase

Myeloperoxidase (MPO) is a peroxidase enzyme that is secreted by activated neutrophils in conjunction with hydrogen peroxide (generated indirectly from NOX complex) for antimicrobial activity. Along with NOX-2 and the mitochondria, MPO is considered to be a contributing component in the oxidant generation that is involved in atherosclerosis (Hazen 1997, Madamanchi 2005). HOCl has also been shown previously in our lab to oxidize 7,8-NP to neopterin (Widner 2000, Parker 2015). This section investigates the role of MPO inhibitors (thiocyanate ions and 4-amino benzoic acid) on the cell viability of U937 cells when exposed to oxLDL. Further research investigates the contribution MPO has to the cytosolic oxidative stress using DHE staining.

### 3.6.1 The effect of thiocyanate ions on the cell viability of U937 cells

Preliminary experiments investigated the cytotoxicity of thiocyanate ions (NaSCN) on U937 cells. The cells were incubated with 0 - 600µM NaSCN for 24 hours to determine if the concentration range caused any cell death before the addition of oxLDL. The results show that there was a slight increase in PI negative cells at 400 - 600µM NaSCN by 10%, although this was non-significant (**Figure 3.6.1**). There were no changes in the PI positive cells suggesting that the cells were unharmed.

Further research investigated the antioxidant properties of SCN ions when incubated with oxLDL. U937 cells were incubated with 200 - 600µM NaSCN for 15 minutes before the incubation with 0.30mg/mL oxLDL for 24 hours. The results showed that there was a 40% decrease in the oxLDL treatment's PI negative cells compared to the cell only control. Furthermore, there was no significant difference in the PI negative cells of the oxLDL only treatment and the NaSCN treatment at any concentration (**Figure 3.6.2**). This suggests that NaSCN is not having a protective effect on U937 cells when exposed to oxLDL

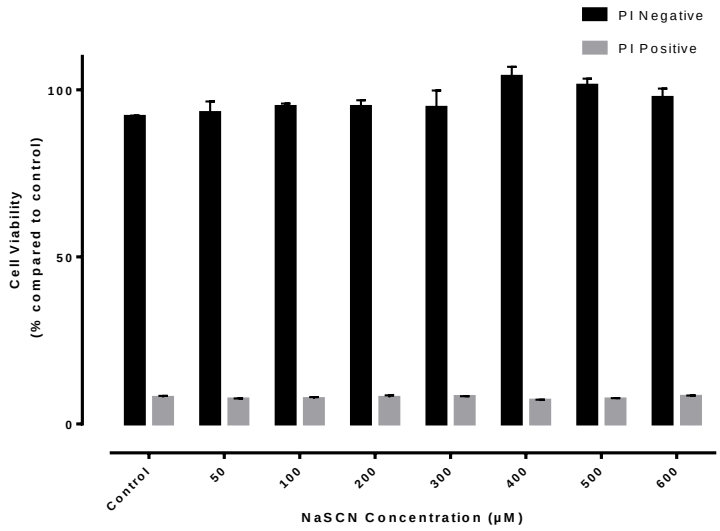


**Figure 3.6.1 The effect of increasing concentrations of NaSCN on cell viability**

U937 cells ($0.5x10^6$ cells/mL) were treated with increasing concentrations of NaSCN for 24 hours in non-phenol red RPMI-1640. Cell viability was measured by PI and the data was expressed as a percentage of the cell only control. The different treatments were aliquoted into centrifuge tube and PI stain was added and incubated for 10minutes in the dark. Results were analyzed by Flow Cytometry under the FL-3 filter. Significance was a two way ANOVA and is indicated from the cell only control, however, there was no significance.

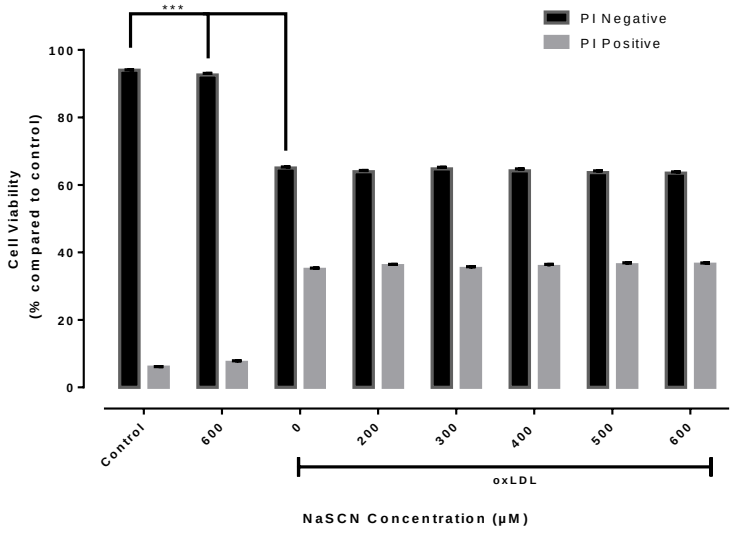


**Figure 3.6.2 The effect of increasing concentrations of NaSCN on cells that have been exposed to 0.30mg/mL oxLDL.**

U937 cells ($0.5x10^6$ cells/mL) were treated with increasing concentrations of NaSCN and 0.30mg/mL oxLDL for 24 hours in non-phenol red RPMI-1640. Cell viability was measured by PI and the data was expressed as a percentage of the control with no oxLDL. The different treatments were aliquoted into centrifuge tube and PI stain was added and incubated for 10minutes in the dark. Results were analyzed by Flow Cytometry under the FL-3 filter. Significance was a two way ANOVA and is indicated from the oxLDL (0µM SCN) control. Significance levels are indicated as: (*) $p \leq 0.05$, (**) $p \leq 0.01$ and (***) $p \leq 0.001$.

### 3.6.2 The effect of ABAH on the cell viability of U937 cells

The possible role of MPO was further examined using MPO inhibitor, 4-amino benzoic acid (ABAH), on the oxLDL induced cell death. U937 cells were incubated with increasing concentrations of ABAH for 24 hours to determine if there were any preliminary cytotoxic effects occurring to the cells. The results showed that there was no significant change in PI negative cells when exposed to 0 - 300µM ABAH (**Figure 3.6.3**), indicating there is no cytotoxic effect at that concentration range with just ABAH.

U937 cells were then incubated with 0 - 300µM with 0.20mg/mL oxLDL for 24 hours to determine if there were any protective effects occurring to the PI negative cells. The results showed that there was a 5% increase in PI negative cells treated with 5 and 100µM ABAH with oxLDL compared to the other treatments (**Figure 3.6.3**). This indicates that ABAH provided little or no protection from the oxLDL induced toxicity.

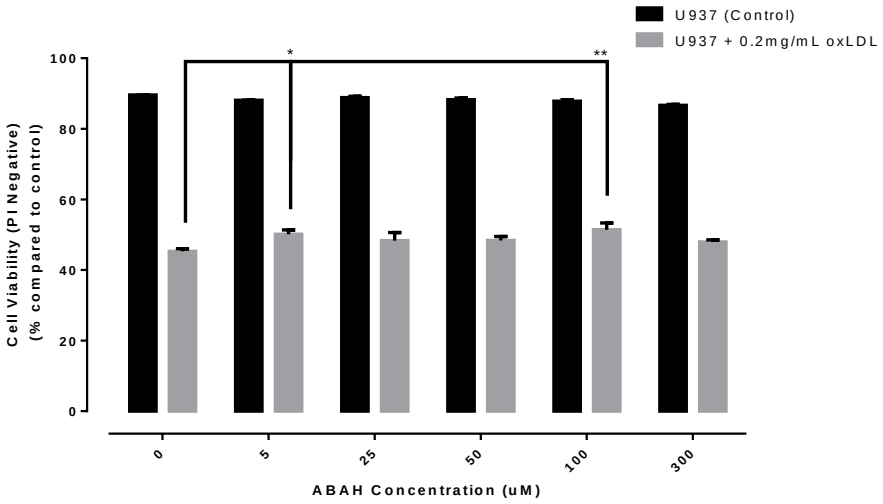


**Figure 3.6.3 The effect of increasing concentration of ABAH on cells treated with oxLDL.**

U937 cells ($0.5x10^6$ cells/mL) were treated with increasing concentrations of ABAH and 0.20mg/mL oxLDL for 24 hours in non-phenol red RPMI-1640. Cell viability was measured by PI and the data was expressed as a percentage of the control with no oxLDL. The different treatments were aliquoted into centrifuge tube and PI stain was added and incubated for 10minutes in the dark. Results were analyzed by Flow Cytometry under the FL-3 filter. Significance was a two way ANOVA and is indicated from the oxLDL (0µM ABAH) control. Significance levels are indicated as: (*) $p \leq 0.05$, (**) $p \leq 0.01$ and (***) $p \leq 0.001$.

### 3.6.3 The effect of ABAH on the cytosol intracellular oxidative stress

Further research investigated the contribution MPO/hypochlorite had to the cytosol intracellular oxidative stress generated when U937 cells are incubated with oxLDL. Research by this laboratory has seen an increase in DHE staining when U937 cells are incubated with oxLDL (Katouah 2015); however, it is unknown if hypochlorite contributes to the oxidative stress. Preincubating U937 cells with ABAH would establish whether superoxide or hypochlorite is the major oxidant that is causing the oxidative stress when U937 cells are exposed to oxLDL. The results (**Figure 3.6.4**) showed that U937 cells that are incubated with oxLDL for 6 hours, there is a 60% significant increase in mean cellular fluorescence compared to the cell only control. However, there is no significant difference between the oxLDL control (0µM ABAH) or 5 - 300µM ABAH plus oxLDL treatments suggesting that hypochlorite does not contribute towards the DHE staining present within U937 cells. There was a decrease in mean cellular fluorescence at the 25µM ABAH with oxLDL treatment, although, this was not a significant decrease. The results indicate that the intracellular DHE staining is likely to be superoxide anions and hypochlorite is unlikely to be contributing towards the oxidative stress.

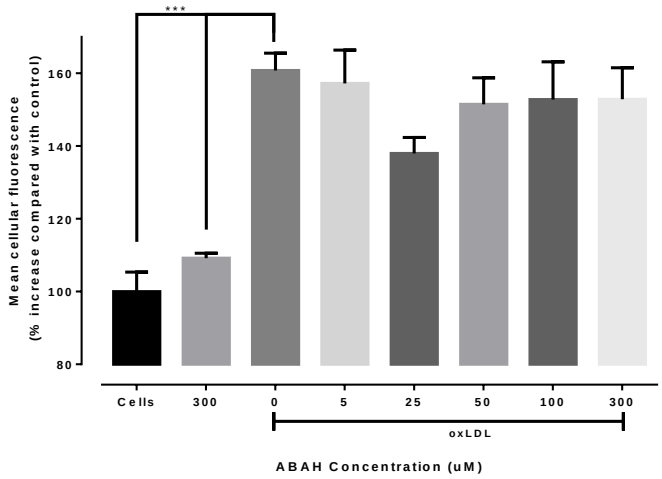


**Figure 3.6.4 The effect of increasing concentrations of ABAH on the intracellular oxidative stress produced by oxLDL.**

U937 cells ($0.5x10^6$ cells/mL) were treated with increasing concentrations of ABAH and 0.30mg/mL oxLDL for 6 hours in non-phenol red RPMI-1640. The cells were washed and incubated with 10µM DHE for 20minutes in the dark to measure the intracellular superoxide production from oxLDL. The cells were measured by Flow Cytometry under the FL2 filter. The data was expressed as a percentage increase of the 0 hour control and significance is relative to the 0-hour control. Significance was a one way ANOVA and is indicated from the oxLDL (0µM ABAH) control. Significance levels are indicated as: (*) $p \leq 0.05$, (**) $p \leq 0.01$ and (***) $p \leq 0.001$.

## 3.7 Cultured Plaque sections

Live plaque tissue was excised from patients undergoing an endarterectomy surgery and sections were cultured for 96 hours to measure the change in neopterin, total neopterin, 7,8-dihydroneopterin and lactate output in to the media. Analysis of the plaque media was conducted through HPLC, measuring the neopterin and total neopterin of each samples in duplicate (**section 2.2.9**). The 7,8-NP was calculated through the subtraction of neopterin from total neopterin and lactate was measured through an assay kit from Roche diagnostics (**section 2.2.8**).

### 3.7.1 The effect of sub-lethal oxLDL on cultured plaque sections

The effect of oxLDL has been extensively studied in cell culture research, however, little is known what effect it has in physiological conditions. OxLDL was added to plaque tissue sections to determine if there were significant changes in the neopterin or 7,8-NP production. Every 24 hours fresh media was added to the sections along with a sub lethal concentration of oxLDL (0.25mg/mL) for a total of 72 hours. The samples were stored at -80°C before analysis of neopterin, total neopterin and lactate of each sample. Analysis of the neopterin **(Figure 3.7.1)** over the 0 - 72 hours revealed a significant increase in sections 5 and 6 after 72 hours, with a significant increase of neopterin production in sections 1 and 7 at 48 hours and a subsequent decrease at 72 hours. Section 8's 0-hour treatment displayed a significant production of neopterin however, this decreased significantly once oxLDL was added at 24hours. Total neopterin **(Figure 3.7.2)** produced by the oxLDL treated plaque had no significant change of total neopterin in all plaque sections between 0 – 72 hours oxLDL incubation. This indicates that sub-cytotoxic levels of oxLDL has no inflammatory effect within the plaque that lead to macrophage activation and up regulation of 7,8-NP production. This was confirmed by the 7,8-NP graph **(Figure 3.7.3)** as the levels of 7,8-NP remained constant in sections 1-7 throughout the 72 hour oxLDL incubation. This was an exception for section 8 with 7,8-NP production significantly increased at 24 hours. The lactate measurement **(Figure 3.7.4)** indicates that in all of the sections, there was no significant decrease in lactate production indicating that the cells metabolism are still intact, suggesting that the oxLDL concentration was non-toxic as expected. The lactate production in sections 1-7 slowly increased between the 0-48 hours and plateau at 72 hours, this suggests that

the plaque is becoming more glycolytic in response to the non-toxic concentration of oxLDL. Therefore the results indicate there is no immune activation or up-regulation of 7,8-NP production and a significant increase in plaque metabolism in the first 24 hours when incubated with oxLDL. Interestingly, there was a significant increase in neopterin production suggesting an oxidative environment occurring within the plaque.

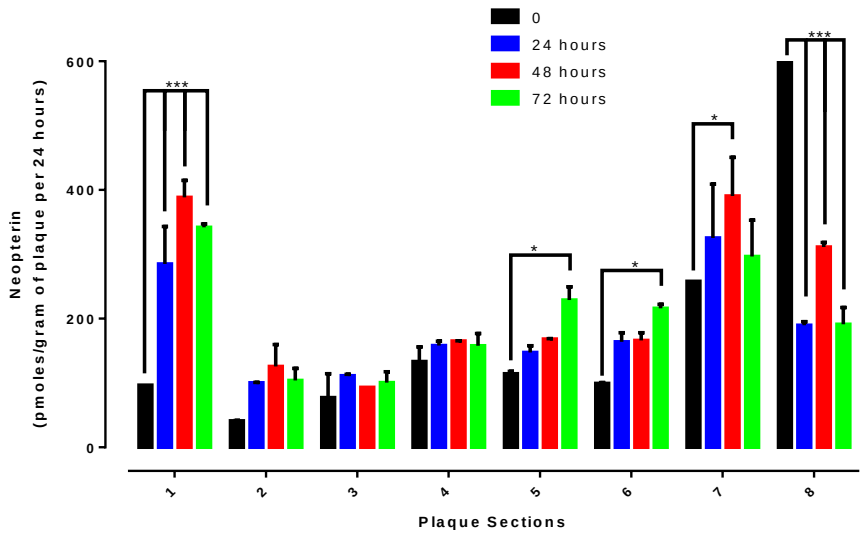


**Figure 3.7.1 The effect of oxLDL on Plaque 113 neopterin production.**

Plaque 113 was sliced into 8 sections and incubated at 37ºC with RPMI 1640 with phenol red, 10% human serum, penstrep and 0.25mg/mL oxLDL. After 24, 48, 72 and 96 hours the media was collected and analyzed for neopterin through the HPLC. Two way ANOVA significance is indicated from the 0 hour media control. The data is in duplicate from a single experiment. Significance levels are indicated as: (*) $p \leq 0.05$, (**) $p \leq 0.01$ and (***) $p \leq 0.001$.

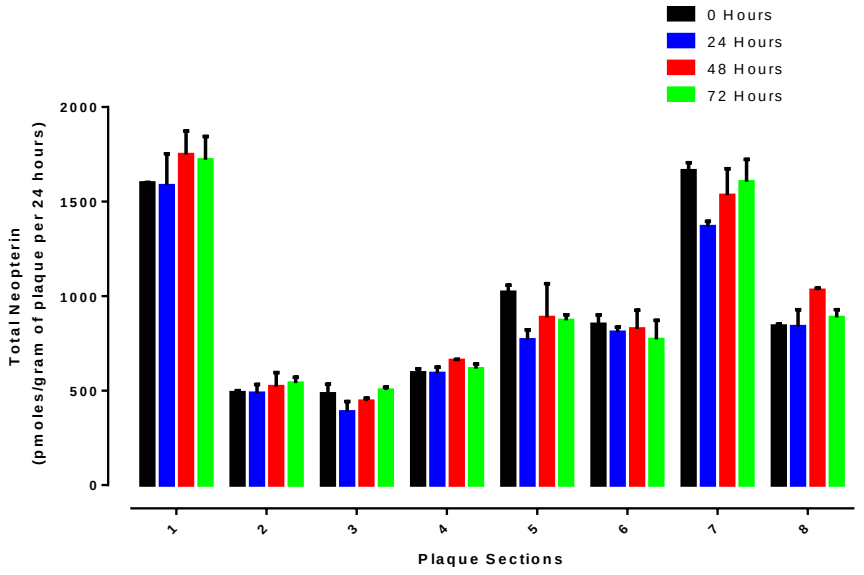


**Figure 3.7.2 The effect of oxLDL on Plaque 113 total neopterin production.**

Plaque 113 was sliced into 8 sections and incubated at 37ºC with RPMI 1640 with phenol red, 10% human serum, penstrep and 0.25mg/mL oxLDL. After 24, 48,72 and 96 hours the media was collected and analyzed for neopterin through the HPLC. Data is presented in duplicate. Two way ANOVA significance is indicated from the 0 hour media control. The data is in duplicate from a single experiment. Significance levels are indicated as: (*) $p \leq 0.05$, (**) $p \leq 0.01$ and (***) $p \leq 0.001$.

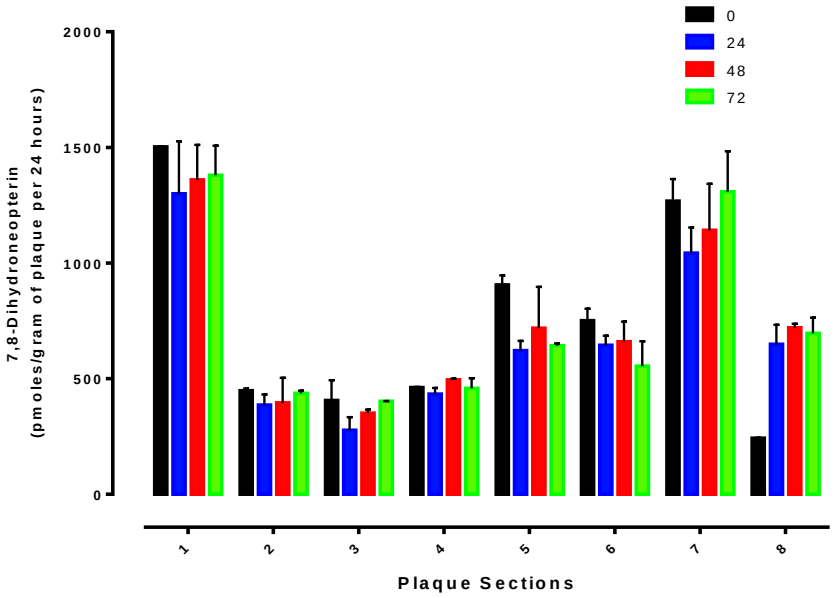


**Figure 3.7.3 The effect of oxLDL on Plaque 113 7,8-dihydroneopterin production.**

Data represents the difference between neopterin and total neopterin values Data is presented in duplicate. Two way ANOVA significance is indicated from the 0 hour media control. The data is in duplicate from a single experiment. Significance levels are indicated as: (*) $p \leq 0.05$, (**) $p \leq 0.01$ and (***) $p \leq 0.001$.

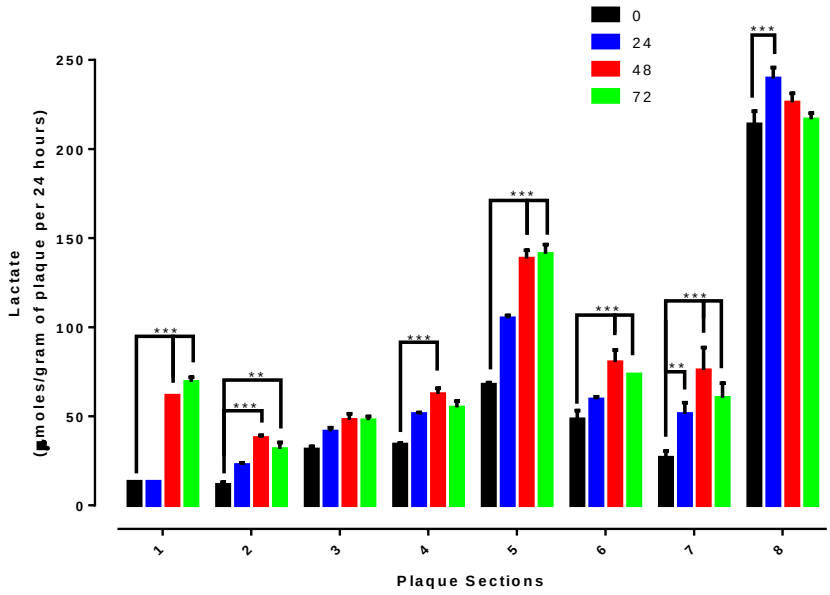


**Figure 3.7.4 The effect of oxLDL on Plaque 113 lactate production.**

Plaque 113 was sliced into 8 sections and incubated at 37ºC with RPMI 1640 with phenol red, 10% human serum, penstrep and 0.25mg/mL oxLDL. After 24, 48,72 and 96 hours the media was collected and stored at -80ºC before being analyzed on the Roche Diagnostics Lactate determination assay. Two way ANOVA significance is indicated from the 0 hour media control. The data is in duplicate from a single experiment. Significance levels are indicated as: (*) $p \leq 0.05$, (**) $p \leq 0.01$ and (***) $p \leq 0.001$.

### 3.7.2 The effect of γ-interferon on cultured plaque sections

γ-Interferon is an inflammatory cytokine that is important in the activation of macrophages to respond against viral and bacterial infections (Schoenborn 2007). γ-Interferon (500units per mL) was added to the plaque culture to stimulate the immune cells within the plaque and to determine the magnitude of immune activation over the 72-hour period. Stimulated macrophages release 7,8-NP, however, subsequent oxidation will form it's oxidative product, neopterin, which can be utilized as a biomarker to quantify the oxidative stress within the plaque (Schumacher 1997, Fuchs 2009). Total neopterin was measured to determine the 7,8-NP output from macrophage activation.

Analysis of the neopterin (**Figure 3.7.5**) over 0 – 72 hours revealed a significant increase of neopterin production in plaque sections 1 – 7 compared to 0 hours starting point. This showed that a single dose of γ-interferon amplifies the inflammatory response after every 24 hours and stimulates the macrophages to release oxidants into the environment. Total neopterin (**Figure 3.7.6**) showed a significant increase in all of the time points compared to 0 hour γ-interferon exposure, except for section 1 where the 48 and 72 hour exposure plateaued. The 7,8-NP graph (**Figure 3.7.7**) showed in sections 1 – 4 there was a significant increase in 7,8-NP between 0 – 48 hours although a decline in 7,8-NP production at 72 hours. This indicates that oxidative stress is occurring in sections 1-4 at 48 -72 hours, depleting the levels of 7,8-NP. There was a gradual increase of 7,8-NP in sections 5-7 over the 72 hours except for 48 hour with a reduction in 7,8-NP production.

Lactate production (**Figure 3.7.8**) in sections 1-7, shows that there was no significant difference over the 72 hours, indicating that each plaque section is maintaining a stable metabolism and γ-interferon is not cytotoxic to the plaque sections.
The data shows the decay of a single treatment of γ-interferon at 24 hours significantly increases oxidative stress and the 7,8-NP production of the plaque sections for 48 hours. The oxidative burst resulted in the oxidation of 7,8-NP and causing increasing concentrations of neopterin to leak out into the media.

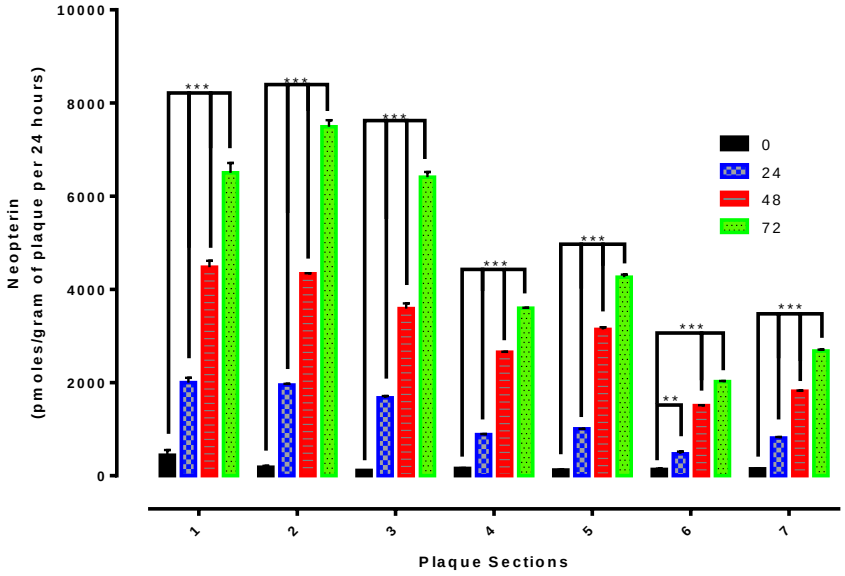


**Figure 3.7.5 The effect of γ-Interferon on Plaque 112 neopterin production.**

Plaque 112 was sliced into 7 sections and incubated at 37ºC with RPMI 1640 with phenol red, 10% human serum and penstrep. After 24 hours, γ-interferon (500 units per mL) then subsequent media changes at 48, 72 and 96 hours. The media was collected and analyzed for neopterin through the HPLC. Two way ANOVA significance is indicated from the 0 hour media control. The data is in duplicate from a single experiment. Significance levels are indicated as: (*) $p \leq 0.05$, (**) $p \leq 0.01$ and (***) $p \leq 0.001$. Sample collection and analysis was in conjunction with Hannah Prebble.

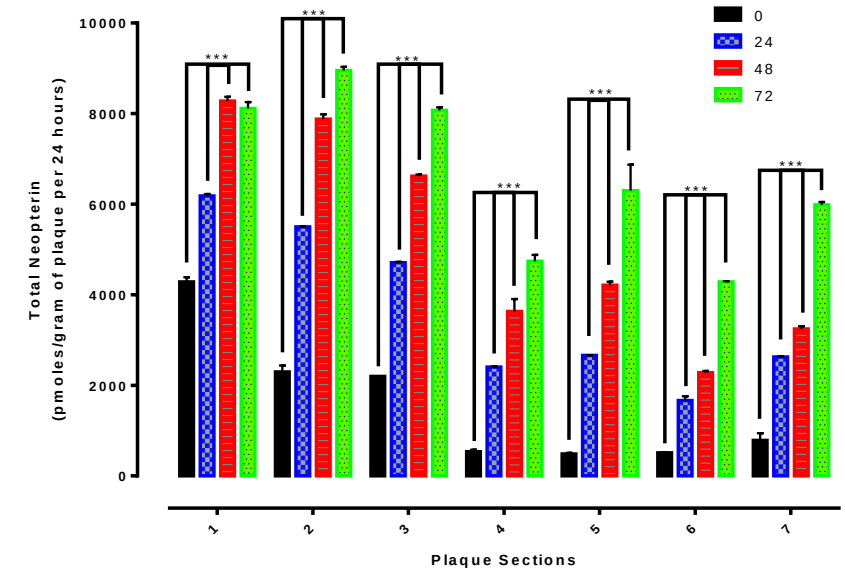


**Figure 3.7.6 The effect of γ-Interferon on Plaque 112 total neopterin production.**

Plaque 112 was sliced into 7 sections and incubated at 37ºC with RPMI 1640 with phenol red, 10% human serum and penstrep. After 24 hours, γ-interferon (500 units per mL) then subsequent media changes at 48, 72 and 96 hours. The media was collected and analyzed for neopterin through the HPLC. Two way ANOVA significance is indicated from the 0 hour media control. The data is in duplicate from a single experiment. Significance levels are indicated as: (*) $p \leq 0.05$, (**) $p \leq 0.01$ and (***) $p \leq 0.001$. Sample collection and analysis was in conjunction with Hannah Prebble.

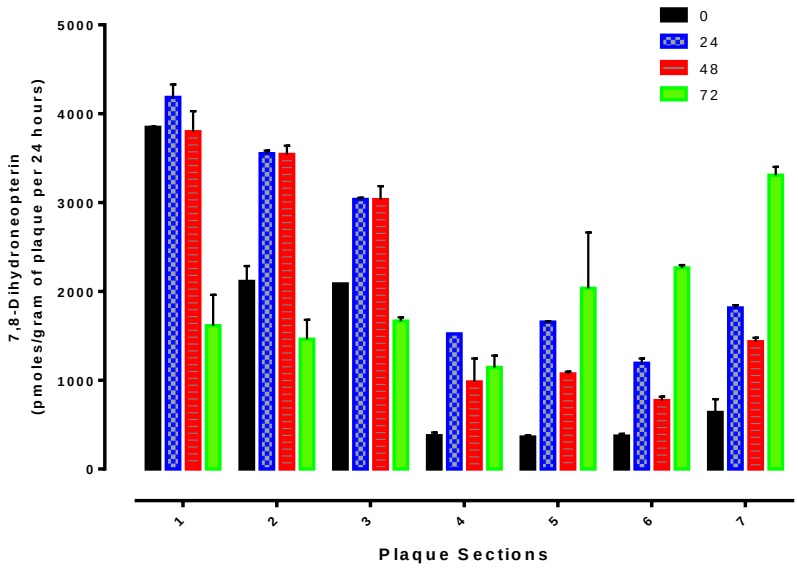


**Figure 3.7.7 The effect of γ-interferon on Plaque 112 7,8-dihydroneopterin production.**

Data represents the difference between neopterin and total neopterin values. Two way ANOVA significance is indicated from the 0 hour media control. The data is in duplicate from a single experiment.

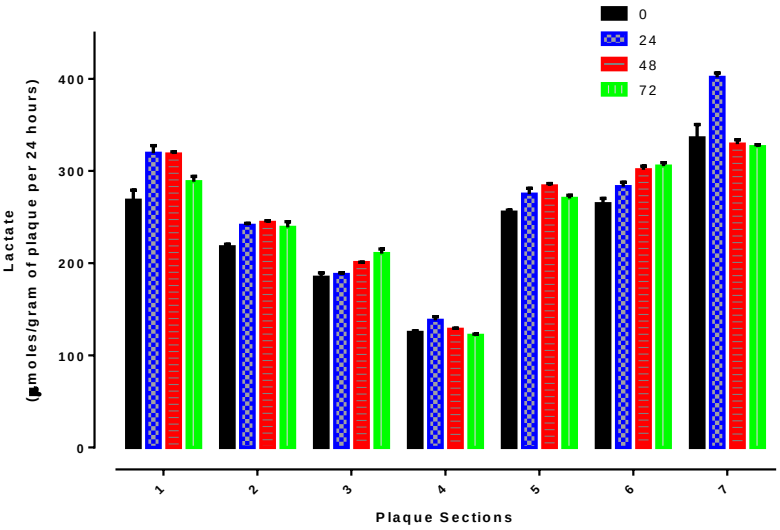


**Figure 3.7.8 The effect of γ-interferon on Plaque 112 lactate production.**

Plaque 112 was sliced into 7 sections and incubated at 37ºC with RPMI 1640 with phenol red, 10% human serum, penstrep. After 24 hours, γ-interferon (500 units per mL) then subsequent media changes at 48, 72 and 96 hours. The media was collected and stored at -80ºC before being analyzed on the Roche Diagnostics Lactate determination assay. Two way ANOVA significance is indicated from the 0 hour media control. The data is in duplicate from a single experiment. Significance levels are indicated as: (*) $p \leq 0.05$, (**) $p \leq 0.01$ and (***) $p \leq 0.001$. Sample collection and analysis was in conjunction with Hannah Prebble.

### 3.7.3 The effect of PMA on cultured plaque sections

Phorbol myristate acetate (PMA) has been shown to directly stimulate protein kinase C that in turn activates the NOX complex by phosphorylation of $p47^{phox}$. Activation of NOX induces extracellular release of oxidants, causing an oxidative stress environment (Karlsson 2000). Cultured live plaque sections were treated with 5µM PMA to stimulate T-cell activation in the plaque which is in turn was thought to stimulate the production of 7,8-NP. The activation of NOX has been reported to induce the release of oxygen radicals which react with 7,8-NP, forming it's oxidative product, neopterin.

The effect of PMA on plaque sections was investigated through analysis of lactate (**Figure 3.7.12**), neopterin (**Figure 3.7.9**) and 7,8-NP production (**Figure 3.7.10 & 3.7.11**) over 72 hours. The plaque was incubated in RPMI -1640 with 10% human serum media for 24 hours to determine the baseline of 7,8-NP and neopterin production. PMA was added to the plaque media after 24 (PMA day 1) and 48 (PMA day 2). Analysis of the neopterin (**Figure 3.7.9**) over 0-72 hours revealed a significant increase in neopterin production in all of the plaque sections except 4 and 5. There was a significant increase in neopterin production at PMA day 1 in all of the sections except 4 and 5 compared to the media only control. There was another significant increase in neopterin production in all of the plaque sections except 4 and 5 at PMA day 2, suggesting second day of PMA exposure the plaque has the biggest response to PMA. Total neopterin (**Figure 3.7.10**) showed a significant increase in all of the sections except 5 and 8 over the PMA exposure. This suggests that the plaque sections are up regulating the 7,8-NP production in response to PMA exposure. This was confirmed in **Figure 3.7.11** as there was a significant increase in 7,8-NP production in sections 1-3 compared to the media control. In sections 4-8 there was still a slight increase in 7,8-NP production suggesting this is occurring throughout the plaque sections.

The lactate graph (**Figure 3.7.12**) shows a significant increase in lactate production at PMA day 1 and 2 in sections 2-3, 6-8. This indicates that the PMA is increasing the plaque metabolism in both PMA days 1 & 2 which is shown by an increase in lactate production, however in section 1, there is a significant decrease in lactate production suggesting a decrease in plaque metabolism in response to PMA.

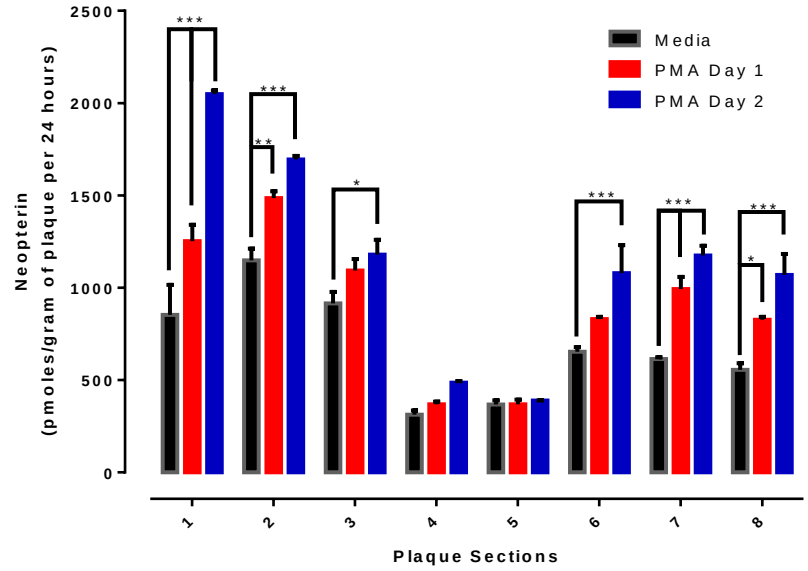


**Figure 3.7.9 The effect of 5µM PMA on Plaque 120 neopterin production.**

Plaque 120 was sliced into 8 sections and incubated at 37ºC with RPMI 1640 with phenol red, 10% human serum and penstrep. After 0, 24, 48, and 72 hours the media was collected and analyzed for neopterin through the HPLC. Two way ANOVA significance is indicated from the 0 hour media control. The data is in duplicate from a single experiment. Significance levels are indicated as: (*) $p \leq 0.05$, (**) $p \leq 0.01$ and (***) $p \leq 0.001$.

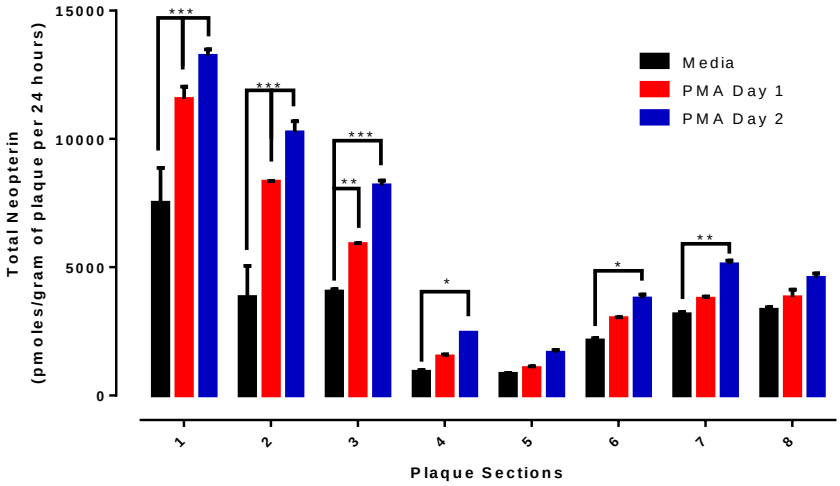


**Figure 3.7.10 The effect of 5µM PMA on Plaque 120 total neopterin production.**

Plaque 120 was sliced into 8 sections and incubated at 37ºC with RPMI 1640 with phenol red, 10% human serum and penstrep. After 24, 48,72 and 96 hours the media was collected and analyzed for neopterin through the HPLC. Two way ANOVA significance is indicated from the 0 hour media control. The data is in duplicate from a single experiment. Significance levels are indicated as: (*) $p \leq 0.05$, (**) $p \leq 0.01$ and (***) $p \leq 0.001$.

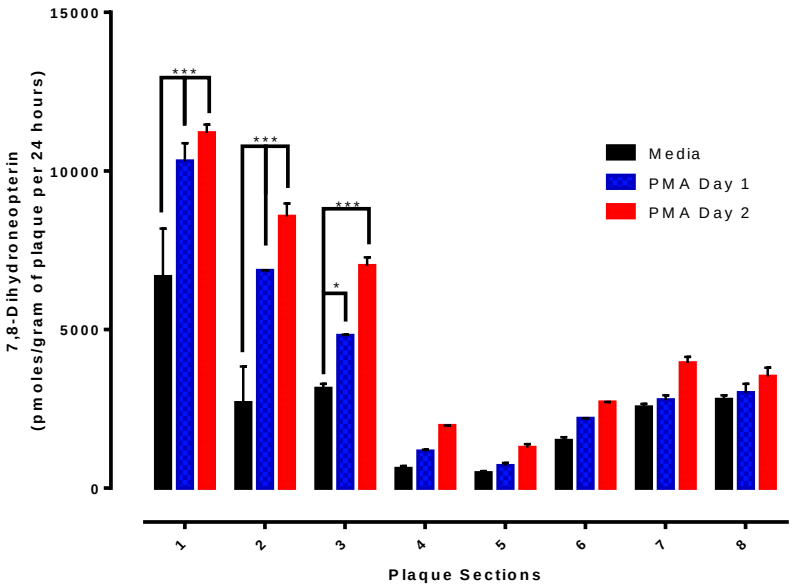


**Figure 3.7.11 The effect of 5µM PMA on Plaque 120 7,8-dihydroneopterin production.**

Data represents the difference between neopterin and total neopterin values. Two way ANOVA significance is indicated from the 0 hour media control. The data is in duplicate from a single experiment. Significance levels are indicated as: (*) $p \leq 0.05$, (**) $p \leq 0.01$ and (***) $p \leq 0.001$.

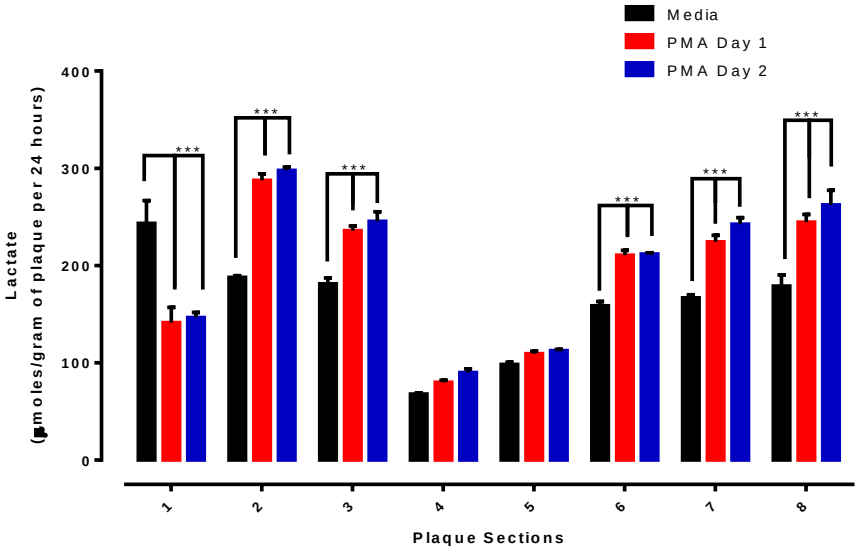


**Figure 3.7.12 The effect of 5µM PMA on Plaque 120 lactate production.**

Plaque 120 was sliced into 8 sections and incubated at 37ºC with RPMI 1640 with phenol red, 10% human serum, penstrep. After 24, 48,72 and 96 hours the media was collected and stored at -80ºC before being analyzed on the Roche Diagnostics Lactate determination assay. Two way ANOVA significance is indicated from the 0 hour media control. The data is in duplicate from a single experiment. Significance levels are indicated as: (*) $p \leq 0.05$, (**) $p \leq 0.01$ and (***) $p \leq 0.001$.

### 3.7.4 The effect of PMA and apocynin on cultured plaque section

As explained in **Section 1.7.2**, apocynin is a non-specific NOX inhibitor and functions by preventing the assembly of NADPH oxidase (NOX). The plaque was incubated in RPMI -1640 with 10% human serum media for 24 hours to determine the baseline of 7,8-NP and neopterin production. PMA was added to the plaque media after 24 hours to increase the oxidative stress within the plaque and PMA + apocynin was added after 48 hours to determine the effect the apocynin had on the neopterin production.

Analysis of the neopterin (**Figure 3.7.13**) showed a significant increase in neopterin production compared to the media control when incubated with 5µM PMA, similar to what was observed in **Figure 3.7.9**. A second incubation with 5µM PMA and 20µM apocynin showed a plateau or reduction of neopterin production in plaque sections 1-4. The plateau suggests that the apocynin reduced the NOX activity, minimizing the number of oxidants available to react with 7,8-NP. Section 4 showed a significant decrease in neopterin when apocynin was added; however, plaque section 8 showed a continuous increase over the duration. Interestingly, the total neopterin (**Figure 3.7.14**) showed a significant increase in all of the sections after the incubation with both PMA + apocynin, contrasting **Figure 3.7.13** where total neopterin plateau when apocynin was added. This suggests that apocynin is likely to have inhibited the NOX activity, preventing the production of oxidants and subsequent oxidation of 7,8-NP. This view was supported by the 7,8-NP graph (**Figure 3.7.15**), showing a significant burst of 7,8-NP production in all sections except 8 when apocynin + PMA was added compared to PMA only treatment. This suggests that the apocynin is inhibiting oxidant production and leaving excess 7,8-NP within the plaque.

The lactate graph (**Figure 3.7.16**) indicates the cell metabolism when exposed to PMA or apocynin. Sections 1 and 3 show a dramatic increase in metabolism once the PMA has been added. Results show a significant crash in lactate production once the PMA + apocynin has been added. Sections 2 and 4-8 show a gradual decrease in metabolism media only. This suggests that the PMA is changing the cellular metabolism or apocynin is causing the cell to undergo redox stress as apocynin has been shown to significantly increase intracellular glutathione concentrations, causing damage to the cell. However, the cell is still producing large amounts of 7,8-NP suggesting that the cellular processes are still intact and still functioning normally.

Therefore the results indicate that treatment of apocynin significantly decreased the oxidative stress produced by PMA and prevented the oxidation of 7,8-NP. Production of 7,8-NP suggests that the plaque is alive and functioning, although this conflicts with the lactate data that suggests that the plaques metabolism has significantly decreased. This indicates that the apocynin or PMA is changing the cell's metabolism.

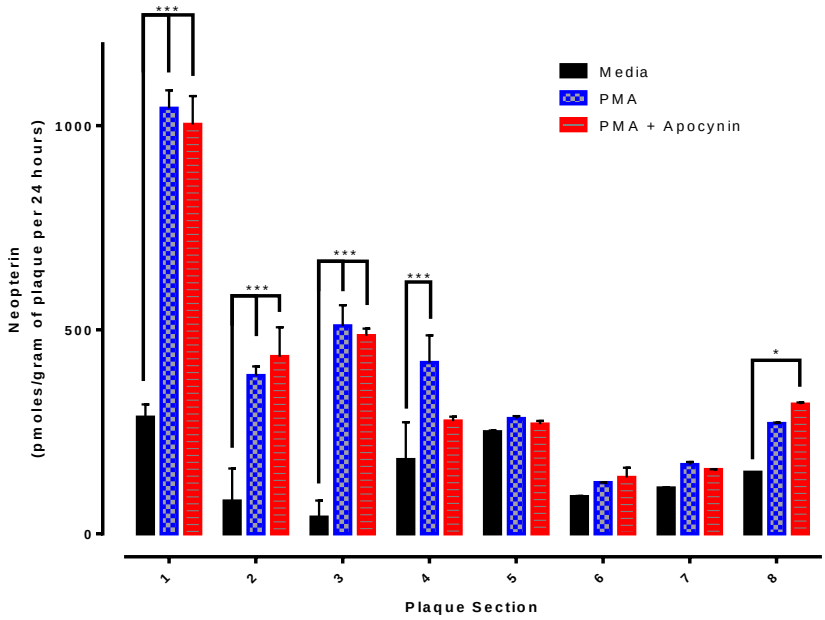


**Figure 3.7.13 The effect of PMA and apocynin on Plaque 114 neopterin production.**

Plaque 114 was sliced into 8 sections and incubated at 37ºC with RPMI 1640 with phenol red, 10% human serum and penstrep. After 0, 24, 48, and 72 hours the media was collected and analyzed for neopterin through the HPLC. Two way ANOVA significance is indicated from the 0 hour media control. The data is in duplicate from a single experiment. Significance levels are indicated as: (*) $p \leq 0.05$, (**) $p \leq 0.01$ and (***) $p \leq 0.001$.

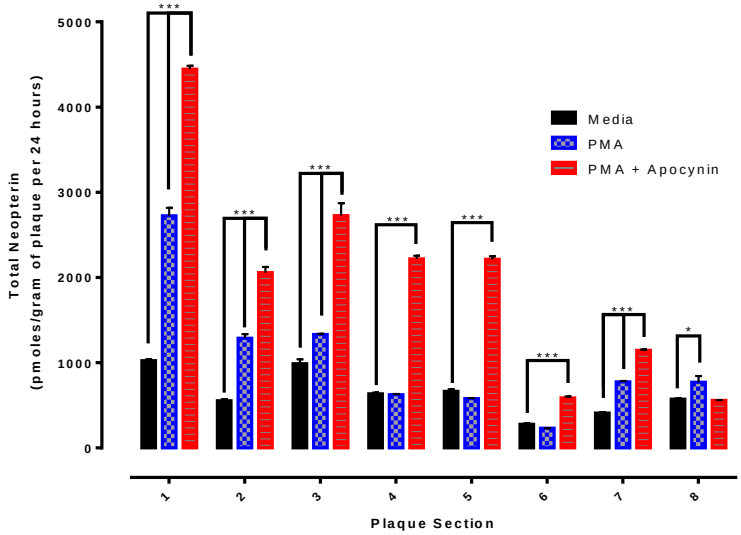


**Figure 3.7.14 The effect of PMA and apocynin on Plaque 114 total neopterin production.**

Plaque 114 was sliced into 8 sections and incubated at 37ºC with RPMI 1640 with phenol red, 10% human serum and penstrep. After 24, 48,72 and 96 hours the media was collected and analyzed for neopterin through the HPLC. Two way ANOVA significance is indicated from the 0 hour media control. The data is in duplicate from a single experiment. Significance levels are indicated as: (*) $p \leq 0.05$, (**) $p \leq 0.01$ and (***) $p \leq 0.001$.

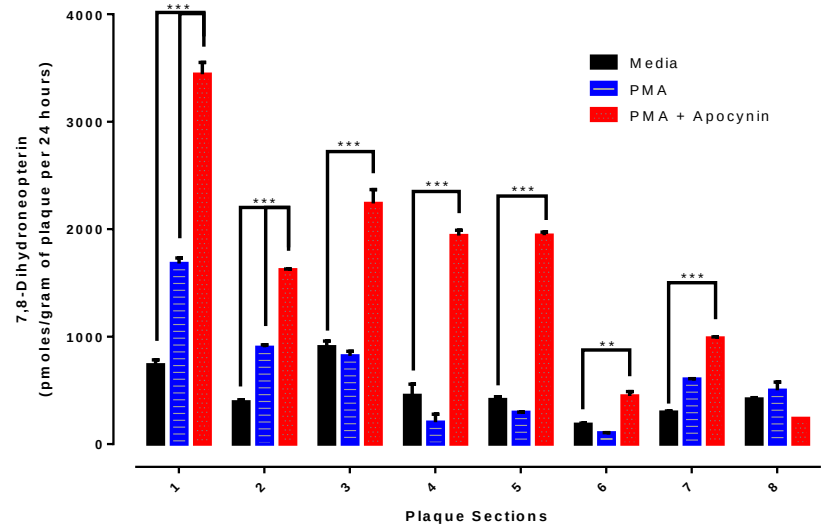


**Figure 3.7.15 The effect of PMA & apocynin on Plaque 114 7,8-dihydroneopterin production.**

Data represents the difference between neopterin and total neopterin values. Two way ANOVA significance is indicated from the 0 hour media control. The data is in duplicate from a single experiment. Significance levels are indicated as: (*) $p \leq 0.05$, (**) $p \leq 0.01$ and (***) $p \leq 0.001$.

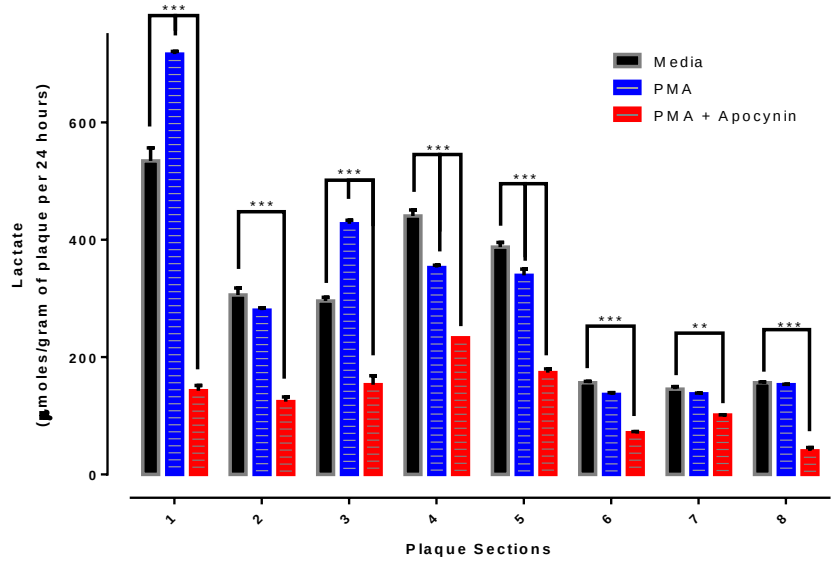


**Figure 3.7.16 The effect of PMA & apocynin on Plaque 114 lactate production.**

Plaque 114 was sliced into 8 sections and incubated at 37ºC with RPMI 1640 with phenol red, 10% human serum, penstrep. After 24, 48,72 and 96 hours the media was collected and stored at -80ºC before being analyzed on the Roche Diagnostics Lactate determination assay. Two way ANOVA significance is indicated from the 0 hour media control. The data is in duplicate from a single experiment. Significance levels are indicated as: (*) $p \leq 0.05$, (**) $p \leq 0.01$ and (***) $p \leq 0.001$.

### 3.7.5 The effect of PMA and gp91ds-tat on cultured plaque sections

Gp91ds-tat is a peptide that is designed to inhibit the assembly of the NOX complex, reducing the extracellular superoxide production. This experiment was a follow-up from the PMA + apocynin research that targets the NOX complex to reduce the oxidation of 7,8-NP to its highly fluorescent product, neopterin.

Apocynin and gp91ds-tat have similar mechanisms of inhibiting the assembly and activation of NOX complex. Therefore, similar trends were expected to have been seen such as a plateau effect occurring to the neopterin production as seen in **Figure 3.7.13** and increasing 7,8-NP after each media change as seen in **Figure 3.7.15** due to T-cell activation from PMA.

The plaque was incubated in RPMI-1640 with 10% human serum media for 24 hours to determine the baseline of 7,8-NP and neopterin production. PMA was added to the plaque media after 24 hours to increase the production of oxidative stress within the plaque and PMA plus gp91ds-tat was added after 48 hours to determine the effect the peptide inhibitor had on the neopterin production when NOX activity was significantly reduced.

Analysis of the neopterin (**Figure 3.7.17**) showed a significant increase in neopterin production compared to the media control when incubated with 5µM PMA, similar to what was observed in **Figure 3.7.9**. However, second incubation with 5µM PMA and 0.5µM gp91ds-tat showed an significant increase in neopterin production in plaque sections 1-7. This suggests that the gp91ds-tat was not inhibiting the NOX complex or preventing the oxidation of 7,8-NP. Total neopterin (**Figure 3.7.18**) showed a significant increase in sections 1-7 after the 48 hours incubation with both PMA plus gp91ds-tat. The 7,8-NP concentrations (**Figure 3.7.19**) were significantly increased in sections 1 – 7 after gp91ds-tat + PMA exposure compared to PMA only treatment.

The lactate (**Figure 3.7.20**) showed an increase in lactate production in sections 1-7 when PMA added but a decrease in lactate production occurred with PMA plus gp91ds-tat treatment. These results are similar findings to what was observed in the initial PMA only study (**Figures 3.7.9 - 12**) suggesting that there is no inhibitory effect occurring when 0.5µM gp91ds-tat was added to the plaque media. Future research could investigate higher concentrations (1µM) of the inhibitor to see if there is a reduction in neopterin.

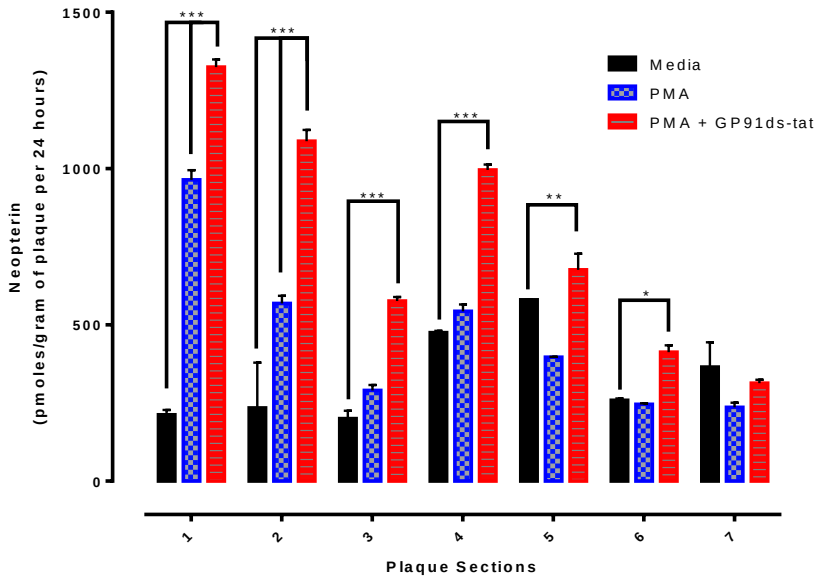


**Figure 3.7.17 The effect of 5µM PMA and 0.5µM gp91ds-tat on Plaque 116 neopterin production.**

Plaque 116 was sliced into 7 sections and incubated at 37ºC with RPMI 1640 with phenol red, 10% human serum and penstrep. After 24, 48, 72 and 96 hours the media was collected and analyzed for neopterin through the HPLC. Two way ANOVA significance is indicated from the 0 hour media control. The data is in duplicate from a single experiment. Significance levels are indicated as: (*) $p \leq 0.05$, (**) $p \leq 0.01$ and (***) $p \leq 0.001$.

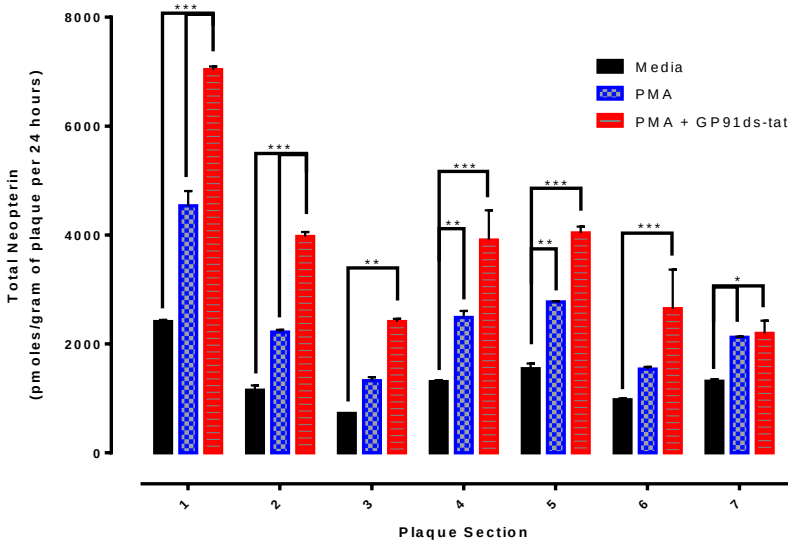


**Figure 3.7.18 The effect of 5µM PMA and 0.5µM gp91ds-tat on Plaque 116 total neopterin production.**

Plaque 116 was sliced into 7 sections and incubated at 37ºC with RPMI 1640 with phenol red, 10% human serum and penstrep. After 24, 48, 72 and 96 hours the media was collected and analyzed for total neopterin through the HPLC. Two way ANOVA significance is indicated from the 0 hour media control. The data is in duplicate from a single experiment. Significance levels are indicated as: (*) $p \leq 0.05$, (**) $p \leq 0.01$ and (***) $p \leq 0.001$.

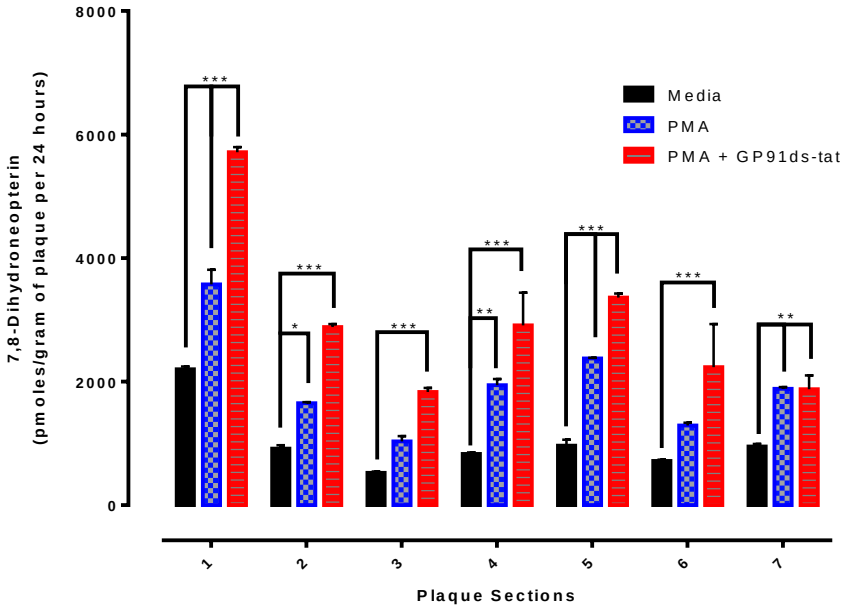


**Figure 3.7.19 The effect of gp91ds-tat on Plaque 116 7,8-dihydroneopterin production.**

Data represents the difference between neopterin and total neopterin values. Two way ANOVA significance is indicated from the 0 hour media control. The data is in duplicate from a single experiment. Significance levels are indicated as: (*) $p \leq 0.05$, (**) $p \leq 0.01$ and (***) $p \leq 0.001$.

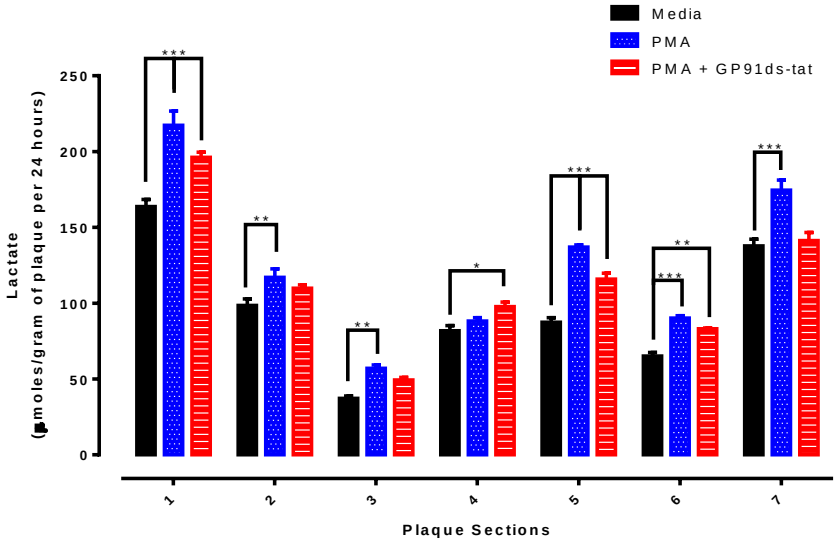


**Figure 3.7.20 The effect of 5µM PMA and 0.5µM gp91ds-tat on Plaque 116 lactate production.**

Plaque 116 was sliced into 7 sections and incubated at 37ºC with RPMI 1640 with phenol red, 10% human serum, penstrep and 0.25mg/mL oxLDL. After 24, 48,72 and 96 hours the media was collected and stored at -80ºC before being analyzed on the Roche Diagnostics Lactate determination assay. Two way ANOVA significance is indicated from the 0 hour media control. The data is in duplicate from a single experiment. Significance levels are indicated as: (*) $p \leq 0.05$, (**) $p \leq 0.01$ and (***) $p \leq 0.001$.

# 4. DISCUSSION

Previous studies have shown that oxLDL toxicity is caused by an over production of intracellular oxidants indicated by an increase of cellular DHE staining (**Figure 3.3.1**), loss of cellular glutathione (Kappler 2007, Gieseg 2010 B), reduction in essential metabolic enzyme activity (Katouah 2015) and loss of caspase function (Baird 2004, Gieseg 2008). Metabolic dysfunction and inactivation of caspase-3 through the oxidative damage to the thiol groups result in the inability of the cell to undergo apoptosis and defaults to necrosis (Baird 2004, Katouah 2015). This study investigated the source of the cytotoxic oxidative stress triggered by the presence of oxLDL in U937 monocyte like cells. The research investigated whether NADPH oxidase, myeloperoxidase or uncoupled mitochondria generated intracellular oxidants in response to oxLDL.

## 4.1 NADPH oxidase (NOX) & Oxidative stress

### 4.1.1 NOX, a primary source of oxidative stress

Chen (2012) investigated the role of NOX-2 in the intracellular superoxide generation in response to oxLDL and this study follows on from their previous research. This research explored the hypothesis of oxLDL inducing a hyper activation of the NOX complex and generating an overproduction of intracellular oxidants causing significant U937 cell death.

This research utilized a highly specific peptide NOX inhibitor called gp91ds-tat that was designed by Rey (2001). This inhibitor specifically binds to $P47_{phox}$ subunit and prevents the assembly and activation of NOX. Gp91ds-tat showed a significant reduction of intracellular superoxide generation when U937 cells were incubated with oxLDL (**Figure 3.4.3 and 3.4.5**). The significant reduction of intracellular superoxide suggests that NOX is the major source of oxLDL-induced oxidative stress. This is in concert with what was observed in Rey (2001), as they showed that gp91ds-tat caused a 35% decrease of NOX activity in human neutrophils and an 80% reduction in superoxide production in a cell free assay. Other research utilising this inhibitor found it to be very effective causing an 80% reduction in superoxide production in bovine pulmonary artery endothelial cells (BPAEC) (Jaimes 2004).

Rey (2001) states that gp91ds-tat is capable of inhibiting other NOX homologs that contain the $gp91_{phox}$ and $P47_{phox}$ subunits. However, there is little evidence in the literature of other NOX homologs present in phagocytic cell lines or research of gp91ds-tat concentration toxicity occurring in other cell lines (Bánfi 2001, Bánfi 2003).

It was expected that the reduction in superoxide generation would prevent oxidative damage occurring to the cell and a subsequent increase of cell viability. However, the inhibitor provided virtually no cell viability protection when U937 cells were incubated with oxLDL (**Figure 3.4.4 and 3.4.6**). This laboratory has shown previously that apocynin reduced intracellular superoxide production in U937 cells, like gp91ds-tat, apocynin only provided a 20% protection against oxLDL induced cell death (Chen 2012). Apocynin has been shown to cause the cell to undergo reductive stress by inducing an up regulation of GSH production (Lapperre 1999). It is unknown if gp91ds-tat induces the same effect as GSH was not measured.

The lack of cell viability protection could also be a result of chronic oxLDL exposure and the cell is already committed to cell death (Tabas 1997, Tabas 2010) or the residual oxidative stress is inducing significant oxidative damage to the cell. Gp91ds-tat inhibited the intracellular oxidative stress by 70 – 90% (**Figure 3.4.5 & 3.4.3**) and there is a number of theories that could explain the residual 10 – 30% oxidative stress and the lack of cell viability.

Dihydroethidium is a known fluorescent probe that reacts with intracellular superoxide and intercalates in the DNA, emitting a red fluorescence (Peshavariya 2007). There is some conjecture on whether the probe is an accurate representation of oxLDL-induced oxidative stress or if the gp91ds-tat inhibition is a gross-exaggeration of the events that are occurring. It is unknown if the cells are exposed to more oxidative stress than what is being detected with DHE, potentially explaining the lack of cell viability protection.

Another explanation is the possibility of a secondary source contributing to the residual oxidative stress. It is possible that oxLDL activates other NOX homologs and causes them to produce oxidants. In genetically modified phagocytic cells (PLB-985

leukaemia and X-CGD CD34+ PBSC cells), Geiszt (2003) demonstrated that a complete NOX2 knockout showed an up regulation of other NOX homologs to compensate for the NOX-2 deficiency (Geiszt 2003). However, it is highly unlikely as complete NOX-2 inhibition in U937 cells would be unable to up regulate other NOX isoforms within 6 hours of oxLDL exposure.
Additionally, it was demonstrated that NOX4 was inducible in human macrophages and monocytes treated with oxLDL (Lee 2010). Although, Othman (2015) demonstrated in U937 cells, that VAS2870 (NOX4 inhibitor) did not reduce the intracellular oxidative stress or provided no cell viability protection against oxLDL (Othman 2015). This suggests that NOX4 is not induced by oxLDL in the U937 cell oxidative stress mechanism.

OxLDL could be inducing additional sources of intracellular oxidative stress (the mitochondria (**Section 4.3.2**), myeloperoxidase (**Section 4.2**) and xanthine oxidase), which may contribute to the production of intracellular oxidants. Xanthine oxidase catalyses the degradation of hypoxanthine and xanthine to uric acid and giving off superoxide as a byproduct (Schulze 2005). Xanthine oxidase activity has been reported to increase by 200% and closely associated with increased vascular oxidative stress in patients with chronic heart failure (Landmesser 2002). However, there is little evidence of oxLDL stimulating xanthine oxidase to produce oxidative stress in isolated macrophages.

The most convincing explanation is that gp91ds-tat is a competitive inhibitor for the binding site on the $P47_{phox}$ subunit, inhibiting the activation of the NOX-2 complex. The inhibitor can reversibly bind to the binding site and is competing with the $gp91_{phox}$ subunit that activates the complex, generating superoxide (Rey 2001).
This explains why at lower gp91ds-tat concentrations, there is less inhibitor competing for the $p47_{phox}$-binding site, with the intracellular oxidative stress decreasing with increasing inhibitor concentration (**Figure 3.4.5 & 3.4.3**). However, even at maximum inhibitor concentrations, there was not 100% NOX inhibition because the $gp91_{phox}$ subunit was still competing for the binding site and activating complex, generating the residual oxidative stress. This provides insight that the oxidative mechanism is not as clear-cut as previously thought, as partial removal of NOX does not protect U937 cells from oxLDL induced death. This suggests that the

cells are either committed to the oxLDL induced cell death as soon as 6 hours through ER stress (Tabas 2010, Tsukano 2010) or the residual oxidative stress is still causing extensive damage to the cell.

An important question arising from this study is whether the increase of intracellular oxidative stress (**Figure 3.3.1**) was solely superoxide or a combination of hypochlorite and superoxide. Dihydroethidium fluorescent probe is supposed to react specifically with superoxide anions however, hypochlorite needed to be eliminated from the equation to ensure that the intracellular oxidative stress was entirely superoxide. A potent MPO inhibitor (ABAH) was utilized as a tool to inhibit the generation of hypochlorite (Kettle 1997), the experiment showed that the intracellular oxidative stress was specifically superoxide and not hypochlorite (**Figure 3.6.4**). This suggests that the intracellular oxidative stress generated in response to oxLDL exposure is superoxide (Katouah 2015). This is important as it supports the theory that oxLDL is inducing overproduction of superoxide generated from the NOX complex.

### 4.1.2 NOX is causing the intracellular oxidation of 7,8-NP

Neopterin has been extensively used as a clinical marker of immune cell activation in a variety of inflammatory diseases, including cardiovascular disease (Berdowska 2001, Gieseg 2008). It is often stated that neopterin is the oxidative product of 7,8-dihydroneopterin (Firth 2008, Mangge 2014), however, the mechanism of neopterin generation in cells is currently unknown. 7,8-Dihydroneopterin has been shown to have antioxidant capabilities, by providing cell viability protection (**Figure 3.1.4**) and causing a reduction of intracellular oxidative stress (**Figure 3.3.2**) in U937 cells. These results are in agreement with Gieseg (2010 B) as they saw 7,8-NP cell viability protection in HMDM.

#### *In vitro* study

Previous *in vitro* research has implicated NOX in the intracellular superoxide generation by treating oxLDL exposed U937 cells to apocynin. It was shown that apocynin significantly reduced the intracellular superoxide generation and restored the glutathione (Chen 2012). Additionally, it was demonstrated in peritoneal macrophages that administration of apocynin suppressed oxidant generation and

expression of atherogenic cytokines (Kinoshita 2013). NOX2 was further implicated in the oxLDL-induced mechanism as NOX-2 expression was equally elevated in oxLDL or PMA treated U937 cells, suggesting that oxLDL can activate the NOX2 complex and generate oxidants (Katouah 2015). This sections objective was to investigate the involvement of NOX-2 in the oxidation of 7,8-NP to neopterin in oxLDL exposed U937 cells. It was shown that oxLDL induced a significant elevation of intracellular neopterin in U937 cells at 6 hours, corresponding to oxLDL-induced 7,8-NP oxidation (**Figure 3.3.7 – 3.3.9**). Similar findings were found in a previous studies with HMDM, observing a significant generation of intracellular neopterin between 6 – 12 hours oxLDL exposure (Shchepetkina 2013). This suggests that oxLDL is inducing an increased production of intracellular oxidants that is oxidizing 7,8-NP to neopterin. This research has suggested that NOX-2 is implicated in the acute oxLDL toxicity mechanism (**Figure 3.4.3 & 3.4.5**) along with superoxide anions (**Figure 3.6.4**). This led to the hypothesis that superoxide is causing the intracellular oxidation of 7,8-NP to neopterin in HMDM and U937 cells. U937 cells that were incubated with a potent NOX inhibitor (apocynin) showed a significant reduction of intracellular neopterin generation after 12 hours (**Figure 3.3.10 – 3.3.11**). Similar results were shown in our laboratory with HMDM, showing a significant reduction of neopterin production after 12 hour incubation with both oxLDL and apocynin compared to the oxLDL only treatment (Shchepetkina 2013). This suggests that NOX-2 plays an important role in the intracellular oxidation of 7,8-NP and confirming that superoxide is the major intracellular oxidant in both U937 cells and HMDM. A notable difference between this research and Shchepetkina (2013) (besides the different cell type) was the concentration of apocynin and the length of preincubation before the addition of oxLDL. HMDM were preincubated with 200µM apocynin for 3 hours before the addition of oxLDL and showed a significant reduction of intracellular neopterin at 6 hours (Shchepetkina 2013). When U937 cells were preincubated with 20µM apocynin for 15 minutes before the addition of oxLDL, there was a significant reduction of neopterin at 12 hours. Ignoring the differences between cell types, this indicates that apocynin requires a prolonged preincubation period to effectively prevent NOX assembly and subsequent oxLDL induced 7,8-NP oxidation.

## *In vivo* study

Previous research in this lab has mainly focused on *in vitro* studies, utilizing cell lines to mimic the conditions of what macrophages would experience in an atherosclerotic plaque. The following research focused on culturing atherosclerotic plaques and comparing to what is being observed *in vitro* research. It is commonly accepted that NOX-2 plays an important role in the oxidative events that are occurring within the atherosclerotic plaque. Previous research has developed a clear link between atherosclerotic plaque susceptible (ApoE $^{-/-}$) mice have elevated levels of NOX-2 expression and through the deletion of NOX2, resulted in the inhibition of lesion development (Judkins 2010). Additionally, atherosclerotic lesions had significant superoxide staining accompanied with increased NOX2 expression (Sorescu 2002). These studies suggested that NOX2 has a more prominent role in atherosclerotic lesion development than expected.

Like the *in vitro* research, this sections objective was to investigate the involvement of NOX-2 in the oxidation of 7,8-NP to neopterin in atherosclerotic plaque sections. PMA is an inflammatory cytokine that directly stimulates protein kinase C (PKC) which in turn induces the production of 7,8-NP and assembly of the NOX-2 complex in activated macrophages (Karlsson 2000). This research investigated the use of NOX inhibitors (apocynin and gp91ds-tat) to see if they prevented the oxidation of 7,8-NP in immune activated plaque sections. Apocynin treated plaque sections (**Figure 3.7.13 - 15**) showed significant reduction in 7,8-NP oxidation and neopterin formation. These results were in agreement to what was observed in apocynin treated cell culture experiments (**Figure 3.3.10 – 3.3.11**) with a reduction of 7,8-NP oxidation through the inhibition of oxidants generated from the NOX-2 complex. This indicates that the apocynin has inhibited the oxidant production by blocking the activation of NOX that in turn prevents further oxidation of 7,8-NP. Gp91ds-tat activated plaque sections (**Figure 3.7.17 - 19)** did not prevent the 7,8-NP oxidation, suggesting that NOX-2 was not inhibited. We suspect that a higher concentration of gp91ds-tat was required to see similar results to what was found in the apocynin-treated plaque sections (**Figure 3.3.10 – 3.3.11**). Additionally, hypercholesteremic (ApoE$^{-/-}$/LDLR$^{-/-}$) mice treated with apocynin marked a significant reduction of atherosclerotic lesion size in thoracic and abdominal aorta. This suggested that apocynin attenuates the progression of

atherosclerotic lesions in ApoE$^{-/-}$ mice by inhibiting the generation of superoxide from the NOX complex (Kinkade 2013). Collectively, the data suggests that NOX-2 is the primary source of oxidative stress in both oxLDL-exposed U937 cells and PMA activated plaque sections. Additionally, NOX-generated superoxide appears to be the major intracellular oxidant that is generated causing the extensive oxidative damage and subsequent cell death. OxLDL-induced cell death is a key player in the development of the necrotic core, driving the progression of the atherosclerotic plaque.

## 4.2 Myeloperoxidase (MPO)

Myeloperoxidase has been considered to be another potential source of oxidative damage to the cell and resulting in subsequent cell death. Sugiyama (2004) demonstrated that MPO-positive macrophages can disrupt the endothelial cell monolayer and induce cell death. The concentrations of hypochlorite that were reported in Sugiyama (2004) were within range of what is found in sites of inflammation (Epstein 1989). Hypochlorite has been shown to be a common substituent in atherosclerotic plaque, suggesting that MPO is highly active within this site (Hazen 1997). Hypochlorite can directly induce endothelial dysfunction (Zhang 2001), degrade the extracellular matrix proteins between endothelial cells (Vissers 1997), and activate dormant metalloproteinase which can make the atherosclerotic plaque unstable (Galis 1994, Fu 2001). *In vitro* research has shown hypochlorite to induce cell death by decreasing cellular ATP levels (Schraufstätter 1990) and rapidly provoke endothelial apoptosis, likely through GSH depletion, Bcl-2 degradation and cytochrome c release from the mitochondria (Sugiyama 2004). As MPO and its oxidative products have been extensively found within atherosclerotic lesions, this research investigated the link between oxLDL exposure and MPO induced oxidative stress in U937 cells. It was hypothesized that U937 cells incubated with MPO inhibitors (thiocyanate & ABAH) would prevent hypochlorite formation thus preventing oxidative damage occurring to the cell and restore the cell viability. U937 cells incubated with thiocyanate (SCN) ions showed no protective effects occurring to the cell viability when exposed to oxLDL (**Figure 3.6.2**). Thiocyanate has been shown to provide protective effects in human lung epithelial cell line (Calu-3) against hypochlorite and hydrogen peroxide cytotoxicity (Xu 2009). U937 cells treated with

ABAH showed virtually no protection against oxLDL treatments (**Figure 3.6.3**), suggesting that MPO does not play a part in the oxLDL induced cell death mechanism. However, ABAH has been shown to provide significant cell viability protection against oxidant-generated apoptosis in myeloid leukaemia cells (HL-60, NB4 and UF-1). This was due to ABAH causing a significant reduction in MPO activity, oxidant production and a subsequent increase in cell viability (Nakazato, 2007). Both ABAH and thiocyanate have been shown to be potent inhibitors against hypochlorite and hydrogen peroxide mediated cell death. In our experiments no protection against oxLDL induced cell death was observed with these inhibitors. This suggests that U937 cells are dying of the oxLDL-induced toxicity regardless of MPO inhibition, suggesting that MPO does not play a part in the *in vitro* oxLDL induced U937 cell death mechanism. An experiment performed by Kramarenko (2006) showed that U937 cells had undetectable MPO activity suggesting that U937 cells do not secrete activated MPO enzyme (Kramarenko 2006). This explains the lack of cell viability protection with MPO inhibitors because U937 cells have little MPO activity to begin with.

## 4.3 Mitochondria induced oxidative stress

Mitochondria produce a basal level of superoxide anions as a result of electron leakage from complex I and III (Lenaz 2002). It was considered that if the mitochondria had received significant damage that the reverse electron transport chain phenomenon would produce a large amount of oxidative stress within the cell (Liu 2002). This suggested that the mitochondria could be a potential source of intracellular oxidative stress as significant oxLDL damage to U937 cells could produce oxidative stress.

### 4.3.1 JC-1 assay provided inconclusive evidence

Our research set out to investigate the effect oxLDL on the mitochondria, what time frame is this damage was occurring and whether 7,8-NP protected the mitochondria from the oxLDL-induced damage. We expected to determine the effect oxLDL had on the mitochondria and show that it was an oxidative stress damaging the mitochondria. The JC-1 staining technique functions by forming aggregates within the mitochondria membrane and enabling the quantification of mitochondrial function. Healthy

mitochondria exhibit a high mitochondrial potential through red-aggregation of the dye, while the dye forms green monomers at low membrane potential. Mitochondria that exhibit a strong red fluorescence (FL-2) have a high mitochondrial potential whereas mitochondria that have a high green fluorescence (FL-1) have a low mitochondrial membrane potential (Galluzzi 2007, Honeychurch 2012). The results showed that oxLDL induced a significant depolarization of the mitochondria membrane potential at 6 hours (**Figure 3.5.1& 3.5.2)** and that 7,8-NP did not protect the mitochondria depolarization (**Figure 3.5.5 & 3.5.6)**. However, the oxLDL treatment dot plots did not display the intermediate stages of what was shown in the cell only control (healthy mitochondria - high FL-2 and a low FL-1) and the CCCP control (unhealthy mitochondria - decrease in FL-2 with an increase in FL-1). The FL-2:FL-1 ratio graphs (**Figure 3.5.1& 3.5.2**) displayed a clear trend of a significant reduction of FL-2 with a proportional increase of FL-1 between the two controls (cell only and CCCP). As there was no consistency between these two data sets, we are unable to draw conclusions from these findings, as we believe there is a fundamental problem residing in the JC-1 assay. In comparison to research presenting JC-1 dot plots, sea urchin sperm cells showed a significant 89% decrease in the FL-2 dot plots compared to the healthy control, but did not see an increase of FL-1 green monomers (Binet 2014). Similar research examining the JC-1 dot plots of horse sperm cells, showed a decrease in FL-2 with an increase of FL-1 fluorescence (Gravance 2000). The dot plots from Gravance (2000) displayed similar trends to what was stated by the manufactures (decrease in FL-2 with a subsequent increase of FL-1 fluorescence for unhealthy mitochondria) that was not observed in this research or Binet (2014). Further research should utilize another mitochondria specific marker to assess the mitochondria membrane potential as a result of oxLDL exposure.

### 4.3.2 The involvement of the mitochondria in oxidative stress

The mitochondria is considered to be one of the major sources of oxidative stress in the cell, capable of generating superoxide anions, hydrogen peroxide, and hydroxyl radicals within the cell (Esposito 1999). Inhibition of the mitochondria electron transport chain by antimycin A (complex III inhibitor) results in a significant increase in mitochondrial superoxide (Boveris 1973, Boveris 1975) and hydrogen peroxide production (Kwong 1998, Chen 2003). This results in the phenomenon observed in Liu (2002) of reverse electron flow on to molecular oxygen, generating superoxide

anions. Significant oxidative damage to the mitochondria through oxLDL could result in the decoupling of mitochondrial ATP generation and increased oxidant production from the mitochondria. OxLDL-induced damage to the mitochondria could contribute to either increased intracellular oxidative stress or the cell undergoing a cell death as the mitochondria is known to have an essential role in an apoptotic programmed cell death (Murphy 2009). Previous research using MitoSOX dye in our laboratory suggested there was significant generation of mitochondrial superoxide within U937 cells when incubated with increasing concentrations of oxLDL (Chen 2012). Comparison between the DHE staining and the mitochondrial superoxide production suggested that mitochondrial superoxide generation could be a secondary event initiated by excess cytoplasmic oxidative stress. This indicated that the mitochondria oxidant generation was a later event rather than a primary source (Chen 2012). Although the JC-1 mitochondrial data did not provide an accurate conclusion, previous research suggests that the mitochondria could contribute to the oxLDL-induced intracellular oxidative stress through mitochondria dysfunction. As the mitochondria is involved in cell survival and death, extensive oxidative damage could cause cell death and eventuate to necrotic core development and disease progression.

## 4.4 General discussion

Atherosclerosis is a complex disease that is a caused by constant inflammation of the inner arterial intima due to death of macrophages as a result of oxLDL exposure (Libby 2002). Previous literature suggests that oxLDL induces its cytotoxicity through cholesterol accumulation and ER stress (Myoishi 2007, Tsukano 2010, Scull 2011). However, from this research it can be hypothesized that oxLDL can induce two mechanisms, a rapid cytotoxicity (oxidative stress generation) and a chronic toxicity (ER stress). This research extensively studies the acute toxicity of oxLDL, inducing significant oxidant generation within U937 cells (**Figure 3.3.1**) and causing significant cell death (**Figure 3.1.1**). The hypothesized cytotoxicity mechanisms of oxLDL and the findings from this research have been summarized in **Figure 6.1**.

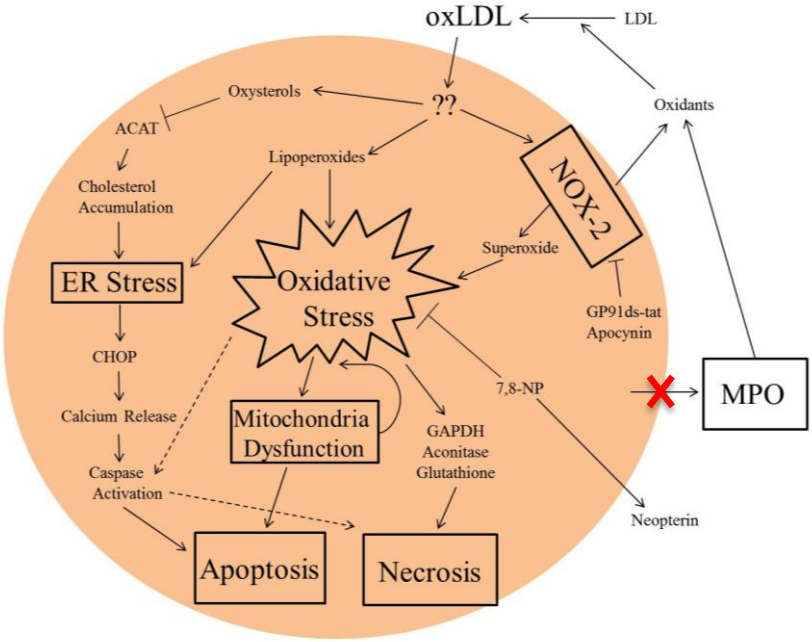


**Figure 4.1 Overview of the intracellular oxidative mechanisms occurring when U937 cells interact with oxLDL**

OxLDL can induce a range of intracellular responses to U937 cells, by causing a rapid generation of intracellular oxidative stress through NOX-2 activation, oxidizing essential enzymes involved in metabolism, cell death mechanism or cellular defence. Alternatively oxLDL can induce the accumulation of intracellular cholesterol, causing prolonged ER stress and subsequent caspase activation. Both mechanisms result in either an apoptotic or necrotic cell death mechanism, contributing to the development of the necrotic core.

Myeloperoxidase (MPO) was shown to not be involved in the U937 cell line oxidative stress mechanism (**Figure 6.1**), however, traditional sources of MPO include blood neutrophils (Sugiyama 2001) and lesional macrophages in atherosclerosis (Daugherty, 1994). Additionally, hypochlorite has been shown to be a common substituent in atherosclerotic plaque, suggesting that MPO is highly active within this site (Hazen 1997). Hypochlorite induced a significant loss of intracellular GSH, GAPDH activity and subsequent loss of cell viability in human monocyte-derived macrophages (HMDM) (**Figure 6.1**) (Schraufstätter 1990, Sugiyama 2004, Yang 2012 B). Collectively, this indicates that although MPO was not present in the U937 cells mechanism, once human neutrophils or lesional macrophages produce hypochlorite, it is capable of causing extensive oxidative damage to the cell resulting in a necrotic cell death (Yang 2012 B).

Our research has provided strong evidence that NOX-2 is involved in the generation of intracellular superoxide in response to oxLDL and induces the cytotoxic effects as seen above (**Figure 6.1**). It has been shown that acute oxLDL toxicity is capable of inducing different cellular responses dependent on the cell type. For example, oxLDL

induces THP-1 apoptosis with caspase activation (Baird 2004) while in HMDM and U937 cells, oxLDL causes an increase of oxidative stress and subsequent necrotic cell death without caspase activation (**Figure 6.1**) (Gieseg 2008, Gieseg 2010 B, Katouah, 2015). However, the exact cause of this variation in acute oxLDL cytotoxicity remains unknown. It is unknown if oxLDL is solely inducing the activation of NOX oxidative stress, generating the intracellular oxidative stress or if oxLDL is causing a combination of oxidative induced damage and ER stress, resulting in cell death (**Figure 6.1**). Understanding the mechanisms of how oxLDL exerts its toxicity on a cell type allows for future research into prevention of cell death. Cell death causes constant inflammation of the arterial intima and subsequent development of the necrotic core. By reducing the oxLDL mediated radical generation, it may be possible to prevent the inflammatory events that lead to progressive macrophage recruitment and plaque growth.

## 4.5 Future Research

Future research should investigate the mechanism between NOX inhibition and the secondary source of oxidative stress. This could be achieved by incubating U937 cells with gp91ds-tat plus 7,8-NP and determine (through PI-cell viability and DHE assay) if the background oxidative stress is completely inhibited through 7,8-NP protection.

There is a possible avenue to verify the trends seen in U937 NOX inhibition with other cell lines such as human monocyte derived macrophages (HMDM) or THP-1 cells, to determine if what is observed is a cell line specific response.

Another area that is yet to be explored is the link between the oxLDL-induced oxidative stress and the reduction in mitochondria membrane potential. Utilizing a different fluorescent dye would be beneficial to determine if the decrease in membrane potential is a result of oxidative damage or if the cell is undergoing a cell death mechanism. *In vivo* research could investigate the effect of higher GP91ds-tat concentrations (1-2µM) or the effect of ABAH on human plaque sections to determine if there is a reduction in 7,8-NP oxidation to neopterin.

## 4.6 Summary

This research confirms that oxLDL is inducing significant increase of intracellular oxidative stress, followed by a subsequent cell death in U937 cells. Myeloperoxidase did not contribute to the intracellular oxidative mechanism nor did MPO inhibitors protect the cells from dying an oxLDL-induced cell death. The research supports the hypothesis that NOX is the major source of oxidative stress in oxLDL induced U937 cells and immune activated plaque sections. Further research into the mechanism of oxLDL cell death is required, including investigating possible additional sources of oxidative stress. Further research is required to rule out the mitochondria in the oxidative stress mechanism induced by oxLDL.

# REFERENCES


Al Ghouleh, I., et al. (2011). "Oxidases and peroxidases in cardiovascular and lung disease: New concepts in reactive oxygen species signaling." Free Radical Biology and Medicine **51**(7): 1271-1288.

Alvarez, R. H. K., Hagop M;Cortes, Jorge E (2006). "Biology of Platelet-Derived Growth Factor and Its Involvement in Disease." ProQuest Health & Medical Complete **81**(9): 1241 - 1257.

Andert, S., et al. (1992). "Neopterin release from human endothelial cells is triggered by interferon-gamma." Clinical & Experimental Immunology **88**(3): 555-558.

Avelar-Freitas, B., et al. (2014). "Trypan blue exclusion assay by flow cytometry." Brazilian Journal of Medical and Biological Research **47**(4): 307-3015.

Aviram, M. (1996). "Interaction of Oxidized Low Density Lipoprotein with Macrophages in Atherosclerosis, and the Antiatherogenicity of Antioxidants." Eur J Clin Chem Clin Biochem **34**: 599-608.

Baird, S. K., et al. (2004). "Oxidized LDL triggers phosphatidylserine exposure in human monocyte cell lines by both caspase-dependent and -independent mechanisms." FEBS Lett **578**(1-2): 169-174.

Baird, S. K., et al. (2005). "OxLDL induced cell death is inhibited by the macrophage synthesised pterin, 7,8-dihydroneopterin, in U937 cells but not THP-1 cells." Biochim Biophys Acta **1745**(3): 361-369.

Ballinger, S. W. (2005). "Mitochondrial dysfunction in cardiovascular disease." Free Radic Biol Med **38**(10): 1278-1295.

Ballinger, S. W., et al. (2000). "Hydrogen peroxide–and peroxynitrite-induced mitochondrial DNA damage and dysfunction in vascular endothelial and smooth muscle cells." Circ Res **86**(9): 960-966.

Banerjee, A. K., et al. (2003). "Oxidant, antioxidant and physical exercise." Molecular and cellular biochemistry **253**(1-2): 307-312.

Bánfi, B., et al. (2003). "Two novel proteins activate superoxide generation by the NADPH oxidase NOX1." Journal of Biological Chemistry **278**(6): 3510-3513.

Bánfi, B., et al. (2001). "A Ca2+-activated NADPH oxidase in testis, spleen, and lymph nodes." Journal of Biological Chemistry **276**(40): 37594-37601.

Bedard, K. and K.-H. Krause (2007). "The NOX family of ROS-generating NADPH oxidases: physiology and pathophysiology." Physiological reviews **87**(1): 245-313.

Bellavite, P. (1988). "The superoxide-forming enzymatic system of phagocytes." Free Radical Biology and Medicine **4**(4): 225-261.

Berdowska, A. and K. Zwirska-Korczala (2001). "Neopterin measurement in clinical diagnosis." Journal of clinical pharmacy and therapeutics **26**(5): 319-329.

Binet, M., et al. (2014). "Use of JC-1 to assess mitochondrial membrane potential in sea urchin sperm." Journal of Experimental Marine Biology and Ecology **452**: 91-100.

Bobryshev, Y. V. (2006). "Monocyte recruitment and foam cell formation in atherosclerosis." Micron **37**(3): 208-222.

Borén, J., Olin, K., Lee, I., Chait, A., Wight, T., Innerarity, T. (1998). "Identification of the Principal Proteoglycan-binding Site in LDL." The American Society for Clinical Investigation **101**(12): 2658 - 2664.

Boullier, A., et al. (2001). "Scavenger receptors, oxidized LDL, and atherosclerosis." Annals of the New York Academy of Sciences **947**(1): 214-223.

Boveris, A. and E. Cadenas (1975). "Mitochondrial production of superoxide anions and its relationship to the antimycin insensitive respiration." FEBS Lett **54**(3): 311-314.

Boveris, A. and B. Chance (1973). "The mitochondrial generation of hydrogen peroxide. General properties and effect of hyperbaric oxygen." Biochemical Journal **134**(3): 707-716.

Brandes, R. P. and J. Kreuzer (2005). "Vascular NADPH oxidases: molecular mechanisms of activation." Cardiovascular Research **65**(1): 16-27.

Brandes, R. P., et al. (2010). "NADPH oxidases in cardiovascular disease." Free Radical Biology and Medicine **49**(5): 687-706.

Brennan, M.-L., et al. (2001). "Increased atherosclerosis in myeloperoxidase-deficient mice." The Journal of clinical investigation **107**(4): 419-430.

Brown, A. J. and W. Jessup (1999). "Oxysterols and atherosclerosis." Atherosclerosis **142**(1): 1-28.

Brown, A. J., et al. (2000). "Cholesterol and oxysterol metabolism and subcellular distribution in macrophage foam cells: accumulation of oxidized esters in lysosomes." Journal of lipid research **41**(2): 226-236.

Brown, M. G., J. (1986). "A Receptor-Mediated Pathway for Cholesterol Homeostasis." American Association for the Advancement of Science **232**(4746): 34-47.

Chandler, J. D. and B. J. Day (2012). "Thiocyanate: a potentially useful therapeutic agent with host defense and antioxidant properties." Biochem Pharmacol **84**(11): 1381-1387.

Channon, K. (2004). "Tetrahydrobiopterin: regulator of endothelial nitric oxide synthase in vascular disease." Trends in cardiovascular medicine **14**(8): 323-327.

Chen, Q., et al. (2003). "Production of reactive oxygen species by mitochondria central role of complex III." Journal of Biological Chemistry **278**(38): 36027-36031.

Chen, Y. A. (2012). Role of Intracellular Oxidant Release in Oxidised Low Density Lipoprotein- Induced U937 Cell Death. School of Biological Sciences. Christchurch, University of Canterbury. **Master of Science in Biochemistry:** 154.

Colles, S. M., Maxson, J M., Carlson, S G., Chisolm, G M. (2001). "Oxidized LDL-Induced Injury and Apoptosis in Atherosclerosis." Trends Cardiovasc Med **11**: 131 - 138.

Cross, A. R. and A. W. Segal (2004). "The NADPH oxidase of professional phagocytes—prototype of the NOX electron transport chain systems." Biochimica et Biophysica Acta (BBA) - Bioenergetics **1657**(1): 1-22.

Daugherty, A., et al. (1994). "Myeloperoxidase, a catalyst for lipoprotein oxidation, is expressed in human atherosclerotic lesions." Journal of Clinical Investigation **94**(1): 437.

Davies, M. J. (2011). "Myeloperoxidase-derived oxidation: mechanisms of biological damage and its prevention." Journal of clinical biochemistry and nutrition **48**(1): 8.

Debaisieux, S., et al. (2012). "The Ins and Outs of HIV-1 Tat." Traffic **13**(3): 355-363.

DeVries-Seimon, T., et al. (2005). "Cholesterol-induced macrophage apoptosis requires ER stress pathways and engagement of the type A scavenger receptor." J Cell Biol **171**(1): 61-73.

Douglas, G. and K. M. Channon (2014). "The pathogenesis of atherosclerosis." Medicine **42**(9): 480-484.

El-Benna, J., et al. (2010). "Peptide-based inhibitors of the phagocyte NADPH oxidase." Biochem Pharmacol **80**(6): 778-785.

Elmore, S. (2007). "Apoptosis: a review of programmed cell death." Toxicol Pathol **35**(4): 495-516.

Epstein, F. H. and S. J. Weiss (1989). "Tissue destruction by neutrophils." New England Journal of Medicine **320**(6): 365-376.

Ermak, N., et al. (2010). "Differential apoptotic pathways activated in response to Cu-induced or HOCl-induced LDL oxidation in U937 monocytic cell line." Biochem Biophys Res Commun **393**(4): 783-787.

Esposito, L. A., et al. (1999). "Mitochondrial disease in mouse results in increased oxidative stress." Proceedings of the National Academy of Sciences **96**(9): 4820-4825.

Esterbauer, H., Dieber-Rotheneder, M., Waeg, G., Striegl, G., Jurgens, G. (1990). "Biochemical, Structural, and Functional Properties of Oxidized Low-Density Lipoprotein." Chemical Research in Toxicology **3**(2): 77-92.

Evanko, S. P., Raines, E W., Ross, R., Gold, L I., Wight, T N. (1998). "Proteoglycan Distribution in Lesions of Atherosclerosis Depends on Lesion Severity, Structural Characteristics, and the Proximity of Platelet Derived Growth Factor and Transforming Growth Factor-B." American Journal of Pathology **152**(2).

Evans, M. D., et al. (1997). Reactive Oxygen Species and their Cytotoxic Mechanisms. Advances in Molecular and Cell Biology. E. E. Bittar, Elsevier. **Volume 20:** 25-73.

Exner, M., et al. (2004). "Thiocyanate catalyzes myeloperoxidase-initiated lipid oxidation in LDL." Free Radic Biol Med **37**(2): 146-155.

Falk, E. (1983). "Plaque rupture with severe pre-existing stenosis precipitating coronary thrombosis. Characteristics of coronary atherosclerotic plaques underlying fatal occlusive thrombi." British heart journal **50**(2): 127-134.

Feng, B., et al. (2003). "The endoplasmic reticulum is the site of cholesterol-induced cytotoxicity in macrophages." Nature cell biology **5**(9): 781-792.

Firth, C. A., et al. (2008). "Macrophage mediated protein hydroperoxide formation and lipid oxidation in low density lipoprotein are inhibited by the inflammation marker 7,8-dihydroneopterin." Biochim Biophys Acta **1783**(6): 1095-1101.

Fu, S., Davies, M J., Stocker, R., Dean, R T. (1998). "Evidence for roles of radicals in protein oxidation in advanced human atherosclerotic plaque." Biochem. J. **333**: 519-525.

Fu, X., et al. (2001). "Hypochlorous acid oxygenates the cysteine switch domain of pro-matrilysin (MMP-7) A mechanism for matrix metalloproteinase activation and atherosclerotic plaque rupture by myeloperoxidase." Journal of Biological Chemistry **276**(44): 41279-41287.

Fuchs, D., et al. (2009). "The role of neopterin in atherogenesis and cardiovascular risk assessment." Current medicinal chemistry **16**(35): 4644-4653.

Fuchs, D., et al. (1989). "Urinary neopterin concentrations vs total neopterins for clinical utility." Clinical chemistry **35**(12): 2305-2307.

Galis, Z. S., Sukhova G K., Lark, M W., Libby P. (1994). "Increased Expression of Matrix Metalloproteinases and Matrix Degrading Activity in Vulnerable Regions of Human Atherosclerotic Plaques." The American Society for Clinical Investigation **94**: 2493 - 2503.

Galluzzi, L., et al. (2007). "Methods for the assessment of mitochondrial membrane permeabilization in apoptosis." Apoptosis **12**(5): 803-813.

Geiszt, M., et al. (2003). "NAD (P) H oxidase 1, a product of differentiated colon epithelial cells, can partially replace glycoprotein 91phox in the regulated production of superoxide by phagocytes." The Journal of Immunology **171**(1): 299-306.

Geng, Y.-j., et al. (1995). "Expression of the Macrophage Scavenger Receptor in Atheroma Relationship to Immune Activation and the T-Cell Cytokine Interferon-γ." Arterioscler Thromb Vasc Biol **15**(11).

Gieseg, S. P., Amit, Z., Yang, Y., Shchepetkina, A., Katouah, H. (2010 B). "Oxidant Production, oxLDL Uptake, and CD36 Levels in Human Monocyte–Derived Macrophages Are Downregulated by the Macrophage-Generated Antioxidant 7,8-Dihydroneopterin." Antioxidants and REDOX Signaling **13**(10).

Gieseg, S. P., et al. (2008). "Potential to inhibit growth of atherosclerotic plaque development through modulation of macrophage neopterin/7,8-dihydroneopterin synthesis." Br J Pharmacol **153**(4): 627-635.

Gieseg, S. P., Crone, E., Amit, Z. (2010 A). "Oxidized Low Density Lipoprotein Cytotoxicity and Vascular
Disease." Endogenous Toxins. Diet, Genetics, Disease and Treatment **2**.

Gieseg, S. P., Esterbauer, H. (1994). "Low density lipoprotein is saturable by pro-oxidant copper." FEBS Lett **343**: 188-194.

Gieseg, S. P., et al. (2008). "Macrophage antioxidant protection within atherosclerotic plaques." Frontiers in bioscience (Landmark edition) **14**: 1230-1246.

Gieseg, S. P., et al. (2001 B). "Protection of erythrocytes by the macrophage synthesized antioxidant 7,8 dihydroneopterin." Free Radical Research **34**(2): 123-136.

Gieseg, S. P., et al. (2003). "Protein Hydroperoxides are a Major Product of Low Density Lipoprotein Oxidation During Copper, Peroxyl Radical and Macrophage-mediated Oxidation." Free Radical Research **37**(9): 983-991.

Gieseg, S. P., et al. (1995). "7, 8 Dihydroneopterin inhibits low density lipoprotein oxidation in vitro. Evidence that this macrophage secreted pteridine is an anti-oxidant." Free Radical Research **23**(2): 123-136.

Gieseg, S. P., Whybrow, J., Glubb, D., Rait, C. (2001 A). "Protection of U937 Cells from Free Radical Damage by the Macrophage Synthesized Antioxidant 7,8-Dihydroneopterin " Free Rad Res **35**: 311-318.

Golstein, P. and G. Kroemer (2007). "Cell death by necrosis: towards a molecular definition." Trends in Biochemical Sciences **32**(1): 37-43.

Goncharov, N., et al. (2015). "Reactive Oxygen Species in Pathogenesis of Atherosclerosis." Current Pharmaceutical Design **21**(9): 1134-1146.

Gravance, C., et al. (2000). "Assessment of equine sperm mitochondrial function using JC-1." Theriogenology **53**(9): 1691-1703.

Hampton, M. B., et al. (1998). "Inside the neutrophil phagosome: oxidants, myeloperoxidase, and bacterial killing." Blood **92**(9): 3007-3017.

Han, D., et al. (2003). "Effect of glutathione depletion on sites and topology of superoxide and hydrogen peroxide production in mitochondria." Molecular pharmacology **64**(5): 1136-1144.

Hansson, G. K. and A. Hermansson (2011). "The immune system in atherosclerosis." Nature immunology **12**(3): 204-212.

Hazen, S. L. and J. W. Heinecke (1997). "3-Chlorotyrosine, a specific marker of myeloperoxidase-catalyzed oxidation, is markedly elevated in low density lipoprotein isolated from human atherosclerotic intima." The Journal of clinical investigation **99**(9): 2075.

He, C., et al. (2013). "7-Ketocholesterol induces autophagy in vascular smooth muscle cells through Nox4 and Atg4B." The American journal of pathology **183**(2): 626-637.

Hemnani, T. and M. Parihar (1998). "Reactive oxygen species and oxidative DNA damage." Indian journal of physiology and pharmacology **42**: 440-452.

Henriksen, T., et al. (1979). "Injury to human endothelial cells in culture induced by low density lipoproteins." Scandinavian journal of clinical and laboratory investigation **39**(4): 361-368.

Heumüller, S., et al. (2008). "Apocynin is not an inhibitor of vascular NADPH oxidases but an antioxidant." Hypertension **51**(2): 211-217.

Honeychurch, J., et al. (2012). "Antibody-induced nonapoptotic cell death in human lymphoma and leukemia cells is mediated through a novel reactive oxygen species-dependent pathway." Blood **119**(15): 3523-3533.

Hort, M. A., et al. (2014). "Diphenyl diselenide protects endothelial cells against oxidized low density lipoprotein-induced injury: Involvement of mitochondrial function." Biochimie **105**: 172-181.

Hsieh, C.-C., et al. (2001). "Oxidized low density lipoprotein induces apoptosis via generation of reactive oxygen species in vascular smooth muscle cells." Cardiovascular Research **49**(1): 135-145.

Jaimes, E. A., et al. (2004). "Stable compounds of cigarette smoke induce endothelial superoxide anion production via NADPH oxidase activation." Arterioscler Thromb Vasc Biol **24**(6): 1031-1036.

Jayaraman, S., Gantz, D L., Gursky, O. (2007). "Effects of Oxidation on the Structure and Stability of Human Low-Density
Lipoprotein." Biochemistry **46**: 5790-5797.

Judkins, C. P., et al. (2010). "Direct evidence of a role for Nox2 in superoxide production, reduced nitric oxide bioavailability, and early atherosclerotic plaque formation in ApoE−/− mice." American Journal of Physiology-Heart and Circulatory Physiology **298**(1): H24-H32.

Kanegae, M. P. P., et al. (2010). "Diapocynin versus apocynin as pretranscriptional inhibitors of NADPH oxidase and cytokine production by peripheral blood mononuclear cells." Biochem Biophys Res Commun **393**(3): 551-554.

Kappler, M., et al. (2007). "Aqueous peroxyl radical exposure to THP-1 cells causes glutathione loss followed by protein oxidation and cell death without increased caspase-3 activity." Biochim Biophys Acta **1773**(6): 945-953.

Karlsson, A., et al. (2000). "Phorbol myristate acetate induces neutrophil NADPH-oxidase activity by two separate signal transduction pathways: dependent or independent of phosphatidylinositol 3-kinase." Journal of Leukocyte Biology **67**(3): 396-404.

Katouah, H., et al. (2015). "Oxidised low density lipoprotein causes human macrophage cell death through oxidant generation and inhibition of key catabolic enzymes." Int J Biochem Cell Biol **67**: 34-42.

Kettle, A., et al. (1997). "Mechanism of inactivation of myeloperoxidase by 4-aminobenzoic acid hydrazide." Biochem. J **321**: 503-508.

Kettle, A. J., et al. (1995). "Inhibition of myeloperoxidase by benzoic acid hydrazides." Biochem. J **308**: 559-563.

Kim, W.-J. and W.-H. Lee (2004). "LIGHT is expressed in foam cells and involved in destabilization of atherosclerotic plaques through induction of matrix metalloproteinase-9 and IL-8." Immune network **4**(2): 116-122.

Kinkade, K., et al. (2013). "Inhibition of NADPH oxidase by apocynin attenuates progression of atherosclerosis." Int J Mol Sci **14**(8): 17017-17028.

Kinoshita, H., et al. (2013). "Apocynin suppresses the progression of atherosclerosis in apoE-deficient mice by inactivation of macrophages." Biochem Biophys Res Commun **431**(2): 124-130.

Koch, G. L. E. (1990). "The endoplasmic reticulum and calcium storage." BioEssays **12**(11): 527-531.

Kramarenko, G. G., et al. (2006). "Ascorbate enhances the toxicity of the photodynamic action of Verteporfin in HL-60 cells." Free Radical Biology and Medicine **40**(9): 1615-1627.

Kwong, L. K. and R. S. Sohal (1998). "Substrate and site specificity of hydrogen peroxide generation in mouse mitochondria." Archives of Biochemistry and Biophysics **350**(1): 118-126.

Landmesser, U., et al. (2002). "Vascular Oxidative Stress and Endothelial Dysfunction in Patients With Chronic Heart Failure Role of Xanthine-Oxidase and Extracellular Superoxide Dismutase." Circulation **106**(24): 3073-3078.

Lapperre, T. S., et al. (1999). "Apocynin increases glutathione synthesis and activates AP-1 in alveolar epithelial cells." FEBS Lett **443**(2): 235-239.

Lardy, B., et al. (2005). "NADPH oxidase homologs are required for normal cell differentiation and morphogenesis in Dictyostelium discoideum." Biochimica et Biophysica Acta (BBA)-Molecular Cell Research **1744**(2): 199-212.

Larsson, D. A., et al. (2006). "Oxysterol mixtures, in atheroma-relevant proportions, display synergistic and proapoptotic effects." Free Radic Biol Med **41**(6): 902-910.

Lee, C. F., et al. (2010). "Nox4 is a novel inducible source of reactive oxygen species in monocytes and macrophages and mediates oxidized low density lipoprotein–induced macrophage death." Circ Res **106**(9): 1489-1497.

Leitner, K. L., et al. (2003). "Low tetrahydrobiopterin biosynthetic capacity of human monocytes is caused by exon skipping in 6-pyruvoyl tetrahydropterin synthase." Biochemical Journal **373**(3): 681-688.

Lenaz, G., et al. (2002). "Role of mitochondria in oxidative stress and aging." Annals of the New York Academy of Sciences **959**(1): 199-213.

Levitan, I., Volkov, S., Subbaiah, P V. (2010). "Oxidized LDL: Diversity, Patterns of Recognition, and Pathophysiology." Antioxidants and REDOX Signaling **13**(1): 40-75.

Libby, P. (2002). "Inflammation and Atherosclerosis." Circulation **105**(9): 1135-1143.

Libby, P. and M. Aikawa (1998). "New insights into plaque stabilisation by lipid lowering." Drugs **56**(1): 9-13.

Libby, P., et al. (2009). "Inflammation in atherosclerosis: from pathophysiology to practice." J Am Coll Cardiol **54**(23): 2129-2138.

Lindsay, A., et al. (2014). "Measurement of changes in urinary neopterin and total neopterin in body builders using SCX HPLC." Pteridines **25**(2): 53-63.

Liu, S. X., et al. (2006). "Advanced oxidation protein products accelerate atherosclerosis through promoting oxidative stress and inflammation." Arterioscler Thromb Vasc Biol **26**(5): 1156-1162.

Liu, Y., et al. (2002). "Generation of reactive oxygen species by the mitochondrial electron transport chain." Journal of neurochemistry **80**(5): 780-787.

Mach, F., et al. (1997). "Activation of monocyte/macrophage functions related to acute atheroma complication by ligation of CD40 induction of collagenase, stromelysin, and tissue factor." Circulation **96**(2): 396-399.

Madamanchi, N. R. and M. S. Runge (2007). "Mitochondrial dysfunction in atherosclerosis." Circ Res **100**(4): 460-473.

Madamanchi, N. R., et al. (2005). "Oxidative stress and vascular disease." Arterioscler Thromb Vasc Biol **25**(1): 29-38.

Majno, G. and I. Joris (1995). "Apoptosis, oncosis, and necrosis. An overview of cell death." The American journal of pathology **146**(1): 3.

Malle, E., et al. (2007). "Myeloperoxidase: a target for new drug development?" Br J Pharmacol **152**(6): 838-854.

Mangge, H., et al. (2014). "Antioxidants, inflammation and cardiovascular disease." World J Cardiol **6**(6): 462-477.

Mao, G. D., et al. (1993). "Superoxide dismutase (SOD)-catalase conjugates. Role of hydrogen peroxide and the Fenton reaction in SOD toxicity." Journal of Biological Chemistry **268**(1): 416-420.

Matsuura, E., et al. (2006). "Oxidative modification of low-density lipoprotein and immune regulation of atherosclerosis." Prog Lipid Res **45**(6): 466-486.

Meyer, J. W., Schimitt, M E. (2000). "A central role for the endothelial NADPH oxidase in atherosclerosis." FEBS Lett **472**: 1-4.

Morgan, P. E., et al. (2002). "Inhibition of glyceraldehyde-3-phosphate dehydrogenase by peptide and protein peroxides generated by singlet oxygen attack." European Journal of Biochemistry **269**(7): 1916-1925.

Murphy, M. P. (2009). "How mitochondria produce reactive oxygen species." Biochemical Journal **417**(1): 1-13.

Myoishi, M., et al. (2007). "Increased endoplasmic reticulum stress in atherosclerotic plaques associated with acute coronary syndrome." Circulation **116**(11): 1226-1233.

Nakazato, T., et al. (2007). "Myeloperoxidase Is a Key Regulator of Oxidative Stress–Mediated Apoptosis in Myeloid Leukemic Cells." Clinical Cancer Research **13**(18): 5436-5445.

Nozaki, S., et al. (1995). "Reduced uptake of oxidized low density lipoproteins in monocyte-derived macrophages from CD36-deficient subjects." Journal of Clinical Investigation **96**(4): 1859.

Obama, T., et al. (2007). "Analysis of modified apolipoprotein B-100 structures formed in oxidized low-density lipoprotein using LC-MS/MS." Proteomics **7**(13): 2132-2141.

Oh, J., et al. (2012). "Endoplasmic reticulum stress controls M2 macrophage differentiation and foam cell formation." Journal of Biological Chemistry **287**(15): 11629-11641.

Othman, I. (2015). Low Density Lipoprotein Induction of Intracellular Oxidants Production. School of Biological Sciences. Christchurch, University of Canterbury. **Doctor of Philosophy in Biochemistry:** 307.

Park, Y. M. (2014). "CD36, a scavenger receptor implicated in atherosclerosis." Experimental & molecular medicine **46**(6): e99.

Parker, G. (2015). 7,8-Dihydroneopterin oxidation: Identifying the source of cellular neopterin generated during inflammation. School of Biological Sciences. Christchurch, University of Canterbury. **Bachelor of Science (Hons.):** 72.

Peshavariya, H. M., et al. (2007). "Analysis of dihydroethidium fluorescence for the detection of intracellular and extracellular superoxide produced by NADPH oxidase." Free Radical Research **41**(6): 699-712.

Pongnimitprasert, N. (2009). "Atherosclerosis and NADPH Oxidase." Silpakorn U Sci Tech J **3**(1): 13-24.

Prokopowicz, Z., et al. (2012). "Neutrophil myeloperoxidase: soldier and statesman." Archivum immunologiae et therapiae experimentalis **60**(1): 43-54.

Rahaman, S. O., et al. (2006). "A CD36-dependent signaling cascade is necessary for macrophage foam cell formation." Cell Metabolism **4**(3): 211-221.

Rey, F. E., Cifuentes, M E., Kiarash, A., Quinn, M T., Pagano, P J. (2001). "Novel Competitive Inhibitor of NADPH Oxidase Assembly Attenuates Vascular O2- and sysolic Blood Pressure in Mice." Circ Res **89**: 408-414.

Ross, R., et al. (1977). "Response to injury and atherogenesis." The American journal of pathology **86**(3): 675.

Rutherford, L. D. and S. P. Gieseg (2012). "7-ketocholesterol is not cytotoxic to U937 cells when incorporated into acetylated low density lipoprotein." Lipids **47**(3): 239-247.

Santulli, G. (2013). "Epidemiology of cardiovascular disease in the 21st century: updated numbers and updated facts." JCvD **1**(1): 1-2.

Schoenborn, J. R. and C. B. Wilson (2007). "Regulation of interferon-γ during innate and adaptive immune responses." Advances in immunology **96**: 41-101.

Schraufstätter, I., et al. (1990). "Mechanisms of hypochlorite injury of target cells." Journal of Clinical Investigation **85**(2): 554.

Schulze, P. C. and R. T. Lee (2005). "Oxidative stress and atherosclerosis." Current atherosclerosis reports **7**(3): 242-248.

Schumacher, M., et al. (1992). "Neopterin levels in patients with coronary artery disease." Atherosclerosis **94**(1): 87-88.

Schumacher, M., et al. (1997). "Increased neopterin in patients with chronic and acute coronary syndromes." J Am Coll Cardiol **30**(3): 703-707.

Scull, C. M. and I. Tabas (2011). "Mechanisms of ER stress-induced apoptosis in atherosclerosis." Arterioscler Thromb Vasc Biol **31**(12): 2792-2797.

Shchepetkina, A. (2013). Mechanisms of 7,8-dihydroneopterin protection of macrophages from cytotoxicity. School of Biological Science. Christchurch, University of Canterbury. **Doctor of Philosophy in Biochemistry:** 304.

Sies, H. (1997). "Oxidative stress: oxidants and antioxidants." Experimental physiology **82**(2): 291-295.

Silverstein, R. L. (2009). "Inflammation, atherosclerosis, and arterial thrombosis: role of the scavenger receptor CD36." Cleveland Clinic journal of medicine **76**(Suppl 2): S27.

Sorescu, D., et al. (2002). "Superoxide production and expression of nox family proteins in human atherosclerosis." Circulation **105**(12): 1429-1435.

Steinbrecher, U. P. (1991). "Role of Lipoprotein Peroxidation in the Pathogenesis of Atherosclerosis." Clin. Cardiol. **14**: 865-867.

Stocker, R. and J. F. Keaney (2004). "Role of oxidative modifications in atherosclerosis." Physiological reviews **84**(4): 1381-1478.

Stolk, J., et al. (1994). "Characteristics of the inhibition of NADPH oxidase activation in neutrophils by apocynin, a methoxy-substituted catechol." American Journal of Respiratory Cell and Molecular Biology **11**(1): 95-102.

Sugiyama, S., et al. (2004). "Hypochlorous acid, a macrophage product, induces endothelial apoptosis and tissue factor expression involvement of myeloperoxidase-mediated oxidant in plaque erosion and thrombogenesis." Arterioscler Thromb Vasc Biol **24**(7): 1309-1314.

Sugiyama, S., et al. (2001). "Macrophage myeloperoxidase regulation by granulocyte macrophage colony-stimulating factor in human atherosclerosis and implications in acute coronary syndromes." The American journal of pathology **158**(3): 879-891.

Sukhanov, S., et al. (2006). "Novel effect of oxidized low-density lipoprotein: cellular ATP depletion via downregulation of glyceraldehyde-3-phosphate dehydrogenase." Circ Res **99**(2): 191-200.

Sun, P., et al. (2000). "Blood Pressure, LDL Cholesterol, and Intima-Media Thickness A Test of the "Response to Injury" Hypothesis of Atherosclerosis." Arterioscler Thromb Vasc Biol **20**(8): 2005-2010.

Tabas, I. (1997). "Free Cholesterol-InducedCytotoxicity A Possible Contributing Factor to Macrophage Foam Cell Necrosis in Advanced Atherosclerotic Lesions." TCM **7**: 254-263.

Tabas, I. (2010). "The role of endoplasmic reticulum stress in the progression of atherosclerosis." Circ Res **107**(7): 839-850.

Tahboub, Y. R., et al. (2005). "Thiocyanate modulates the catalytic activity of mammalian peroxidases." J Biol Chem **280**(28): 26129-26136.

Takeya, R., et al. (2003). "Novel human homologues of p47phox and p67phox participate in activation of superoxide-producing NADPH oxidases." Journal of Biological Chemistry **278**(27): 25234-25246.

Thony, B., et al. (2000). "Tetrahydrobiopterin biosynthesis, regeneration and functions." Biochemical Journal **347**(1): 1-16.

Touyz, R. M. (2008). "Apocynin, NADPH Oxidase, and Vascular Cells A Complex Matter." Hypertension **51**(2): 172-174.

Tsukano, H., et al. (2010). "The endoplasmic reticulum stress-C/EBP homologous protein pathway-mediated apoptosis in macrophages contributes to the instability of atherosclerotic plaques." Arterioscler Thromb Vasc Biol **30**(10): 1925-1932.

Turrens, J. F. (2003). "Mitochondrial formation of reactive oxygen species." J Physiol **552**(Pt 2): 335-344.

Valko, M., et al. (2007). "Free radicals and antioxidants in normal physiological functions and human disease." Int J Biochem Cell Biol **39**(1): 44-84.

van Dalen, C. J., Whitehouse, M W., Winterbourn, C C., Kettle, A J. (1997). "Thiocyanate and chloride as competing substrates for myeloperoxidase." Biochem. J. **327**: 487-492.

Van den Worm, E., et al. (2001). "Effects of methoxylation of apocynin and analogs on the inhibition of reactive oxygen species production by stimulated human neutrophils." European Journal of Pharmacology **433**(2–3): 225-230.

Vicca, S., et al. (2003). "Apoptotic pathways involved in U937 cells exposed to LDL oxidized by hypochlorous acid." Free Radical Biology and Medicine **35**(6): 603-615.

Vignais, P. V. (2002). "The superoxide-generating NADPH oxidase: structural aspects and activation mechanism." CMLS, Cell. Mol. Life Sci **59**: 1428-1459.

Vindis, C., et al. (2005). "Two distinct calcium-dependent mitochondrial pathways are involved in oxidized LDL-induced apoptosis." Arterioscler Thromb Vasc Biol **25**(3): 639-645.

Vissers, M. C. and C. Thomas (1997). "Hypochlorous acid disrupts the adhesive properties of subendothelial matrix." Free Radical Biology and Medicine **23**(3): 401-411.

Walter, R., et al. (2001). "Tetrahydrobiopterin in the vascular system." Pteridines-Berlin- **12**(3): 93-120.

Wang, Y., et al. (2014). "Macrophage mitochondrial oxidative stress promotes atherosclerosis and nuclear factor-κB–mediated inflammation in macrophages." Circ Res **114**(3): 421-433.

Werner-Felmayer, G., et al. (1990). "Neopterin formation and tryptophan degradation by a human myelomonocytic cell line (THP-1) upon cytokine treatment." Cancer research **50**(10): 2863-2867.

Widner, B., et al. (2000). "Oxidation of 7, 8-dihydroneopterin by hypochlorous acid yields neopterin." Biochem Biophys Res Commun **275**(2): 307-311.

Williams, H. C., Griendling, K K. (2007). "NADPH Oxidase Inhibitors: New Antihypertensive Agents?" J Cardiovasc Pharmacol **50**: 9-16.

Williams, K. J. and I. Tabas (1995). "The response-to-retention hypothesis of early atherogenesis." Arterioscler Thromb Vasc Biol **15**(5): 551-561.

Williams, K. J. and I. Tabas (1998). "The response-to-retention hypothesis of atherogenesis reinforced." Current opinion in lipidology **9**(5): 471-474.

Xu, Y., et al. (2009). "The antioxidant role of thiocyanate in the pathogenesis of cystic fibrosis and other inflammation-related diseases." Proceedings of the National Academy of Sciences **106**(48): 20515-20519.

Yang a, Y. T., et al. (2012). "HOCl causes necrotic cell death in human monocyte derived macrophages through calcium dependent calpain activation." Biochim Biophys Acta **1823**(2): 420-429.

Yang b, Y. T., et al. (2012). "Intracellular glutathione protects human monocyte-derived macrophages from hypochlorite damage." Life Sci **90**(17-18): 682-688.

Yu, E. P. and M. R. Bennett (2014). "Mitochondrial DNA damage and atherosclerosis." Trends Endocrinol Metab **25**(9): 481-487.

Zhang, C., et al. (2001). "Endothelial dysfunction is induced by proinflammatory oxidant hypochlorous acid." American Journal of Physiology-Heart and Circulatory Physiology **281**(4): H1469-H1475.

Zhao, B., et al. (2006). "Constitutive receptor-independent LDL uptake and cholesterol accumulation by macrophages differentiated from human monocytes with M-CSF." Journal of Biological Chemistry.